Title
Dynamics of the Anaerobic Ammonium Oxidizing (Anammox) Microbial Community

Author
Lawrence, Jennifer Elise

Publication Date
2018

Peer reviewed|Thesis/dissertation

Dynamics of the Anaerobic Ammonium Oxidizing (Anammox) Microbial Community

By

Jennifer Elise Lawrence

A dissertation submitted in partial satisfaction of the

requirements for the degree of

Doctor of Philosophy

in

Engineering – Civil and Environmental Engineering

in the

Graduate Division

of the

University of California, Berkeley

Committee in charge:

Professor Lisa Alvarez-Cohen, Chair
Professor David Sedlak
Professor Mary Firestone

Fall 2018

Dynamics of the Anaerobic Ammonium Oxidizing (Anammox) Microbial Community

By

Jennifer Elise Lawrence

Abstract

Dynamics of the Anaerobic Ammonium Oxidizing (Anammox) Microbial Community

by

Jennifer Elise Lawrence

Doctor of Philosophy in Engineering – Civil and Environmental Engineering

University of California, Berkeley

Professor Lisa Alvarez-Cohen, Chair

Anaerobic ammonium oxidation (anammox) is the basis for an innovative, biological treatment process that removes reactive nitrogen from wastewater. To date, over 100 full-scale anammox treatment processes have been installed at municipal and industrial wastewater treatment plants across the globe. Unfortunately, the bacteria responsible for anammox are easily inhibited and express low growth rates within the anammox treatment processes' reactors. Often times, it can take up to six months to initiate a new anammox reactor or to restore the performance of an anammox reactor when an inhibition event occurs, which is unacceptably long for municipalities and industries who must adhere to strict nitrogen discharge limits. Moreover, these problems are compounded by a limited understanding of the complex microbial communities that comprise anammox reactors. The work presented in this dissertation seeks to fill this gap by investigating the temporal dynamics of anammox microbial communities during the start-up and continued operation of laboratory-scale anammox reactors, as well as the spatial dynamics of anammox microbial communities across a nitrogen-contaminated environment.

Chapter 2 begins with a review of previous literature that supports the idea of a core microbial community within anammox reactors. This review is combined with temporal-scale data from 440 days of continuous operation of a laboratory-scale anammox reactor to identify relationships between microbial community composition and associated reactor performance. Results suggest that anammox, denitrifying, and dissimilatory nitrate reducing to ammonium (DNRA) bacteria are omnipresent in the anammox reactor. Furthermore, results suggest that these three groups of nitrogen-cycling bacteria cooperate and maximize reactive nitrogen removal under desirable conditions, but that they compete and sabotage reactive nitrogen removal under undesirable conditions (primarily because they share nitrite as their electron acceptor). More research must be done to understand the conditions that support cooperation over competition among these three groups of nitrogen-cycling bacteria in an anammox reactor.

Chapter 3 builds off Chapter 2 and delves more deeply into the relationship between anammox, denitrifying, and DNRA bacteria in a laboratory-scale anammox reactor. The temporal dynamics of these three groups of nitrogen-cycling bacteria and associated reactor performance are investigated by manipulating the ratio of ammonium to nitrite in the anammox reactor's feedstock. Results indicate that an ammonium to nitrite ratio of 1 to 1.32 in the reactor's feedstock favors the enrichment of anammox bacteria, while lower ammonium to nitrite ratios (1 to 1.1 – 1 to 1.2) favor

the enrichment of a more-diverse bacterial community that contains denitrifying and DNRA bacteria alongside anammox bacteria. Furthermore, results suggest that the more-diverse bacterial community has a greater capacity to remove reactive nitrogen from the feedstock (primarily because denitrifying and DNRA bacteria can transform nitrate, a product of anammox metabolism). Nevertheless, more research must still be done to understand the conditions that support cooperation among these three groups of nitrogen-cycling bacteria in an anammox reactor.

In Chapter 4, the capacity of two support media—polyvinyl alcohol-sodium alginate (PVA-SA) and clinoptilolite zeolite—to improve biomass retention (and hence, decrease startup and recovery times) within anammox reactors is investigated through a series of laboratory-scale anammox reactor experiments. Corresponding shifts in bacterial community structure in the presence of clinoptilolite zeolite are also investigated. Under the conditions provided in this study, results indicate that neither of the support media are capable of improving the performance of the laboratory-scale anammox reactors. Moreover, results indicate that the amendment of clinoptilolite zeolite to the laboratory-scale anammox reactors has no impact on the structure of the bacterial community within it. More research must be done (under different conditions) to definitively rule out the capacity of PVA-SA and clinoptilolite zeolite to improve biomass retention within anammox reactors.

While anammox bacteria have existed in anammox reactors for less than 20 years, they have existed for centuries (quite possibly millennia) in natural habitats. Thus, patterns found in the structure of anammox-containing microbial communities from natural habitats may be able to inform the structure and performance of microbial communities within anammox reactors. To this end, Chapter 5 investigates the abundance and distribution of anammox bacteria across nitrogen-contaminated natural habitats in New Zealand. The results of these investigations indicate that there are many similarities between the structure of anammox microbial communities in natural habitats and of anammox microbial communities in anammox reactors. Moving forward, more research must be done to transfer the patterns found within the structure of anammox-containing microbial communities in New Zealand's natural habitats into anammox reactor conditions. Once equipped with these results, scientists and engineers can begin to enrich an anammox microbial community based on New Zealand's unique natural habitats.

Ultimately, the results of the research described in this dissertation bolster the fundamental understanding of anammox microbial communities and their performance within anammox reactors. This understanding, in turn, will enable a more comprehensive control of the anammox treatment process and help facilitate its widespread adoption at municipal and industrial wastewater treatment plants across the globe.

"Nothing can be done except little by little."

- Charles Baudelaire

Table of Contents

List of Figures

List of Tables

Acknowledgements

I would like to convey my heartfelt gratitude to everyone who supported me during my journey through graduate school. This dissertation is the culmination of the tremendous efforts of a host of people:

Foremost, I would like to thank my adviser, Lisa Alvarez-Cohen, for her support and guidance over the past six years. By allowing me the freedom to explore new ideas and a variety of fields, she has taught me the value of initiative and self-reliance. I would also like to thank all of the members of the Alvarez-Cohen research group for their support and friendship over the past six years; they truly made the day-to-day graduate school experience a joy. In particular, I'd like to thank Edmund Antell, Dr. David Jenkins, Dr. Ray Keren, Dr. Shan Yi, and Dr. Wei-Qin Zhuang for their invaluable advice and support.

I would also like to thank a number of individuals for their specific contributions that made this dissertation possible. Dr. Lijie Zhou constructed and maintained the anammox reactors studied in Chapters 2 and 3. He and Dr. Ke Yu assisted with the DNA extractions and subsequent 16S rRNA sequence processing reported in Chapter 2. Edmund Antell, Emily Gonthier, and Anita Sanchez assisted in the design, construction, and maintenance of the anammox reactors studied in Chapter 4. Sarah Cavin assisted with the DNA extractions reported in Chapter 4. Dr. Gavin Lear provided the 16S rRNA sequence dataset and supporting metadata analyzed in Chapter 5. Joseph Charbonnet and Karina Chavarria proofread the fellowship and grant proposals that made all of this dissertation possible.

My grateful thanks are also extended to Dr. David Sedlak and Dr. Mary Firestone for providing feedback on initial drafts of this dissertation, and to Mason King for coordinating the final submission paperwork.

Finally, I would like to thank my family for their continued support and encouragement. None of this could have happened without them.

Chapter 1:

Introduction and Background

1.1 Nitrogen in the environment

Nitrogen is an essential nutrient for all life on earth (Sylvia et al. 2005). The majority of this element exists in the atmosphere in the form of inert nitrogen gas (N_2). Ironically, it is inaccessible to the vast majority of living organisms in this form. Nitrogen gas must first be transformed (i.e., "fixed") into one of a variety of organic and inorganic forms collectively referred to as reactive nitrogen in order to serve biological function (UNEP 2007).

Historically, microorganisms have been responsible for the majority of reactive nitrogen fixation (Cabello et al. 2004; Nielsen 2005). At the turn of the twentieth century, however, a synthetic nitrogen fixation process called the Haber-Bosch Process was invented. Since its inception, the global rate of nitrogen gas fixation into reactive nitrogen has doubled (UNEP 2007). While these increased volumes of reactive nitrogen are essential for meeting the food demands of an ever-increasing world population, they can cause serious problems when released into the environment.

Coastal ecosystems are particularly vulnerable to reactive nitrogen pollution (UNSD 2018). When excess concentrations of reactive nitrogen are released into these environments, they can spur the proliferation of primary producers. This in turn can lead to eutrophication, the reduction of biodiversity of aquatic plants and animals, and the production of toxins (Camargo and Alonso 2006). Currently, large swaths of coastal ecosystems surrounding all six of the inhabited continents are at high or very high-risk levels of eutrophication (Figure 1.1) (UNSD 2018).

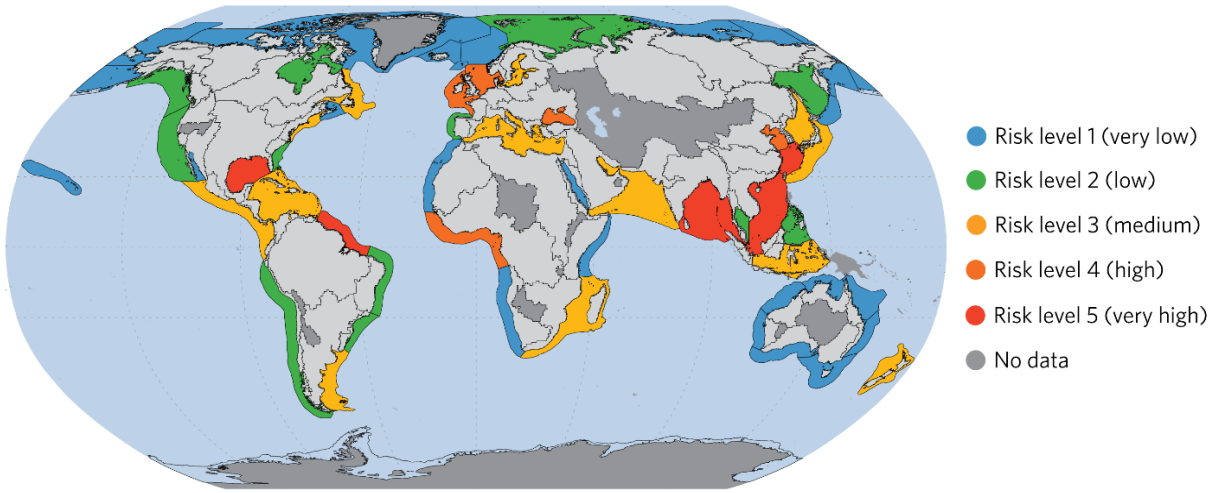

Figure 1.1: Eutrophication risk levels of coastal ecosystems (adapted from UNSD 2018).

Reactive nitrogen pollution originates from many sources, including agricultural runoff, septic tank leachate, municipal and industrial wastewater streams, urban stormwater runoff, and fossil fuel combustion (WRI 2018). To mitigate reactive nitrogen pollution in high-risk coastal ecosystems, reactive nitrogen is generally removed from point-source loads—primarily, municipal wastewater streams—before they are discharged to the environment. To achieve reactive nitrogen removal from a point source, microbiologically-induced transformation processes are employed within an on-site reactor to convert reactive nitrogen back into inert nitrogen gas, thereby completing the nitrogen cycle (Rittmann and McCarty 2001).

1.2 Nitrogen cycling pathways

Microorganisms participating in the nitrogen cycle can be classified according to their metabolic (i.e., nitrogen-transforming) pathways (Figure 1.2) (Cabello et al. 2004; Nielsen 2005). Atmospheric nitrogen gas (N_2) is reduced to ammonium (NH_4^+) in nitrogen fixation. Ammonium is oxidized to and nitrate (NO_3^-) in nitrification. Nitrate is reduced back to nitrogen gas in denitrification. Ammonium and nitrite react to form nitrogen gas in anaerobic ammonium oxidation (anammox). Nitrate is reduced to ammonium in dissimilatory nitrate reduction to ammonium (DNRA) (Arrigo 2005; Sylvia et al. 2005; Tu et al. 2017).

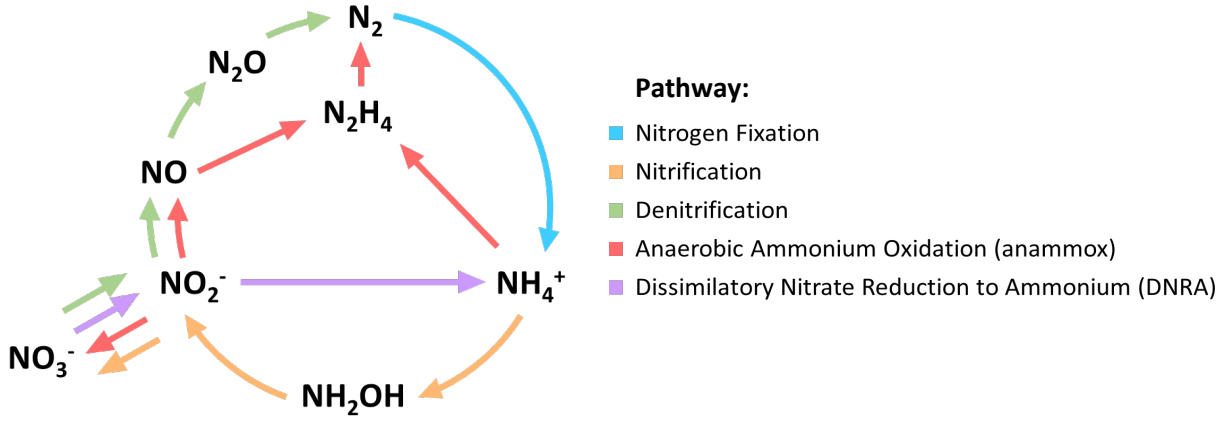

Figure 1.2: Nitrogen cycling pathways.

Some pathways (e.g., anammox) are strongly, though not strictly, linked to phylogeny, while others (e.g., nitrification/denitrification) are spread widely across the bacterial and archaeal domains (Canfield et al. 2010). The metabolic capabilities of microorganisms are particularly important in the design of wastewater reactors, because the microbial communities within them are typically derived from strong selection pressure upon diverse inocula, rather than from bioaugmentation.

1.2.1 Nitrification

Nitrifying microorganisms oxidize ammonium first into nitrite, and then into nitrate, with oxygen as their electron acceptor (Equations 1.1 and 1.2, respectively). In bacteria, the enzymes responsible for Equation 1.1 are ammonia monooxygenase and hydroxylamine oxidoreductase, while the enzyme responsible for Equation 1.2 is nitrite oxidoreductase. Nitrification is typically considered a chemoautotrophic process, but a handful of heterotrophic microorganisms are capable of the process as well. In chemoautotrophic nitrification, energy is produced for ATP synthesis. In heterotrophic nitrification, on the other hand, no energy is produced (Sylvia et al. 2005).

(1.1) $NH_4^+ + 1.5O_2 \rightarrow NO_2^- + 2H^+ + H_2O$

(1.2) $NO_2^- + 0.5O_2 \rightarrow NO_3^-$

Bacteria capable of Equation 1.1 are classified into "Nitroso-" genera within the classes Betaproteobacteria and Gammaproteobacteria within the phylum Proteobacteria. Bacteria capable

of Equation 1.2 are classified into "Nitro-" genera within the classes Alphaproteobacteria, Gammaproteobacteria, and Deltaproteobacteria within the phylum Proteobacteria, and within the class Nitrospira within the phylum Nitrospirae. Additional, heterotrophic nitrifiers include *Alcaligenes* and *Anthrobacter* spp., within the phyla Proteobacteria and Actinobacteria, respectively (Sylvia et al. 2005).

1.2.2 Denitrification

Denitrifying microorganisms typically harvest energy through the heterotrophic reduction of nitrite or nitrate to nitrogen gas (Equations 1.3 and 1.4, respectively). (Some denitrifiers are autotrophic as well.) In bacteria, denitrification—an anaerobic process—proceeds in four reductive steps: first, nitrate is reduced to nitrite via the nitrate reductase enzyme; second, nitrite is reduced to nitric oxide via the nitrite reductase enzyme; third, nitric oxide is reduced to nitrous oxide via the nitrous oxide reductase enzyme; and fourth, nitrous oxide is reduced to nitrogen gas via the nitrous oxide reductase enzyme (Sylvia et al. 2005).

(1.3) $3CH_2O + 4NO_2^- + 4H^+ \rightarrow 2N_2 + 3CO_2 + 5H_2O$

(1.4) $5CH_2O + 4NO_3^- + 4H^+ \rightarrow 2N_2 + 5CO_2 + 7H_2O$

Denitrifying bacteria represent a wide range of taxonomic groups, including members of the genera *Alcaligenes, Agrobacterium, Aquaspirillum, Azospirillum, Blastobacter, Bradyrhizobium, Branhamella, Chromobacterium, Dechloromonas, Denitratisoma, Hyphomicrobium, Neisseria, Paracoccus, Pseudomonas, Rhodoplanes, Thauera,* and *Wolinella* within the classes Alphaproteobacteria, Betaproteobacteria, Gammaproteobacteria, and Epsilonproteobacteria within the phylum Proteobacteria, members of the genus *Bacillus* within the phylum Firmicutes, members of the genera *Cytophaga*, *Flavobacterium*, and *Flexibacter* within the phylum Bacteroidetes, and members of the genus *Propionibacterium* within the phylum Actinobacteria (Sylvia et al. 2005; Pereira et al. 2017).

1.2.3 Anaerobic ammonium oxidation (anammox)

Anammox bacteria obtain their energy for growth from the anaerobic, chemolithoautotrophic conversion of ammonium and nitrite into nitrogen gas (Equation 1.5). This conversion proceeds via three coupled redox reactions with two intermediates: nitric oxide and (highly toxic) hydrazine (Kartal et al. 2004). First, nitrite reduction is carried out by the nitrite reductase enzyme. Second, hydrazine is synthesized by the hydrazine synthase enzyme. Third, the four-electron oxidation of hydrazine is carried out by the hydrazine dehydrogenase enzyme (Kartal et al. 2004).

In anammox bacteria's overall metabolism, Equation 1.5 is coupled with the oxidation of nitrite and the reduction of bicarbonate for biomass synthesis (Equation 1.6). Nitrite plays a dual role, acting both as an electron acceptor in the energy-generating reaction, and as an electron donor in the biosynthesis reaction. As a consequence, anammox growth is always associated with the production of nitrate (Strous et el. 1998; Kuenen 2008; Kartal et al. 2012).

(1.5) $NH_4^+ + NO_2^- \rightarrow N_2 + 2H_2O$

(1.6) $NH_4^+ + 1.32NO_2^- + 0.066HCO_3^- + 0.13H^+ \rightarrow 1.02N_2 + 0.26NO_3^- + 2.03H_2O + 0.066CH_2O_{0.5}N_{0.15}$

Currently, all of the identified anammox bacteria are members of the order Brocadiales and the phylum Planctomycetes. Within the order Brocadiales, five "Candidatus" anammox genera—*Anammoxoglobus*, *Brocadia*, *Jettenia*, *Kuenenia*, and *Scalindua*—and 16 anammox species within these genera have been identified (Sonthiphand et al. 2014; Connan et al. 2016).

1.2.4 Dissimilatory nitrate reduction to ammonium (DNRA)

DNRA microorganisms gain energy from the reduction of nitrate to ammonium, with nitrite as an intermediate. In bacteria, nitrate is reduced to nitrite via the nitrate reductase enzyme, and nitrite is reduced to ammonium via the nitrite reductase enzyme via anaerobic processes (Sylvia et al. 2005). DNRA bacteria have been found to use both organic carbon and sulfur compounds as their electron donors (Equations 1.7 and 1.8, respectively) (van de Leemput et al. 2014; Preisler et al. 2007).

(1.7) $2CH_2O + NO_3^- + 2H^+ \rightarrow NH_4^+ + 2CO_2 + H_2O$

(1.8) $4S(0) + 3NO_3^- + 7H_2O \rightarrow 4SO_4^{2-} + 3NH_4^+ + 2H^+$

Several genera of bacteria are capable of DNRA, including members of *Clostridium*, *Selenomonas*, and *Veillonella* within the phylum Firmicutes, and members of *Desulfovibrio*, *Wolinella*, *Citrobacter*, *Enterobacter*, *Erwinia*, *Escherichia*, *Klebsiella*, *Photobacterium*, *Salmonella*, *Serratia*, and *Vibrio* within the classes Gammaproteobacteria, Deltaproteobacteria, and Epsilonproteobacteria within the phylum Proteobacteria (Sylvia et al. 2005).

1.3 Nitrogen removal technologies

Reactive nitrogen enters municipal wastewater treatment plants primarily in the form of ammonium. The plant's primary wastewater stream (i.e., mainstream) accounts for approximately 95% of the plant's overall flow and contains approximately 20-40 mg NH_4^+-N L^{-1} (Lackner et al. 2014; Laureni et al. 2016). The plant's recycled reject waters (i.e., sidestream, including supernatant liquids from anaerobic digesters and centrate/filtrate streams from sludge dewatering processes) account for the remaining 5% of the plant's overall flow and contain approximately 800 – 2,500 mg NH_4^+-N L^{-1} (Pugh 2012; van der Star et al. 2008). Thus, 65-75% of municipal wastewater's total nitrogen load lies within the mainstream, while the remaining 25-35% of the load lies within the sidestreams.

Depending on the sensitivity of the receiving water body, the concentration of reactive nitrogen in the wastewater treatment plant's effluent can be regulated to as little as 0.4 mg N L^{-1} (EPA 2016). To meet effluent nitrogen regulations, a wastewater treatment plant may choose to remove reactive nitrogen from its mainstream, its sidestreams, or a combination of both. Using traditional technologies, it costs roughly $15.00 to remove a kilogram of reactive nitrogen from mainstream, versus $4.50 to remove a kilogram of reactive nitrogen from sidestreams (Grow and Graham 2018).

1.3.1 Biological nutrient removal (BNR)

Biological nutrient removal (BNR) is the established technology for ammonium and total reactive nitrogen removal from mainstream and sidestreams at municipal wastewater treatment plants (Hu et al. 2012). While there are a number of BNR process configurations available, they are all based

around the sequencing of aerobic zones of nitrification and anaerobic zones of denitrification for ammonium and total reactive nitrogen removal. In nitrification, the wastewater stream's ammonium concentration is converted to nitrate. In denitrification, the produced nitrate is cycled to nitrogen gas. Some of the most common BNR process configurations include: the modified Ludzack-Ettinger (MLE) process, the A^2/O process, the step feed process, the Bardenpho process, the modified Bardenpho process, the sequencing batch reactor process, the modified University of Cape Town process, and the oxidation ditch continuous flow process (EPA 2007).

1.3.2 Deammonification

Deammonification is a new, innovative technology that removes ammonium and total reactive nitrogen from wastewater streams. Similar to BNR, there are a number of deammonification process configurations available. All of the process configurations are based around the sequencing of aerobic zones of partial nitritation (PN) and anaerobic zones of anammox (Kartal et al. 2012; Paques 2018). In PN, a fraction of the wastewater stream's ammonium concentration is converted to nitrite by AOB. AOB are selected over NOB through a careful control of temperature, dissolved oxygen concentration, hydraulic retention time, and sludge retention time (Lackner et al. 2014). The PN process is highly sensitive to these controls (Shalini and Joseph 2012). In anammox, the produced nitrite and remaining ammonium are cycled to nitrogen gas.

The deammonification process can be implemented sequentially (in two separate reactors, where PN is physically separated from anammox), or in a single reactor (where the AOB and anammox bacteria are directly mixed) (Regmi et al. 2014). Many treatment plants have successfully applied the two-stage deammonification process to ammonium-rich wastewaters, including the reject water from anaerobic digestion, digested black water, and mixed agricultural-digestate (de Graaff et al. 2011; Dosta et al. 2015; Scaglione et al. 2015). More recently, single-stage reactors have been gaining popularity because they permit significant investment cost savings through minimized equipment, footprint, and labor requirements (Jeanningros et al. 2010; Stinson 2018). Currently available single-stage deammonification process configurations include: the ANAMMOX granular sludge process, the ANITAMox attached growth moving bed bioreactor process, the DEMON suspended growth sequencing batch reactor process, the Cleargreen suspended growth sequencing batch reactor process, and the TerraMox hybrid suspended and attached growth process (Stinson 2018). While these process configurations are typically applied to sidestream conditions, current efforts seek to adapt them to mainstream conditions (Laureni et al. 2016; Li et al. 2018).

1.4 Motivation

Unlike the conventional BNR process, deammonification operates with minimal aeration and does not require an organic carbon supplement (WWW 2015). As a result, full-scale, single-stage deammonification consumes 60% less energy, produces 90% less waste biomass, and emits a significantly smaller volume of greenhouse gases than its full-scale BNR counterpart (Paques 2018). To date, just over 100 full-scale deammonification reactors have been installed across the globe (representing a mere fraction of the number of BNR reactors) (Lackner et al. 2014; Li et al. 2018). If deammonification could be applied on a wider scale, the energy and environmental savings would be immense (Dodds et al. 2009).

Unfortunately, anammox bacteria have very low growth rates (doubling times ranging from 7-22 days) in deammonification reactors treating municipal wastewater streams and are easily inhibited by a variety of factors, including: temperature, pH, and variable substrate and metabolite concentrations (Jin et al. 2012; Carvajal-Arroyo et al. 2013; Ali and Okabe 2015a; Kallistova et al. 2016). Furthermore, a deammonification reactor's performance can take up to six months to recover following an inhibition event, which is unacceptably long for municipalities who must adhere to strict discharge limits (Klaus et al. 2016).

These problems are compounded by what is now only a cursory understanding of the microbial communities responsible for stable and robust anammox performance (Gonzalez-Martinez et al. 2015b). In order for the widespread application of the deammonification process to be realized, a more comprehensive understanding of the complex processes occurring both within and among the numerous bacterial species within an anammox reactor must be attained.

1.5 Dissertation overview

This dissertation describes investigations into the dynamics of anammox bacterial communities. All of the investigations share a guiding theme of informing the design of more effective anammox reactors for the deammonification process. The remainder of this dissertation is organized into four chapters detailing these investigations, followed by an additional chapter summarizing the results and suggesting future directions based on these findings.

Chapter 2 begins with a review of previous literature that supports the idea of a core microbial community within anammox reactors. This review is combined with temporal-scale data from 440 days of continuous operation of a laboratory-scale anammox reactor to identify trends in bacterial community composition and associated reactor performance. Bacterial community members that may be responsible for the destabilization of anammox reactors are identified.

Chapter 3 delves more deeply into the relationship between the anammox, denitrifying, and DNRA pathways in a stable anammox reactor. Through the interpretation of performance data, nitrogen flows through these three pathways are quantified. Results are bolstered with supporting data from 16S rRNA gene sequencing analyses.

In Chapter 4, two new support media—polyvinyl alcohol-sodium alginate (PVA-SA) and clinoptilolite zeolite—are identified to improve biomass retention (and hence, decrease startup time) within an anammox reactor. Their efficacies are investigated through a series of laboratory-scale batch, column, and upflow anaerobic sludge blanket (UASB) reactor experiments. Corresponding bacterial community shifts to new lifestyles in the presence of these support media are interpreted through 16S rRNA gene sequencing analyses.

Chapter 5 investigates the abundance and distribution of anammox bacteria across a nitrogen-contaminated environment. Statistical analyses are performed to draw correlations between anammox microbial communities in engineered reactors and anammox microbial communities in this natural environment. Implications for the enrichment of anammox bacteria from non-traditional sources, primarily its practicality, are discussed.

Conclusions drawn from these investigations and suggestions for future work are summarized in Chapter 6.

Chapter 2:

Temporal Dynamics of the Anammox Bacterial Community

2.1 Introduction

In anammox reactors, many different microbial species (not only the anammox species) interact with each other to maintain reactor function and stability (van der Star et al. 2007). Most notably, anaerobic nitrogen cycling bacteria cooperate to remove not only ammonium and nitrite, but also nitrate—the product of anammox metabolism—from wastewater streams (Bagchi et al. 2016; Lawson et al. 2016; Shu et al. 2016; Castro-Barros et al. 2017). When external carbon sources are absent, the detritus secreted from actively growing anammox bacteria (including soluble microbial products (SMPs), extracellular polymeric substances (EPSs), and volatile fatty acids (VFAs)), as well as the decaying anammox bacterial cells themselves, support heterotrophic nitrogen removal performed by denitrifying and DNRA bacteria (Vlaeminck et al. 2010; Ni et al. 2012; Hou et al. 2015; Castro-Barros et al. 2017).

Previous research has also suggested that a core microbial community exists within anammox reactors (Li et al. 2009; Cho et al. 2010; Kartal et al. 2010; Park et al. 2010; Gonzalez-Martinez et al. 2014; Gonzalez-Martinez et al. 2015a; Gonzalez-Martinez et al. 2015b; Chu et al. 2015; Pereira et al. 2017). Uncultured members of the phyla Acidobacteria, Bacteroidetes, Chlorobi, Chloroflexi, and Proteobacteria have been identified in the majority of anammox reactors. Since these phyla have primarily been identified through 16S rRNA gene sequencing analyses, their roles in maintaining and/or inhibiting anammox performance have yet to be elucidated (Kindaichi et al. 2012; Pereira et al. 2017; Tang et al. 2018).

Acidobacteria, metabolically diverse heterotrophic organisms, may be capable of nitrite and nitrate reduction (Ward et al. 2009). Similar to anammox bacteria, they may also produce EPSs to support heterotrophic nitrogen removal processes (Kielak et al. 2016). Bacteroidetes, while commonly known for their specialization in degrading high molecular weight compounds, may be capable of the construction of web-like structures that contribute to anammox granule formation (Fernandez-Gomez et al. 2013; Cao et al. 2016). Chlorobi, including the green sulfur bacteria that are capable of oxidizing sulfide to elemental sulfur, may reduce the inhibitory effects of sulfide on anammox bacteria (Dapena-Mora et al. 2007; Hiras et al. 2016). Chloroflexi may help to degrade microbial products derived from biomass decay (Miura et al. 2007; Kindaichi et al. 2012). Proteobacteria, the largest and most diverse phylum in the domain bacteria, contains many microorganisms that are capable of heterotrophic dentrification and DNRA, including Burkholderiales, Pseudomonadales, Rhodocyclales, Rhodospirillales, Rhizobiales, and all of the genera previously listed in Chapter 1.2.2 and 1.2.4 (Pereira et al. 2017). Additional phyla of bacteria, while not consistently present in anammox reactors, may also play crucial roles in maintaining the stable and robust performance of anammox reactors.

While there is a substantial body of literature describing the performance of anammox reactors in response to various perturbations and operational conditions, very few studies have examined the performance of anammox reactors in relation to its core microbial community. The work presented in this chapter seeks to fill this gap by investigating the temporal dynamics of the anammox bacterial community during the start-up and continued operation of a laboratory-scale anammox reactor. Ultimately, the results of this investigation support the fundamental, community-level understanding of the anammox process. This, in turn, should enable the more comprehensive control of the promising anammox technology and help facilitate its widespread adoption at municipal wastewater treatment plants across the globe.

2.2 Materials and methods

2.2.1 Reactor setup and operation

A laboratory-scale, anaerobic membrane bioreactor (MBR) with a working volume of 1L was constructed to enrich the anammox microbial community (Figure 2.1). A polyvinylidene fluoride hollow fiber membrane module with a 0.4 μm pore size and total surface area of 260 cm^2 (Litree Company, China) was mounted in the MBR. An impeller was also mounted in the MBR to provide mixing at a rate of 200 rpm. An electric heating blanket (Eppendorf, Hauppauge, NY) was fitted around the MBR to maintain temperature at 37° C. Mixed gas ($Ar:CO_2$ = 95:5) was supplied continuously to the MBR at a rate of 50 mL min^{-1} to eliminate dissolved oxygen and maintain pH at 7.2. On day 0, the MBR was inoculated with approximately 2 g VSS L^{-1} of biomass collected from a pilot-scale deammonification reactor treating sidestream effluent at San Francisco Public Utilities Commission (SFPUC) in San Francisco, California. The MBR was re-inoculated with similar concentrations of biomass from the same source on days 147 and 203.

The MBR was operated in a continuous flow mode. For the first 145 days, the hydraulic retention time (HRT) was maintained at 48 hours; afterwards it was reduced to 12 hours. No solids were removed from the MBR for the first 100 days of operation; afterwards, the solids retention time (SRT) was reduced to 50 days.

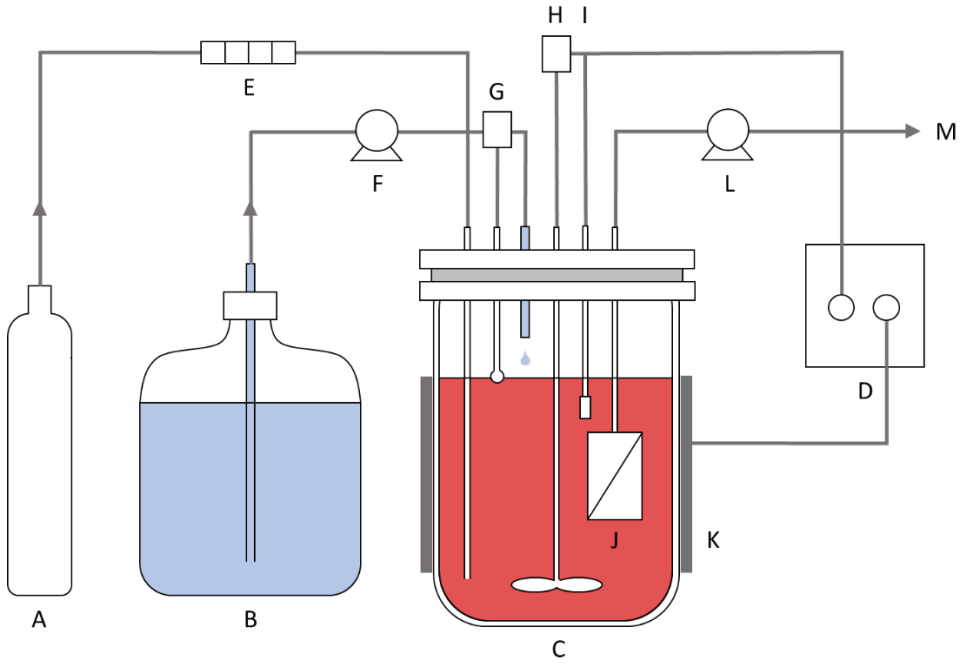

Figure 2.1: Configuration of the laboratory-scale anaerobic membrane bioreactor (MBR). Each letter refers to a different component of the MBR: A – influent gas tank, Ar:CO2 (95:5), B – influent media tank, C – 1L reactor vessel, D – power source and controller, E – flowmeter, F – influent peristaltic pump, G – level controller, H – impeller, I –temperature probe, J – membrane module, K – heating jacket, L – effluent peristaltic pump, and M – effluent media line. This figure is not drawn to scale.

Synthetic medium containing ammonium, nitrite, bicarbonate, and trace nutrients (meant to mimic sidestream effluent at a municipal wastewater treatment plant) was fed to the MBR (Table 2.1). For the first 154 days of operation, the MBR was kept under nitrite-limiting conditions to prevent inhibitory conditions. Influent ammonium and nitrite concentrations ranged from 200-300 mg N L^{-1} and 100-300 mg N L^{-1}, respectively. On day 154, influent ammonium and nitrite concentrations were adjusted to the anammox stoichiometric ratio, 1:1.32 (Kartal et al. 2013). For the remainder of the experiment (aside from days 300 – 365), influent ammonium and nitrite concentrations were maintained at this ratio and ranged from 200-500 mg N L^{-1} and 265-660 mg N L^{-1}, respectively. On day 353, influent concentrations of copper, iron, molybdenum, and zinc were increased based on literature suggestions (van de Graaf et al. 1996; Chen et al. 2014; Liu et al. 2015).

Constituent	Concentration	Unit
$(NH_4)_2SO_4$	40-500	mg-N/L
$NaNO_2$	5-660	mg-N/L
NaCl	1000	mg/L
$MgCl_2 \cdot 6H_2O$	500	mg/L
KH_2PO_4	200	mg/L
KCl	300	mg/L
$CaCl_2 \cdot 2H_2O$	180	mg/L
$KHCO_3$	420	mg/L
*$FeCl_2 \cdot 4H_2O$	7.7; 17.9	mg/L
$CoCl_2 \cdot 6H_2O$	0.24	mg/L
$MnCl_2 \cdot 4H_2O$	0.99	mg/L
*$ZnCl_2$	0.07; 0.20	mg/L
H_3BO_3	0.014	mg/L
*$Na_2MoO_4 \cdot 2H_2O$	0.10; 0.22	mg/L
$NiCl_2 \cdot 6H_2O$	0.19	mg/L
*$CuCl_2 \cdot 2H_2O$	0.002; 0.17	mg/L
$Na_2SeO_3 \cdot 5H_2O$	0.16	mg/L
pH	6.8-7.0	-

Table 2.1: Synthetic medium composition. The concentrations of the four asterisked constituents were increased from their low to high values on day 353.

2.2.2 Chemical analyses

Influent and effluent concentrations of ammonium, nitrite, and nitrate were measured approximately every other day using HACH test kits (HACH, Loveland, CO), as described in the manufacturer's methods 10031, 10019, and 10020, respectively.

2.2.3 Biomass collection and DNA extraction

Biomass samples were extracted via syringe from the MBR every 2-10 days, flash frozen in liquid nitrogen, and stored frozen at -80° C until use. Genomic DNA was extracted from the samples

using the DNeasy PowerSoil Kit (Qiagen, Carlsbad, CA), as described in the manufacturer's protocol. The concentration and purity of extracted DNA was measured with a NanoDrop Spectrophotometer (Thermo Fisher Scientific, Waltham, MA). The concentration of genomic DNA in all samples was normalized to 10 ng μL^{-1} with nuclease-free water (Thermo Fisher Scientific, Waltham, MA). All genomic DNA samples were stored at -80° C until use.

2.2.4 16S rRNA gene sequencing and analysis

Genomic DNA samples were sent to the Institute for Environmental Genomics at the University of Oklahoma (Norman, OK) for amplification of the variable 4 (V4) region of the 16S rRNA gene, library preparation, and amplicon sequencing. The full protocol was previously described in Wu et al. 2015. In summary, the V4 region of the bacterial 16S rRNA gene was amplified from DNA samples using primers 515F (5'-GTGCCAGCMGCCGCGGTAA-3') and 806R (3'-TAATCTWTGGGVHCATCAGG-5'), with barcodes attached to the reverse primer. Amplicons were pooled at equal molality and purified with the QIAquick Gel Extraction Kit (QIAGEN Sciences, Germantown, MD). Paired-end sequencing was then performed on the barcoded, purified amplicons with the Illumina MiSeq sequencer (Illumina, San Diego, CA).

Subsequent sequence processing and data analysis were performed in-house using mothur v.1.39.5, following the MiSeq standard operating procedure (SOP) (Schloss et al. 2009, Kozish et al. 2013). In summary, sequences were demultiplexed, merged, trimmed, and quality filtered. Unique sequences were aligned against the SILVA v.132 16S rRNA gene reference alignment database (Pruesse et al. 2007). Sequences that did not align to the position of the forward primer were discarded. Chimeras were detected and removed. Remaining sequences were clustered into operational taxonomic units (OTUs) within a 97% similarity threshold using the Phylip-formatted distance matrix. Representative sequences from each OTU were assigned taxonomic identities from the SILVA v.132 16S rRNA gene reference alignment database (Pruesse 2007). Sequences that were not classified as bacteria were removed. Remaining OTUs were counted, and the 150 most abundant OTUs (accounting for up to 99% of sequence reads within individual samples) were transferred to Microsoft Excel (Microsoft Office Professional Plus 2016) for downstream interpretation and visualization of their relative abundances. Phylogenetic distances were generated for the 150 most abundant OTUs using Clearcut (Evans et al. 2006).

2.2.5 Statistical analyses

Statistical analyses were performed in Microsoft Excel (Microsoft Office Professional Plus 2016) and RStudio v1.1.383 (RStudio Team 2015) using the ggplot2 and vegan packages. A significance level of $\alpha = 0.05$ was used for all analyses, unless noted otherwise. Details of statistical methods used for additional analyses are given below.

2.2.5.1 Microbial diversity

The Shannon index (*H'*) was chosen to quantify microbial diversity within each biological sample. *H'* was calculated as follows:

$$H' = -\sum_{i=1}^{N} p_i \ln p_i$$

Where $\{p_1, p_2, \ldots, p_N\}$ are the relative abundances of the OTUs within the biological sample of interest and N is the number of observations in the sample (Hill et al. 2006).

2.2.5.2 Nonmetric multidimensional scaling (NMDS)

NMDS was used to collapse information across all of the biological samples onto a two-dimensional plot for visualization and interpretation (Oksanen 2018). In summary, the original positions of each biological sample were defined in multidimensional space based on the rank-order of the relative abundances of OTUs at each timepoint (for simplification, OTUs that were assigned identical taxonomies were merged). An initial, random configuration of the OTUs and timepoints was constructed in two-dimensions. Distances in this initial configuration were regressed against the observed (i.e., measured) distances. The stress (i.e., disagreement) between the initial configuration and predicted values from the regression were determined. Configurations were iterated until the stress value became less than 0.1.

2.3 Results and discussion

2.3.1 Reactor performance

The performance of the MBR was tracked for 440 days from initial seeding, through several performance crashes, to stable and robust anammox activity (Figure 2.2a). Differences in influent and effluent concentrations of reactive nitrogen species were tabulated into nitrogen speciation ratios and the nitrogen removal rate (NRR)—g-N removed, per liter, per day (Figure 2.2b).

In summary, the MBR's performance steadily improved over the first 103 days of operation. At this time, the effluent concentration of nitrite unexpectedly began to rise, so influent concentrations of ammonium and nitrite were decreased to prevent process failure from nitrite toxicity (Lotti 2012). Process failure was successfully avoided, and the MBR's performance was quickly restored. On days 145 – 147, measures were taken to further enhance the MBR's performance. On day 145, the HRT was reduced from 48 hours to 12 hours, and influent ammonium and nitrite concentrations were decreased (to maintain a stable loading rate). On day 147, the MBR was amended with a concentrated stock of biomass from a nearby pilot-scale deammonification process. As expected, the MBR's performance continued to improve. Afterwards, influent ammonium and nitrite concentrations were steadily increased until the NRR approached 2 g-N L^{-1} d^{-1} on day 180. Unfortunately, on day 189, the MBR experienced a technical malfunction and subsequent performance crash, identified by a rapid decrease in the NRR. On day 203, the MBR was again amended with a concentrated stock of biomass from a nearby pilot-scale deammonification process

and the NRR quickly recovered. Influent ammonium and nitrite concentrations were again increased until the NRR approached 2 g-N L^{-1} d^{-1}.

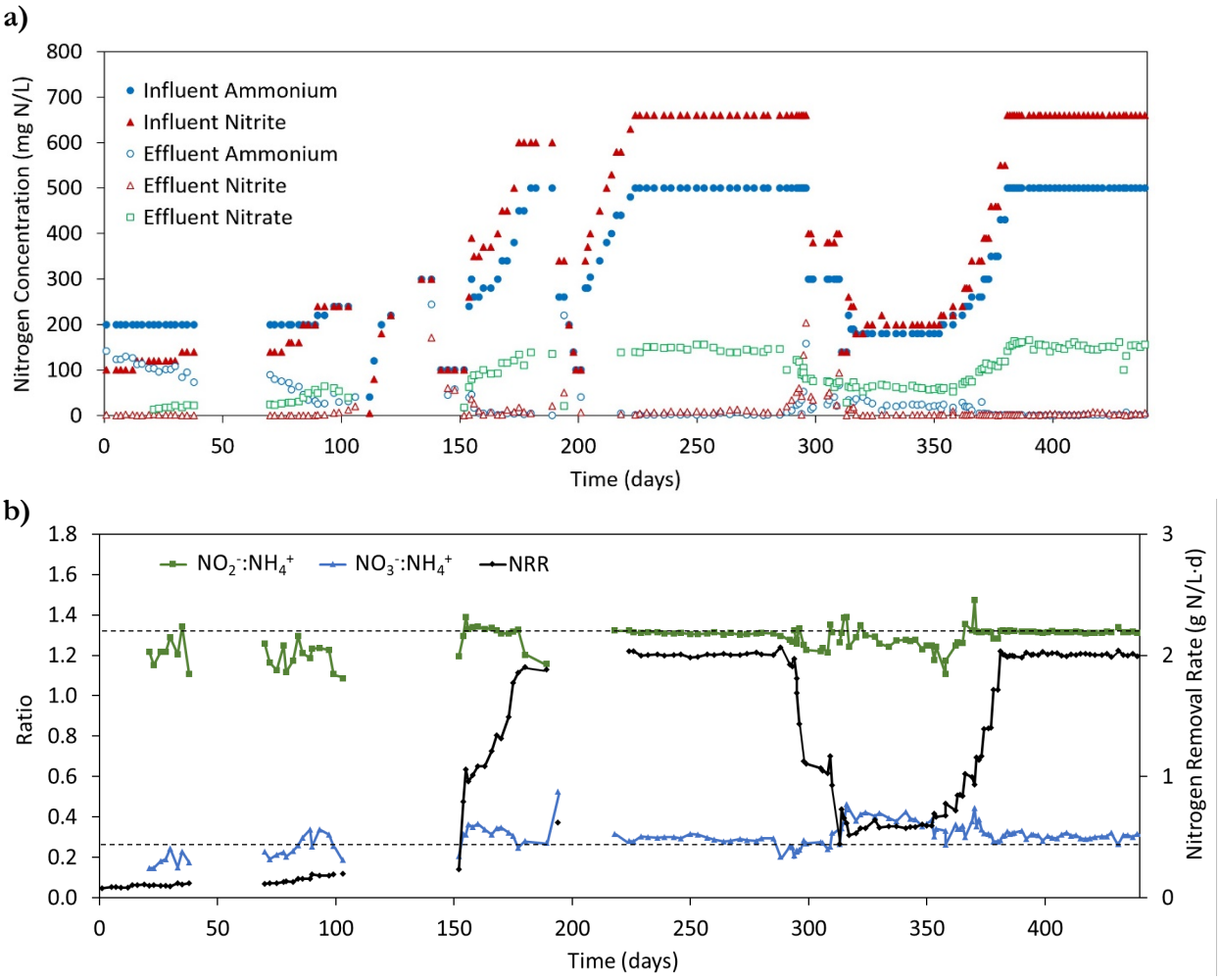

Figure 2.2: MBR performance. The upper panel (a) reports the influent and effluent concentrations of reactive nitrogen species in the MBR over time (influent nitrate concentrations were negligible, so they were not plotted). The lower panel (b) reports the nitrogen speciation ratios (primary y-axis) and NRR (secondary y-axis) in the MBR over time. The dashed lines represent the stoichiometric nitrogen speciation ratios for anammox (Equation 1.6).

The MBR maintained steady performance for approximately 75 days, until day 288, when effluent concentrations of ammonium and nitrite unexpectedly began to increase and nitrate concentrations disproportionately decreased. Seven days later (on day 295), the NRR rapidly plummeted. No technical malfunctions occurred, indicating that a destabilized microbial community may have been responsible for the performance crash. At the time, the cause of the performance decline was not understood, so the MBR was not re-seeded with biomass. For 57 days (from day 297 – day 353), influent concentrations of ammonium and nitrite (and hence, NRR) were intentionally held at lower values to allow the community to stabilize. During this time, less nitrite was consumed per unit of ammonium consumed, and more nitrate was produced per unit of ammonium consumed.

After the 50-day period of lowered performance, concentrations of copper, iron, molybdenum, and zinc were increased in the synthetic wastewater medium based on literature suggestions, and influent concentrations of ammonium and nitrite were ramped up (van de Graaf et al. 1996; Chen et al. 2014; Liu et al. 2015).

Again, the NRR quickly approached 2 g-N L^{-1} d^{-1}. The ratios of nitrite consumption and nitrate production relative to ammonium consumption returned to stoichiometric values for anammox (Equation 1.6). Stable and robust MBR performance was maintained for 50 days, at which point the MBR was transitioned to another experiment, reported in Chapter 3.

2.3.2 Bacterial community structure

The V4 region of 16S rRNA genes was sequenced at 56 distinct timepoints over the lifespan of the MBR study. These timepoints captured the initial enrichment of the anammox bacterial community in the MBR, through two biomass amendments, a technical malfunction, an unexplained destabilization of anammox activity, and finally to stable and robust anammox activity.

A phylogenetic tree was constructed using iTOL (Letunic and Bork 2016) to visualize the overall diversity of the 150 most abundant OTUs in the MBR's bacterial community (Figure 2.3; Appendix 1). Consistent with previous reports of bacterial community structure in anammox reactors, members of the phyla Acidobacteria, Bacteroidetes, Chlorobi (i.e., Ignavibacteria), Chloroflexi, and Proteobacteria accounted for the majority of the recovered OTUs in the MBR (Gonzalez-Martinez et al. 2015b). These phyla accounted for 10, 10, 7, 35, and 44 of the recovered OTUs, respectively. Members of the genus *Brocadia* were identified as the anammox bacteria within the MBR. Six OTUs are associated with this genus.

The remainder of the OTUs were classified into the phyla Actinobacteria, Armatimonadetes, Cyanobacteria, Dadabacteria, Deinococcus-Thermus, Gemmatimonadetes, Nitrospirae, Patescibacteria, Planctomycetes, Spirochaetes, and Verrucomicrobia. Due to the current disagreement on the classification of Ignavibacteria as a class of Bacteroidetes, as a class of Chlorobi, or as its own phylum, it has been depicted here as its own phylum (Parks et al. 2018).

Oligoflexales, a member of the phylum Proteobacteria, appears to be misplaced on the phylogenetic tree. This OTU's relative abundance over the lifespan of the MBR is negligible, so its misplacement is expected to have negligible impacts on downstream analyses.

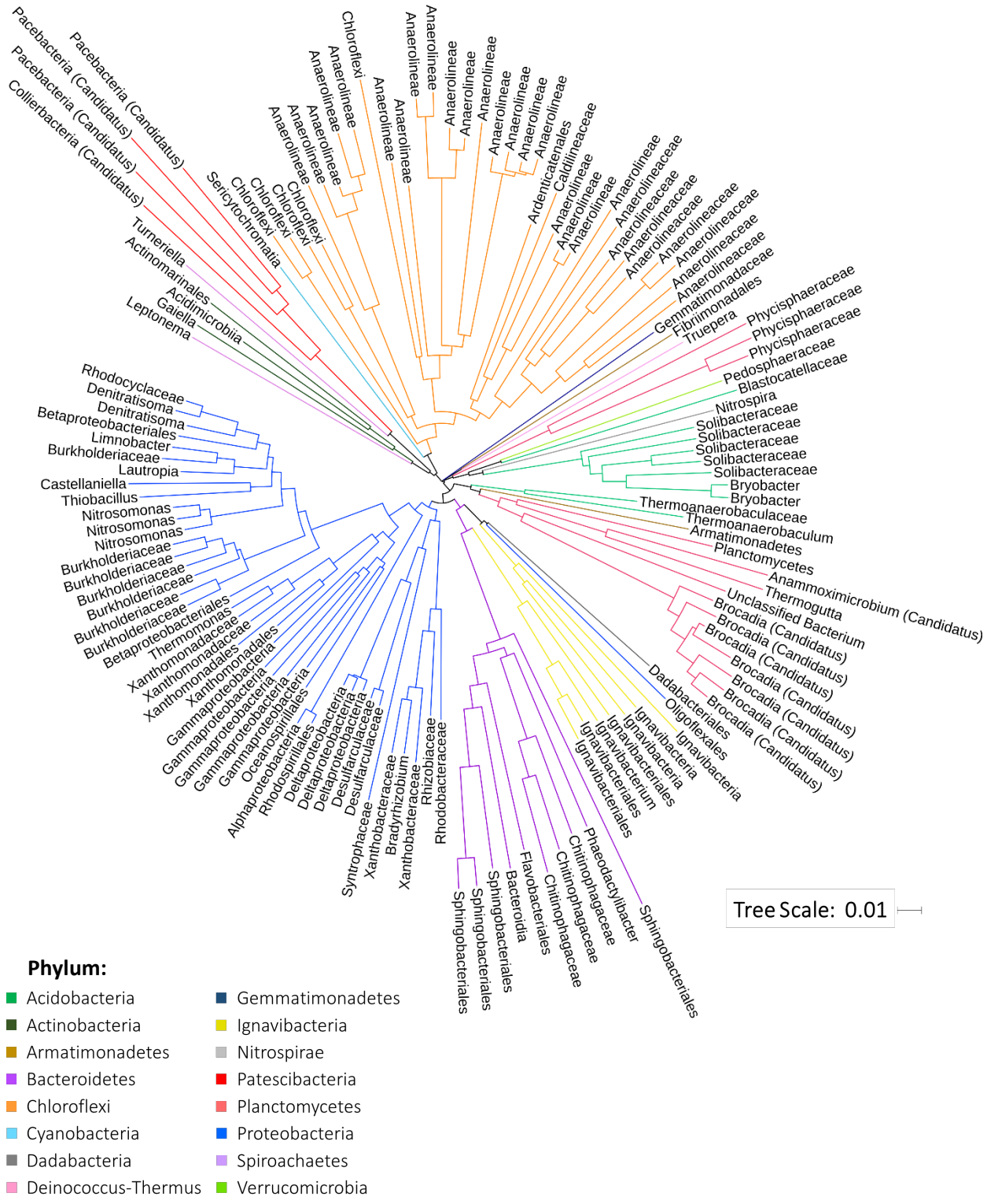

Figure 2.3: Phylogenetic tree of all recovered operational taxonomic units (OTUs) in the MBR.

2.3.2.1 Temporal community dynamics

The relative abundances of OTUs were averaged over three-day increments, resulting in 33 distinct relative abundance profiles over the lifespan of the MBR study (Figure 2.4; Appendix 1). The genus *Brocadia* accounted for a small fraction of bacteria in the MBR's bacterial community at startup. Instead, members of the phyla Acidobacteria, Ignavibacteria, and Proteobacteria dominated the bacterial community. During the first 100 days of the MBR's operation, *Brocadia* increased in relative abundance at the expense of the three aforementioned phyla. Following the MBR's malperformance and subsequent biomass amendment on day 147, the MBR became dominated by a single OTU—a member of the phylum Bacteroidetes and the order Sphingobacteriales—from the biomass amendment. It appears that the MBR was not a favorable environment for this OTU, as its relative abundance steadily declined over the next 100 days.

From day 150 – day 290, *Brocadia* again increased in relative abundance, this time at the expense of the Spingobacteriales OTU and the phylum Proteobacteria. *Brocadia* remained dominant until day 290, when the relative abundances of the order Ignavibacteriales within the phylum Ignavibacteria and the class Anaerolineae within the phylum Chloroflexi dramatically increased at the expense of *Brocadia*. Shortly after this shift, the MBR experienced its unexplained destabilization of anammox activity and subsequent performance crash. Over the next 50 days of lowered MBR performance, the relative abundances of Ignavibacteriales, Anaerolineae, and *Brocadia* remained fairly constant.

After the synthetic medium's trace metals concentrations were increased and the influent concentrations of ammonium and nitrite were ramped up on day 353, the relative abundance of *Brocadia* increased while the relative abundances of Ignavibacteriales and Anaerolineae decreased. For the next 50 days of the MBR's operation, the relative abundances of Brocadia, Ignavibacteriales, and Anaerolineae (as well as the balance of the MBR's OTUs) remained fairly constant.

The aforementioned changes in the relative abundance profiles of bacterial taxa over the lifespan of the MBR, primarily the changes that occurred leading up to, during, and after the destabilization of the MBR's performance (days 290 – 440) merit further attention. In particular, the decline of the relative abundance of *Brocadia* around the same time that effluent concentrations of ammonium and nitrite unexpectedly began to increase and nitrate disproportionately began to decrease (and at least five days before the MBR's NRR rapidly declined) indicate that an instability in bacterial community dynamics may have instigated the unexplained destabilization of anammox activity within the MBR. More specifically, the deviations in the ratios of nitrite consumption and nitrate production relative to ammonium consumption over the exact same timespan indicate that the instability in bacterial community dynamics may be related to an imbalance among the MBR's nitrogen removal processes (i.e., anammox, denitrification, and DNRA).

The following sections describe the statistical analyses that were performed to further investigate the bacterial community's temporal dynamics surrounding the aforementioned events, and to potentially identify a cause for the unexplained destabilization of anammox activity.

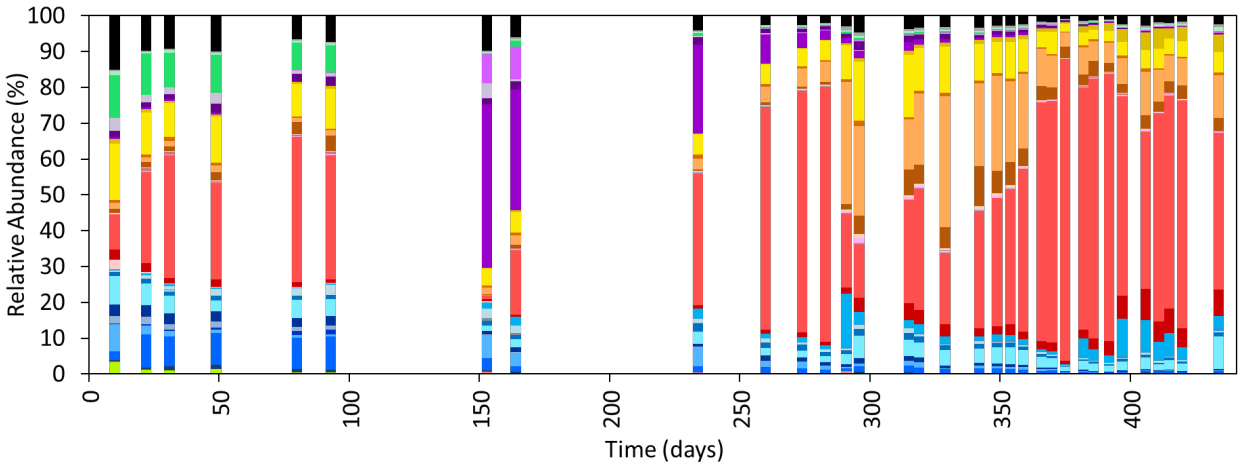

Classification	Phylum
Unclassified	N/A
Others	
Solibacteraceae	Acidobacteria
Blastocatellaceae	
Thermoanaerobaculum	
Bacteroidetes	Bacteroidetes
Bacteroidia	
Chitinophagaceae	
Phaeodactylibacter	
Sphingobacteriales	
Ignavibacteria	Ignavibacteria
Ignavibacteriales	
Chloroflexi	Chloroflexi
Anaerolineae	
Anaerolineaceae	
Ardenticatenales	
Sericytochromatia	
Truepera	Deinococcus-Thermus
Nitrospira	Nitrospirae
Brocadia	Planctomycetes
Phycisphaeraceae	
Anammoximicrobium	
Proteobacteria	Proteobacteria
Rhizobiaceae	
Xanthobacteraceae	
Deltaproteobacteria	
Syntrophaceae	
Gammaproteobacteria	
Betaproteobacteriales	
Burkholderiaceae	
Lautropia	
Thiobacillus	
Nitrosomonas	
Rhodocyclaceae	
Xanthomonadales	
Leptospiraceae	Spirochaetes
Pedosphaeraceae	Verrucomicrobia

Figure 2.4: Relative abundance profiles of bacterial taxa over the lifespan of the MBR. "Others" include taxa that were identified, but their relative abundance profiles never reached 0.5% for any of the sequencing timepoints.

2.3.2.1.1 Microbial diversity

The microbial diversity of each sampling timepoint was quantified using the Shannon diversity index (*H'*) and plotted over the lifespan of the MBR study (Figure 2.5). Over the first 230 days of the MBR's lifespan, *H'* steadily declined from 3.06 to 2.39. Around this time, *Brocadia* began to dominate the MBR's bacterial community, so *H'* declined even further to 1.56 on day 288. When the MBR's performance began to destabilize on day 288, the relative abundance of *Brocadia* rapidly declined, so *H'* was restored to 3.01 (a value similar to that observed at the beginning of the MBR's lifespan).

At first glance, it appears that a decrease in the overall diversity of the bacterial community (due to the dominance of the community by a single bacterium—*Brocadia*) may have caused the destabilization of anammox activity. However, results from the second half of the MBR's lifespan tell a different story. Over the next 57 days (from day 297 – day 353), while the MBR's performance was limited, *H'* remained high. As soon as the MBR's NRR started to improve on day 353, *H'* plummeted to values even lower than those observed during the performance destabilization on day 288 (*H'* bottomed out on day 374, with a value of 0.94.). While the first instance of declining microbial diversity indicated a performance destabilization, the second instance indicated the direct opposite—a performance stabilization.

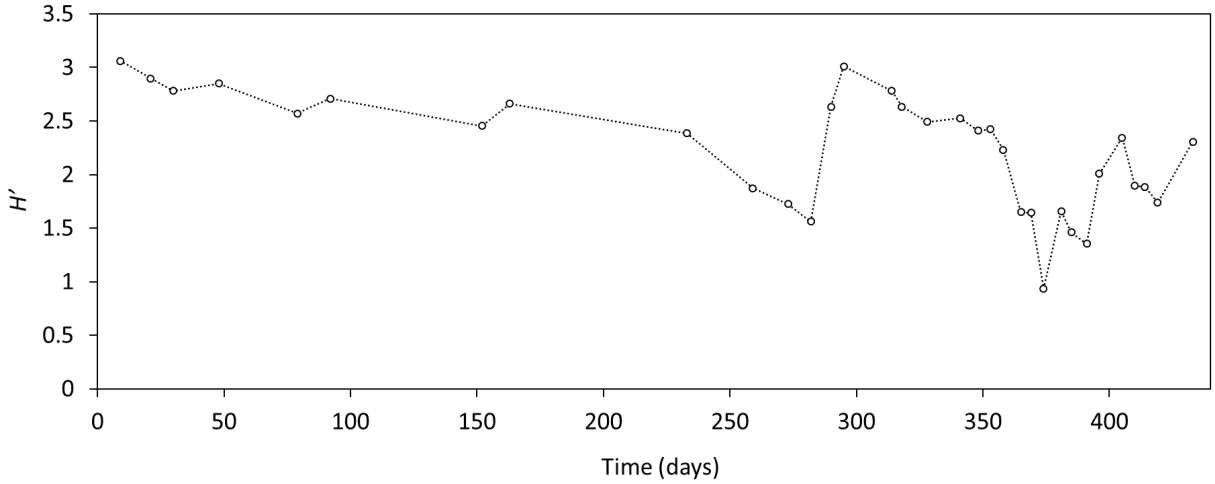

Figure 2.5: Microbial diversity indices over the lifespan of the MBR.

Ultimately, there seems to be no statistically-significant correlation between microbial diversity and anammox activity (measured via NRR) (Appendix 2). While the over-dominance of the *Brocadia* sp. may have been an important factor in the destabilization of the MBR's performance on day 295, its impact cannot be captured by *H'* alone.

2.3.2.1.2 Community grouping

To further examine the correlations between bacterial community structure and anammox activity, nonmetric multidimensional scaling (NMDS) analyses were applied to the relative abundance profiles over the lifespan of the MBR study (Figure 2.6a; Appendix 2). The resulting NMDS projection shows that certain bacterial taxa are associated with specific time periods over the lifespan of the bioreactor. "Startup" taxa are clustered with the MBR's initial sampling timepoints (days 9 – 92). "Pre-Crash" taxa are clustered with the MBR's sampling timepoints leading up to the performance destabilization on day 295 (days 233 – 290). "Mid-Crash" taxa are clustered with the MBR's sampling timepoints during the period of reduced performance (days 295 – 365). "Stable State" taxa are clustered with the MBR's final sampling timepoints that are associated with stable, robust anammox activity (days 381 – 433). The *Brocadia* sp. can be found directly between the "Mid-Crash" and "Stable State" clusters. While the names of the taxa associated with each of the clusters are not plotted in Figure 2.6, they can be found in Table 2.2.

The relative abundances of the taxa associated with each of the aforementioned NMDS clusters were summed and plotted over the lifespan of the MBR study (Figure 2.6b). The "Startup" cluster, containing bacterial species from the phyla Acidobacteria, Bacteroidetes, and Verrucomicrobia, accounted for 20% of the bacterial community at day 9. It appears that the MBR was not a favorable environment for the bacteria in this cluster, as the "Startup" cluster's relative abundance steadily declined over the next 200 days. The "Pre-Crash" cluster, containing uncultivated bacterial species from the phyla Bacteroidetes and Nitrospira, accounted for 10% of the bacterial community at day 150. The bacterial species in this cluster were most likely introduced to the MBR on day 147, when it was amended with a concentrated stock of biomass from a nearby pilot-scale deammonification process. It appears that the MBR was not a favorable environment for the bacteria in this cluster either, as the "Pre-Crash" cluster's relative abundance became negligible after two sampling timepoints. In summary, the relative abundances of the bacterial taxa associated with both the "Startup" and "Pre-Crash" clusters became negligible well before the MBR's performance destabilization on day 295. The loss of the bacterial taxa associated with these clusters may have disrupted the overall balance of the MBR's bacterial community and subsequently caused the MBR's performance destabilization. If this is the case (and the bacterial taxa associated with these clusters were performing some function(s) critical to the health of the MBR), their critical function(s) were replaced by other taxa later on.

Of all four of the NMDS clusters, the "Mid-Crash" cluster contains the largest number of bacterial taxa, including species from the phyla Acidobacteria, Chloroflexi, Deinococcus-Thermus, Ignavibacteria, Proteobacteria, and Spirochaetes. While the relative abundance of the "Mid-Crash" cluster is highest right at the MBR's performance destabilization on day 295 (accounting for 30% of the bacterial community on day 295), the cluster's relative abundance is also high during the first 100 days of the MBR's operation (indicating that the bacterial taxa within this cluster may have played important role(s) in the pilot-scale deammonification process prior to their inoculation into the MBR used in this study). Interestingly, the "Mid-Crash" cluster's relative abundance accounts for at least 5% of the MBR's bacterial community over the entire lifespan of the MBR, including the MBR's final days of robust, stable anammox activity (from day 380 onwards). The bacterial taxa associated with this cluster may have caused (and taken advantage of) the destabilized anammox performance, but they are also present during the MBR's final days of robust, stable anammox activity (from day 380 onwards).

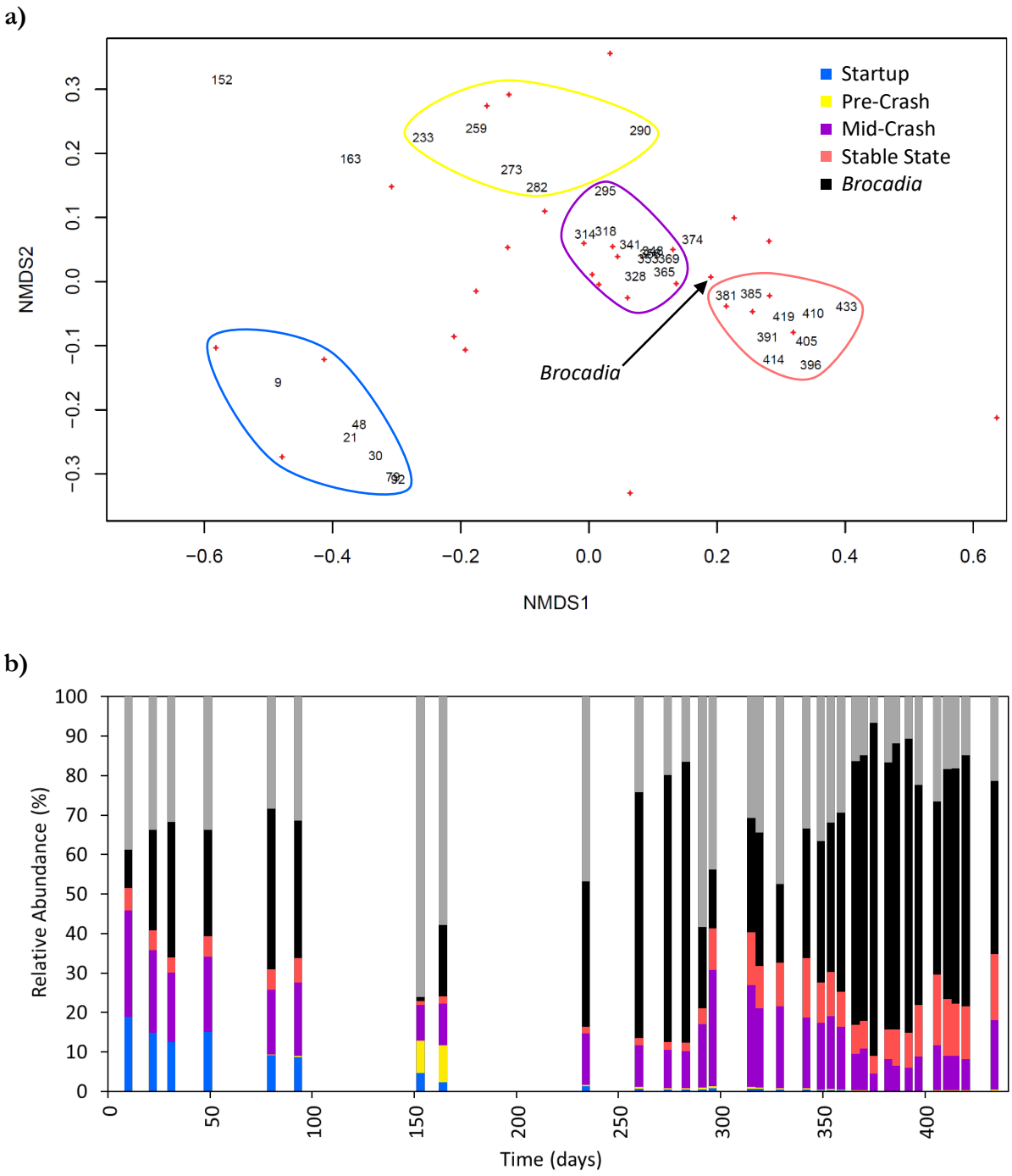

Figure 2.6: Nonmetric multidimensional scaling (NMDS) projection of bacterial taxa and sampling timepoints. In the upper panel (a), bacterial taxa are represented by red crosses and sampling timepoints are represented by their values. Groups of bacterial taxa and sampling timepoints that clustered together are circled and assigned into groups in the legend. In the lower panel (b), the relative abundances of bacterial taxa that were classified into the NMDS groups assigned in panel (a) are plotted over the lifespan of the MBR.

The "Stable State" cluster, containing bacterial species from the phyla Chloroflexi, Ignavibacteria, Plantomycetes, and Proteobacteria, accounted for 10-15% of the bacterial community between days 381 – 433. Similar to the "Mid-Crash" cluster, the "Stable State" cluster is represented over the entire lifespan of the MBR. Interestingly, the relative abundance of the "Stable State" cluster first began to rise on day 290, when the MBR's performance began to destabilize. The bacterial taxa associated with the "Stable State" cluster may have taken advantage of the destabilized anammox performance, but they are also present the MBR's final days of robust, stable anammox activity (from day 380 onwards).

Startup	Pre-Crash	Mid-Crash	Stable State
Bacteroidia	Bacteroidetes	Ardenticatenales	Anaerolineaceae
Blastocatellaceae	Nitrospira	Betaproteobacteriales	Ignavibacteria
Pedosphaeraceae		Chloroflexi	Phycisphaeraceae
		Gammaproteobacteria	Xanthobacteraceae
		Ignavibacteriae	
		Leptonema	
		Solibacteraceae	
		Truepera	

Table 2.2: Bacterial taxa associated with each nonmetric multidimensional scaling (NMDS) cluster.

2.3.3 Conclusions

The temporal dynamics of the anammox bacterial community were investigated from the start-up of a laboratory-scale anammox MBR, through several performance crashes, to stable and robust anammox activity. As anammox bacteria became enriched in the MBR's bacterial community, the relative abundances of other taxa declined, and the community's microbial diversity decreased. An instability in the simplified bacterial community may have caused the relative abundances of Ignavibacteriales (within the phylum Ignavibacteria) and Anaerolineae (within the phylum Chloroflexi) to dramatically increase at the expense of anammox bacteria. Almost immediately thereafter, nitrogen removal deviated from anammox stoichiometry and the NRR rapidly declined. Later into the experimental timeline, however, the simplified bacterial community achieved a robust NRR. While the over-dominance of anammox bacteria may have caused the destabilization of the MBR's performance, it did not prevent robust performance further into the experimental timeline.

Interestingly, the relative abundances of bacterial taxa not only associated with the MBR's limited performance (days 295 – 365), but also with the stable state performance (days 381 – 433), increase on day 295. Under desirable conditions, anammox, denitrifying, and DNRA bacteria may cooperate to maximize nitrogen removal. Under undesirable conditions, however, anammox bacteria may compete with denitrifying and DNRA bacteria for nitrite—their shared electron acceptor. Because anammox bacteria grow more slowly than their heterotrophic companions, anammox bacteria may lose this competition, leading to their out-competition and subsequent inhibition within the reactor (Molinuevo et al. 2009). The MBR's deviation from anammox stoichiometry indicate that "undesirable conditions" may have caused the destabilization of the anammox reactor on day 295.

During the MBR's limited performance, bacterial taxa may be competing with anammox via heterotrophic nitrogen removal processes. Then, during the MBR's stable state performance, these same taxa may be cooperating with anammox via heterotrophic nitrogen removal processes (Unfortunately, several operational parameters were changed within the MBR on day 353, so a clear story cannot be elucidated from the transition from the limited performance to stable state performance periods.).

According to NMDS analyses, neither Ignavibacteriales nor Anaerolineae were associated with the MBR's periods of limited performance or stable state performance. However, other members of these two phyla (Ignavibacteria and Chloroflexi) span the MBR's limited and stable state performance periods. The two remaining phyla within the core anammox microbial community—Acidobacteria and Proteobacteria—are also present in the MBR's stable state period, but none of the analyses presented here help to elucidate their role(s) in the MBR.

In conclusion, the bacterial taxa associated with both limited and stable performance are present over the entire lifespan of the MBR. It appears that these bacterial taxa can either help and hinder the performance of the MBR through their participation in nitrogen cycling. More research must be done to understand that conditions that support each of these conditions. This idea will be further investigated in Chapter 3.

Chapter 3:

The Impact of Nitrogen Speciation on the Performance and Bacterial Community Structure of an Anammox Reactor

3.1 Introduction

Anammox bacteria obtain energy for growth from the conversion of ammonium and nitrite into nitrogen gas. This conversion proceeds via three coupled redox reactions with two intermediates: nitric oxide and hydrazine (Kartal et al. 2004). First, nitrite is reduced to nitric oxide by the nitrite reductase enzyme, NirS (Equation 3.1). Second, nitric oxide and ammonium are synthesized into hydrazine by the hydrazine synthase enzyme, HZS (Equation 3.2). (Interestingly, HZS is unique to anammox bacteria; there are no known homologs in other organisms (Kallistova et al. 2015).) Third, the four-electron oxidation of hydrazine is carried out by the hydrazine dehydrogenase enzyme, HDH (Equation 3.3) (Kartal et al. 2004).

(3.1) $NO_2^- + 2H^+ + e^- \rightarrow NO + H_2O$

(3.2) $NO + NH_4^+ + 2H^+ + 3e^- \rightarrow N_2H_4 + H_2O$

(3.3) $N_2H_4 \rightarrow N_2 + 4H^+ + 4e^-$

When combined, these three redox reactions model anammox catabolism (Equation 3.4).

(3.4) $NH_4^+ + NO_2^- \rightarrow N_2 + 2H_2O$

Anammox bacteria typically (although, not necessarily) utilize bicarbonate as their primary carbon source for the synthesis of cell biomass (Kallistova et al. 2015; Castro-Barros et al. 2017). The reduction of bicarbonate is coupled to the oxidation of nitrite to nitrate, meaning that the growth of anammox bacteria is always accompanied by the production of nitrate (Equation 3.5) (Strous et al. 1998; Lotti et al. 2014; Kallistova et al. 2015).

(3.5) $NO_2^- + 0.26HCO_3^- \rightarrow NO_3^- + 0.26CH_2O_{0.5}N_{0.15}$

The widely-accepted model of the overall anammox metabolism (based on the combination of catabolism and synthesis of cell biomass) is based on data collected in physiological experiments performed by Strous et al. 1998 (Equation 3.6).

(3.6) $NH_4^+ + 1.32NO_2^- + 0.066HCO_3^- + 0.13H^+ \rightarrow 1.02N_2 + 0.26NO_3^- + 2.03H_2O + 0.066CH_2O_{0.5}N_{0.15}$

Recently, the stoichiometric coefficients for the overall anammox metabolism were challenged by Lotti et al. 2014 (Equation 3.7). Lotti et al. proposed that less nitrite was consumed per mole of ammonium and that less nitrate was produced per mole of ammonium, with similar amounts of nitrogen gas and biomass yielded.

(3.7) $NH_4^+ + 1.146NO_2^- + 0.071HCO_3^- + 0.057H^+ \rightarrow 0.986N_2 + 0.161NO_3^- + 2.002H_2O + 0.0071CH_2O_{0.31}N_{0.20}$

Unlike Strous et al.'s experiments which were carried out in sequential batch reactors with a community that was 74% anammox bacteria, Lotti et al.'s experiments were carried out in an MBR with a community that was more-highly enriched for anammox bacteria. These alterations may have

lifted mass transfer limitations on growth and decreased the effects of other microorganisms on the estimation of growth parameters, resulting in more accurate stoichiometric coefficients for the overall anammox reaction (Lotti et al. 2014; Kallistova et al. 2015). Ultimately, however, the stoichiometric coefficients for the overall anammox metabolism in both of the aforementioned studies are based on experimental data with mixed microbial communities. The differences in results suggest that the actual anammox stoichiometry may yet to be elucidated.

While additional studies have continued to debate the stoichiometry of anammox bacteria's metabolism, few have investigated its translation into the greater stoichiometry of the overall anammox community's metabolism (Strous et al. 1998; Puyol et al. 2013; Lotti et al. 2014; Yao et al. 2015; Alejo-Alvarez et al. 2016; Zhu et al. 2017). As discussed in Chapter 2, nitrate—a product of anammox metabolism—can be reduced to nitrite by both denitrifying and DNRA bacteria, and can then be further reduced to nitrogen gas by anammox and denitrifying bacteria, or to ammonium by DNRA bacteria (Figure 3.1).

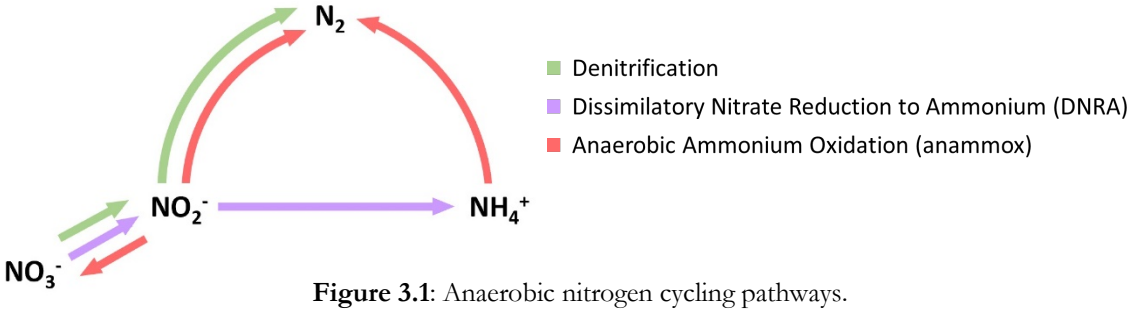

Figure 3.1: Anaerobic nitrogen cycling pathways.

Most studies simply assume that nitrate is removed through denitrification, if at all (Seitzinger 1988; Cornwell et al. 1999). In reality, nitrate has a much more complex fate under various reactor conditions (Figure 3.2) (Burgin and Hamilton 2007).

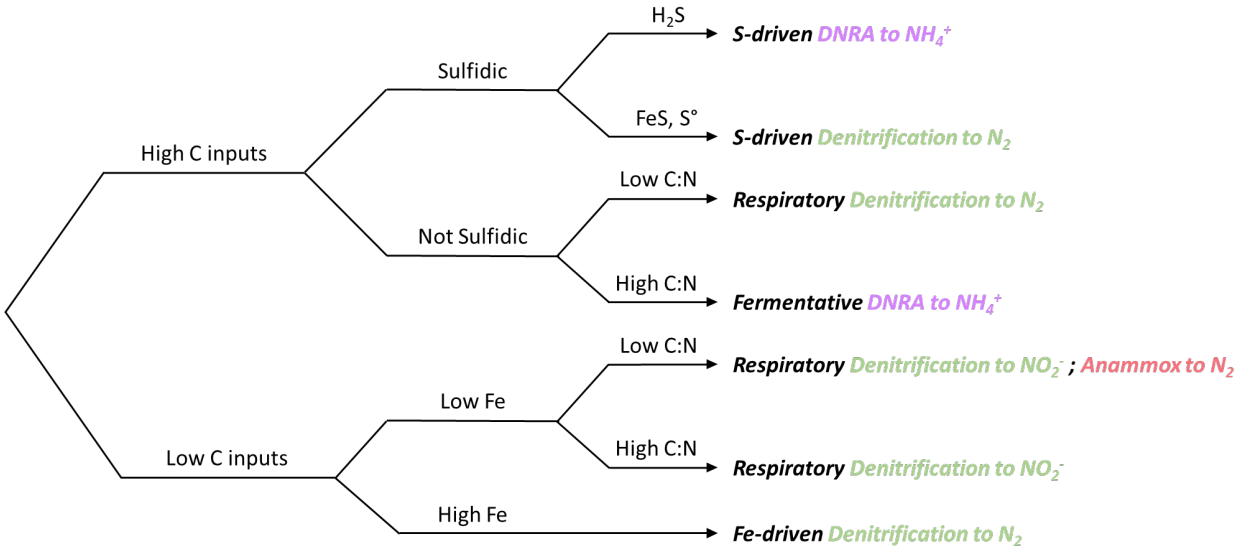

Figure 3.2: Dissimilatory pathways of nitrate removal (adapted from Burgin and Hamilton 2007).

Under the majority of reactor conditions reported in Figure 3.2, nitrate is indeed removed through denitrification (Burgin and Hamilton 2007). However, there are a few exceptions. When an anammox reactor's organic carbon inputs are low, ambient concentrations of iron are low, and ambient ratios of C:N are low, it is expected that nitrate will be reduced to nitrite by denitrifying bacteria, and then further reduced to nitrogen gas by anammox bacteria. This recycle of nitrite into an anammox reactor without a corresponding infusion of ammonium for the anammox process may lead to the accumulation of nitrite to levels that are inhibitory to the anammox process (Lotti et al. 2012). Additionally, when an anammox reactor's organic carbon inputs are high, it is expected that nitrate will be reduced to ammonium by DNRA bacteria, rather than reduced to nitrogen gas by denitrifying bacteria. This recycle of ammonium into an anammox reactor without a corresponding infusion of nitrite for the anammox process may lead to the accumulation of ammonium to levels that are toxic to microorganisms (EPA 2017). In all of the aforementioned scenarios, the fate of nitrate will impact not only the performance of the anammox reactor, but also the stoichiometry of the overall anammox community's metabolism.

The work presented in this chapter investigates the stoichiometry of anammox metabolism within the greater context of anaerobic nitrogen cycling by anammox, denitrifying, and DNRA bacteria. Through the manipulation of a stable-state anammox reactor, nitrogen flows through these three pathways are hypothesized. The hypotheses are bolstered with supporting data from 16S rRNA gene sequencing analyses. Ultimately, the results of this investigation support the fundamental, community-level understanding of the anammox process. This, in turn, should enable the more comprehensive control of the promising anammox technology and help facilitate its widespread adoption at municipal wastewater treatment plants across the globe.

3.2 Materials and methods

3.2.1 Reactor setup and operation

A laboratory-scale, anaerobic MBR with a working volume of 1L was maintained as reported in Chapter 2 (Figure 2.1). A polyvinylidene fluoride hollow fiber membrane module with a 0.4 μm pore size and total surface area of 260 cm^2 (Litree Company, China) was mounted in the MBR. An impeller was also mounted in the MBR to provide mixing at a rate of 200 rpm. An electric heating blanket (Eppendorf, Hauppauge, NY) was fitted around the MBR to maintain temperature at 37° C. Mixed gas ($Ar:CO_2$ = 95:5) was supplied continuously to the MBR at a rate of 50 mL min^{-1} to eliminate dissolved oxygen and maintain pH at 7.2. The MBR was operated in a continuous flow mode. The HRT was maintained at 12 hours; the SRT was maintained at 50 days.

Synthetic medium containing ammonium, nitrite, bicarbonate, and trace nutrients (meant to mimic sidestream effluent at a municipal wastewater treatment plant) was fed to the MBR (Table 3.1) (van de Graaf et al. 1996; Chen et al. 2014; Liu et al. 2015). In order to investigate the stoichiometry of anammox metabolism within the MBR, the influent ratio of ammonium:nitrite was varied between the ratios proposed by Strous et al. 1998 and Lotti et al. 2014. For the first 60 days of operation, influent concentrations of ammonium and nitrite were maintained at 500 mg N L^{-1} and 660 mg N L^{-1}, respectively. During this time, the influent ratio of ammonium:nitrite was 1:1.32, following the stoichiometry proposed by Strous et al. 1998. From day 61 – day 142, influent concentrations of ammonium were increased to 600 mg N L^{-1} while influent concentrations of nitrite remained the

same. During this time, the influent ratio of ammonium:nitrite was reduced to 1:1.1, a ratio slightly lower than that proposed by Lotti et al. 2014. Over the next 60 days, influent concentrations of nitrite were slowly increased from 660 mg N L^{-1} to 720 mg N L^{-1} to increase the influent ammonium:nitrite ratio from 1:1.1 to 1:1.2. After this adjustment period, influent concentrations of ammonium and nitrite were slowly increased to 640 mg N L^{-1} and 768 mg N L^{-1}, respectively (maintaining the ammonium:nitrite ratio at 1:1.2).

Constituent	Concentration	Unit
$(NH_4)_2SO_4$	500-640	mg-N/L
$NaNO_2$	660-768	mg-N/L
NaCl	1000	mg/L
$MgCl_2 \cdot 6H_2O$	500	mg/L
KH_2PO_4	200	mg/L
KCl	300	mg/L
$CaCl_2 \cdot 2H_2O$	180	mg/L
$KHCO_3$	420	mg/L
$FeCl_2 \cdot 4H_2O$	17.9	mg/L
$CoCl_2 \cdot 6H_2O$	0.24	mg/L
$MnCl_2 \cdot 4H_2O$	0.99	mg/L
$ZnCl_2$	0.20	mg/L
H_3BO_3	0.014	mg/L
$Na_2MoO_4 \cdot 2H_2O$	0.22	mg/L
$NiCl_2 \cdot 6H_2O$	0.19	mg/L
$CuCl_2 \cdot 2H_2O$	0.17	mg/L
$Na_2SeO_3 \cdot 5H_2O$	0.16	mg/L
pH	6.8-7.0	-

Table 3.1: Synthetic medium composition.

3.2.2 Chemical analyses

Influent and effluent concentrations of ammonium, nitrite, and nitrate were measured approximately every other day using HACH test kits (HACH, Loveland, CO), as described in the manufacturer's methods 10031, 10019, and 10020, respectively.

3.2.3 Biomass collection and DNA extraction

Biomass samples were extracted via syringe from the MBR every 2-10 days, flash frozen in liquid nitrogen, and stored frozen at -80° C until use. Genomic DNA was extracted from the samples using the DNeasy PowerSoil Kit (Qiagen, Carlsbad, CA), as described in the manufacturer's protocol. The concentration and purity of extracted DNA was measured with a NanoDrop Spectrophotometer (Thermo Fisher Scientific, Waltham, MA). The concentration of genomic DNA in all samples was normalized to 10 ng/μL with nuclease-free water (Thermo Fisher Scientific, Waltham, MA). All genomic DNA samples were stored at -80° C until use.

3.2.4 16S rRNA gene sequencing and analysis

Genomic DNA samples were sent to the Joint Genome Institute (Walnut Creek, CA) for amplification of the variable 4 (V4) region of the 16S rRNA gene, library preparation, and amplicon sequencing. The full protocol was previously described in the Earth Microbiome Project (Kirton 2017; Earth Microbiome Project 2018). In summary, the V4 region of the bacterial 16S rRNA gene was amplified from DNA samples using revised primers 515FB (5'-GTGYCAGCMGCCGCGGTAA-3') and 806RB (3'-TAATCTWTGGGVNCATCAGG-5'), with barcodes attached to the forward primer. Amplicons were pooled at equal molality and purified with the MoBio UltraClean PCR Clean-Up Kit (MoBio Laboratories, Carlsbad, CA). Paired-end sequencing was then performed on the barcoded, purified amplicons with the Illumina MiSeq sequencer (Illumina, San Diego, CA).

Subsequent sequence processing and data analysis were performed in-house using mothur v.1.39.5, following the MiSeq standard operating procedure (SOP) (Schloss et al. 2009, Kozish et al. 2013). In summary, sequences were demultiplexed, merged, trimmed, and quality filtered. Unique sequences were aligned against the SILVA v.132 16S rRNA gene reference alignment database (Pruesse et al. 2007). Sequences that did not align to the position of the forward primer were discarded. Chimeras were detected and removed. Remaining sequences were clustered into operational taxonomic units (OTUs) within a 97% similarity threshold using the Phylip-formatted distance matrix. Representative sequences from each OTU were assigned taxonomic identities from the SILVA v.132 16S rRNA gene reference alignment database (Pruesse 2007). Sequences that were not classified as bacteria were removed. Remaining OTUs were counted, and the 150 most abundant OTUs (accounting for up to 99% of sequence reads within individual samples) were transferred to Microsoft Excel (Microsoft Office Professional Plus 2016) for downstream interpretation and visualization of their relative abundances. Phylogenetic distances were generated for the 150 most abundant OTUs using Clearcut (Evans et al. 2006).

3.2.5 Statistical analyses

Statistical analyses were performed in Microsoft Excel (Microsoft Office Professional Plus 2016) and RStudio v1.1.383 (RStudio Team 2015) using the ggplot2 and vegan packages. A significance level of $\alpha = 0.05$ was used for all analyses, unless noted otherwise. Details of statistical methods used for additional analyses are given below.

3.2.5.1 Microbial diversity

The Shannon index (*H'*) was chosen to quantify microbial diversity within each biological sample. *H'* was calculated as follows:

$$H' = -\sum_{i=1}^{N} p_i \ln p_i$$

Where $\{p_1, p_2, \ldots, p_N\}$ are the relative abundances of the OTUs within the biological sample of interest and *N* is the number of observations in the sample (Hill et al. 2006).

3.3 Results and discussion

3.3.1 Reactor performance

The performance of the MBR was tracked for 215 days, through several manipulations (i.e., phases of experimentation (P)) of the ratio of influent concentrations of ammonium:nitrite (Figure 3.3a). Differences in influent and effluent concentrations of reactive nitrogen species were tabulated into nitrogen speciation ratios and the nitrogen removal rate (NRR)—g-N removed, per liter, per day (Figure 3.3b). For simplification of downstream analyses, effluent concentrations of ammonium, nitrite, and nitrate were averaged over each phase of experimentation (Appendix 3). These averaged concentrations were then used to calculate the performance of the MBR for each phase of experimentation, including the ratio of ammonium consumed to nitrite consumed in the MBR and the ratio of ammonium consumed to nitrate produced in the MBR (Table 3.2).

During phase 1, ammonium and nitrite were fed to the MBR in a 1:1.32 ratio. Ammonium and nitrite were consumed in a similar (1:1.31) ratio within the MBR, and little ammonium and nitrite remained in the effluent. Additionally, 0.31 moles of nitrate were produced for every mole of ammonium fed to the MBR. During phase 2, ammonium and nitrite were fed to the reactor in a 1:1.1 ratio. Almost instantly, ammonium and nitrite consumption changed to a 1:1.21 ratio. Roughly half of the additional ammonium added to the MBR was consumed, while the other half remained in the effluent. Additionally, 0.23 moles of nitrate were produced for every mole of ammonium fed to the MBR. While the ratio of ammonium consumed to nitrate produced in the MBR decreased between phases 1 and 2, the corresponding decrease in the concentration of nitrate in the MBR's effluent was statistically insignificant.

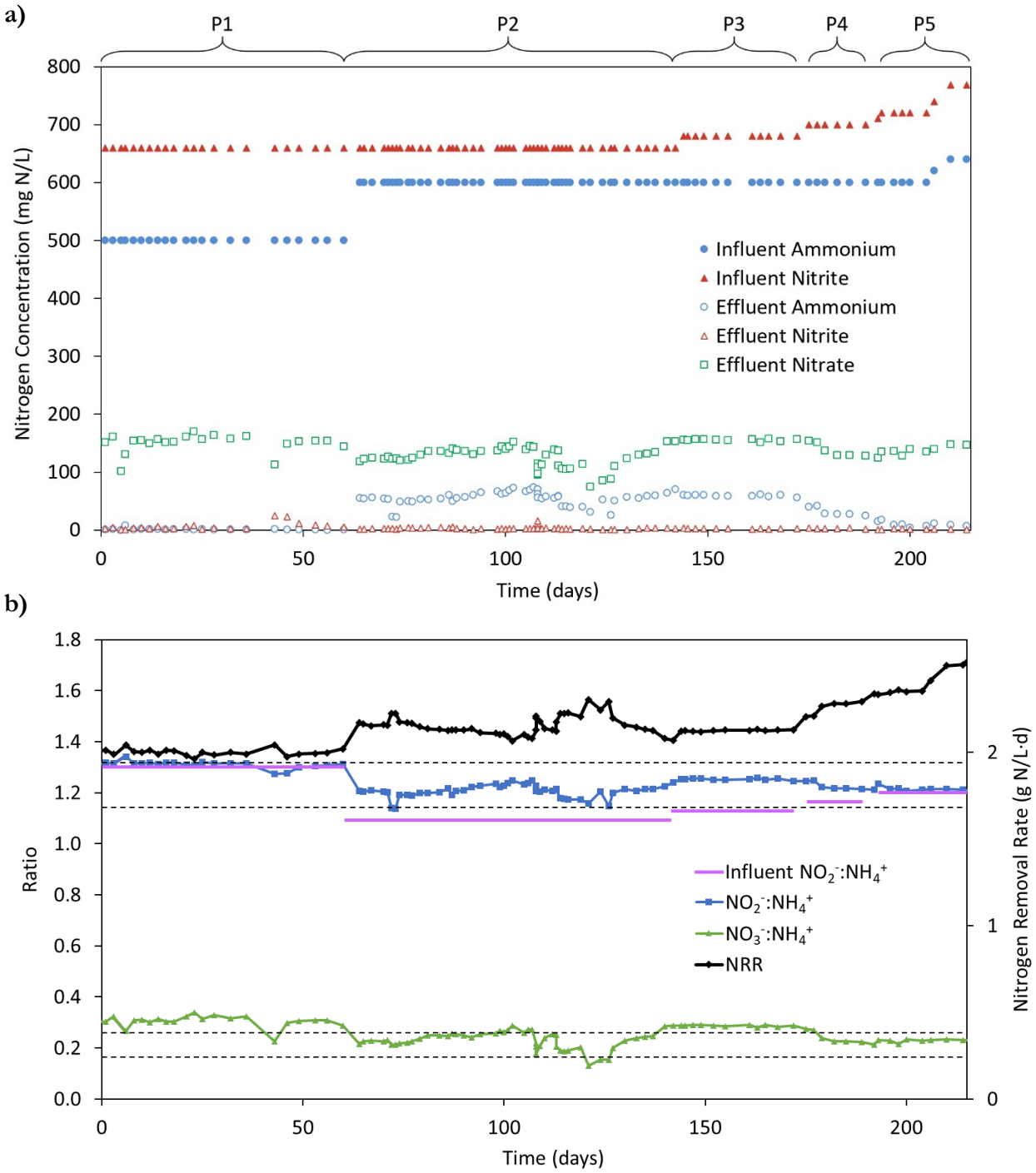

Figure 3.3: MBR performance. The upper panel (a) reports the influent and effluent concentrations of reactive nitrogen species in the MBR over time (influent nitrate concentrations were negligible, so they were not plotted). The five phases (P) of the experiment are delineated on the secondary x-axis. The lower panel (b) reports the nitrogen speciation ratios (primary y-axis) and NRR (secondary y-axis) in the MBR over time. The solid purple line indicates the ratio at which nitrite an ammonium were fed to the reactor, while the blue line, connected by data points, indicates the ratio at which nitrite and ammonium were actually consumed within the reactor. The dashed lines represent the stoichiometric nitrogen speciation ratios for anammox presented in Equations 3.6 and 3.7.

During phases 3 – 5, the ratio of ammonium:nitrite fed to the reactor was steadily increased from 1:1.1 to 1:1.2. At first, the ratio of ammonium:nitrite consumed in the reactor jumped up to 1:1.25, but as the influent ratio of ammonium:nitrite approached 1:1.2, the consumption ratio of ammonium:nitrite decreased to 1:1.22. Additionally, the ratio of ammonium consumed to nitrate produced in the MBR followed a similar pattern: at first, the ratio of ammonium consumed to nitrate produced jumped up to 1:0.29, but as the influent ratio of ammonium:nitrite approached 1:1., the ratio of ammonium consumed to nitrate produced decreased to 1:0.23. While the ratio of ammonium consumed to nitrate produced decreased during phases 3 – 5, the corresponding decrease in the concentration of nitrate in the MBR's effluent was (again) statistically insignificant.

Parameter	P1	P2	P3	P4	P5
NLR (g N/L·d)	2.32	2.52	2.56	2.60	2.64-2.82
Influent NH_4^+ (mg N/L)	500	600	600	600	600-640
Influent NO_2^- (mg N/L)	660	660	680	700	720-768
Influent $NH_4^+ : NO_2^-$	1:1.32	1:1.1	1:1.13	1:1.16	1:1.2
NRR (g N/L·d)	2.00	2.15	2.13	2.26	2.35-2.50
Effluent NH_4^+ (mg N/L)	1	55	59	32	9
Effluent NO_2^- (mg N/L)	6	3	2	2	2
Effluent NO_3^- (mg N/L)	152	125	156	138	139
$NH_4^+ : NO_2^-$	1:1.31	1:1.21	1:1.25	1:1.23	1:1.22
$NH_4^+ : NO_3^-$	1:0.31	1:0.23	1:0.29	1:0.24	1:0.23

Table 3.2: Performance of the MBR during each phase (P) of experimentation.

In summary, the microbial community within the MBR was capable of consuming ammonium and nitrite anywhere between a 1:1.21 and a 1:1.31 ratio. Accordingly, when less nitrite was consumed in relation to ammonium in the MBR, less nitrate was produced in relation to ammonium in the MBR. An influent nitrogen speciation ratio of ammonium:nitrite of 1:1.2 minimized the concentrations of ammonium and nitrite in the MBR's effluent (and hence, maximized the MBR's overall nitrogen removal performance).

Additionally, the almost instantaneous changes in ammonium:nitrite consumption ratios following changes in influent ammonium:nitrite speciation ratios (most notably, between phases 1 and 2) indicate that the existing bacterial community was able to manage the environmental changes by altering its metabolisms, rather than by altering its relative abundance dynamics. The relative abundances of bacterial taxa may have subsequently changed in response to the environmental changes, but such dynamics did not impact the overall function of the MBR.

At the end of phase 5, the concentrations of ammonium and nitrite became negligible in the MBR's effluent, so the MBR was transitioned to another experiment (not included in the scope of this dissertation).

3.3.2 Bacterial community structure

The V4 region of 16S rRNA genes was sequenced at 35 distinct timepoints over the lifespan of the MBR study. These timepoints captured all five phases of experimentation, from the initial influent ammonium:nitrite speciation ratio of 1:1.32, to the final influent ammonium:nitirite speciation ratio of 1:1.2.

A phylogenetic tree was constructed using iTOL (Letunic and Bork 2016) to visualize the overall diversity of the 150 most abundant OTUs in the MBR's bacterial community (Figure 3.4; Appendix 4). The resulting OTUs were very similar to those reported in Chapter 2. The few, small discrepancies can be accounted to the use of updated primers during the amplification process. Members of the phyla Acidobacteria, Bacteroidetes, Chlorobi (i.e., Ignavibacteria), Chloroflexi, and Proteobacteria accounted for the majority of the recovered OTUs in the MBR (Gonzalez-Martinez et al. 2015b). These phyla accounted for 7, 13, 13, 35, and 57 of the recovered OTUs, respectively. Members of the genus *Brocadia* were identified as the anammox bacteria within the MBR. Six OTUs are associated with this genus.

The remainder of the OTUs were classified into the phyla Actinobacteria, Armatimonadetes, Chlamydiae, Cyanobacteria, Deinococcus-Thermus, Dependentiae, Patescibacteria, Planctomycetes, Spirochaetes, and Verrucomicrobia. Due to the current disagreement on the classification of Ignavibacteria as a class of Bacteroidetes, as a class of Chlorobi, or as its own phylum, it has been depicted here as its own phylum (Parks et al. 2018).

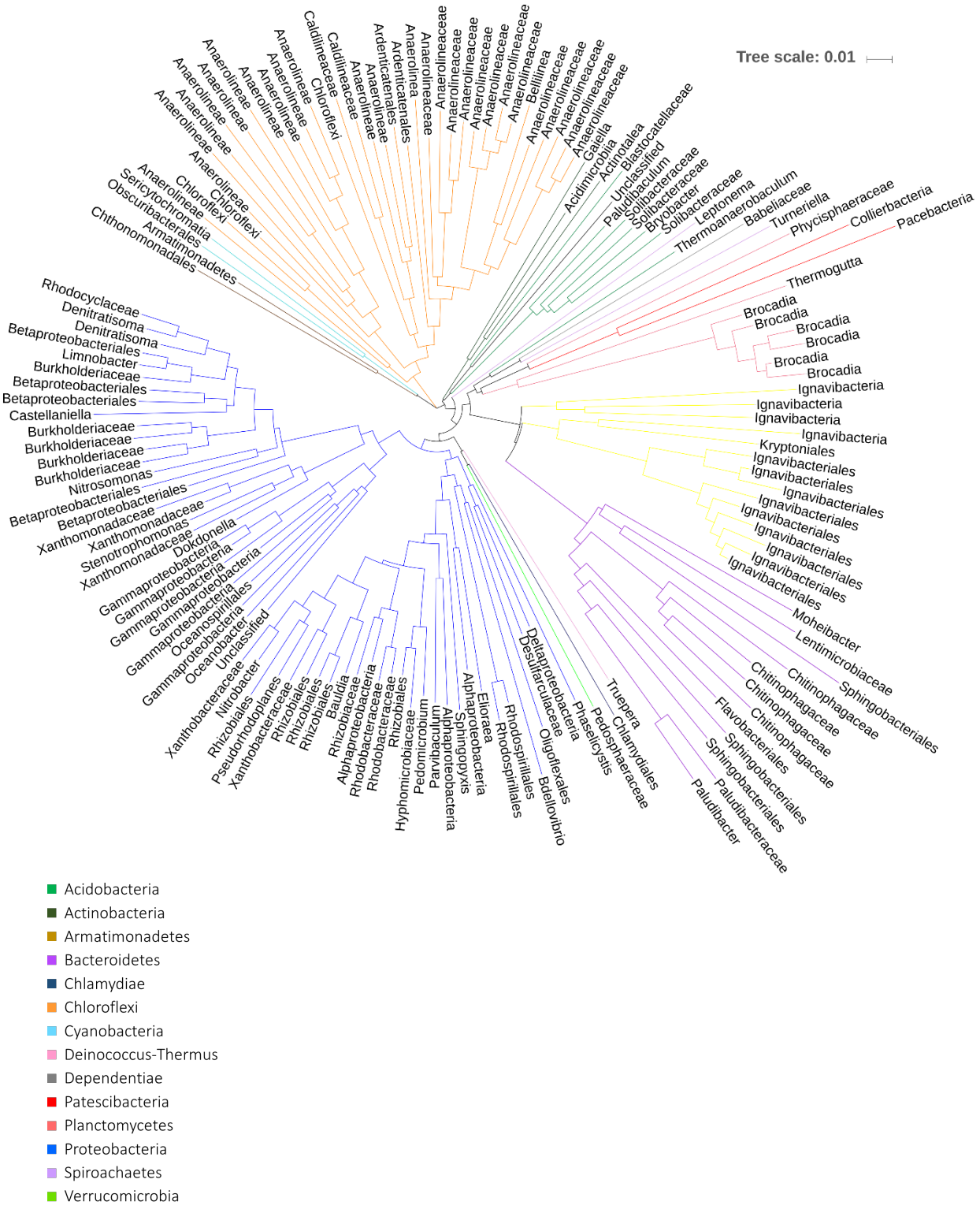

Figure 3.4: Phylogenetic tree of all recovered operational taxonomic units (OTUs) in the MBR.

3.3.2.1 Temporal community dynamics

The relative abundances of OTUs were averaged over three-day increments, resulting in 23 distinct relative abundance profiles over the lifespan of the MBR study (Figure 3.5; Appendix 4). The genus *Brocadia* accounted for 45% of the bacteria in the MBR's bacterial community at the beginning of experimentation. Additionally, members of the phylum Ignavibacteria and of the class Anaerolineae within the phylum Chloroflexi accounted for 11% and 16% of the bacteria in the MBR's bacterial community at the beginning of experimentation, respectively. Over the course of phase 1, the relative abundance of *Brocadia* rose to 73%, while the relative abundances of Ignavibacteria and Anaerolineae decreased to 8% and 8%, respectively. It appears that the influent ammonium:nitrite speciation ratio of 1:1.32 encouraged the enrichment of *Brocadia* at the expense of Ignavibacteria and Anaerolineae, as well as the phylum Proteobacteria.

On day 61, the influent ammonium:nitrite speciation ratio was decreased to 1:1.1. Over the next 35 days, the relative abundances of *Brocadia*, Ignavibacteria, and Anaerolineae remained fairly constant. Then, on day 117, roughly one SRT after the alteration of the influent ammonium:nitrite speciation ratio, the relative abundance of *Brocadia* began to decrease, while the relative abundances of Ignavibacteria and Anaerolineae began to increase. By the end of phase 2 (day 136), the relative abundance of *Brocadia* had fallen to 27%, while the relative abundances of Ignavibacteria and Anaerolineae had risen to 29% and 28%, respectively. It appears that the influent ammonium:nitrite speciation ratio of 1:1.1 discouraged the enrichment of *Brocadia* in favor of the enrichment of Ignavibacteria and Anaerolineae.

From day 143 to day 193, the influent ammonium:nitrite speciation ratio was steadily increased from 1:1.1 to 1:1.2. Over this 50-day period, the relative abundance of *Brocadia* continued to decline. By the commencement of phase 5 (day 194), roughly two and a half SRTs after the initial alteration of the influent ammonium:nitrite speciation ratio, the relative abundance of *Brocadia* had fallen to 27%, while the relative abundances of Ignavibacteria and Anaerolineae had risen to 29% and 28%, respectively.

Interestingly, while the alteration of the influent ammonium:nitrite speciation ratio had minimal impacts on the overall performance of the MBR, it had significant impacts of the relative abundance dynamics of the bacterial community within the MBR. It appears that an influent ammonium:nitrite speciation ratio of 1:1.32 favors the enrichment of the anammox bacterium, *Brocadia*, while lower ammonium:nitrite speciation ratios (1:1.1 – 1:1.2) favor the enrichment of bacteria that are not capable of anammox (here, Ignavibacteria and Anaerolineae). Over the course of the experiment, the community composition and its microbial diversity varied greatly, yet all compositions were consistently capable of robust nitrogen removal performance within the MBR (Appendix 3).

In the following sections, these conflicting results are combined with previous knowledge of nitrogen cycling in attempts to explain the dynamics occurring among anammox, denitrifying, and DNRA bacteria in this experiment.

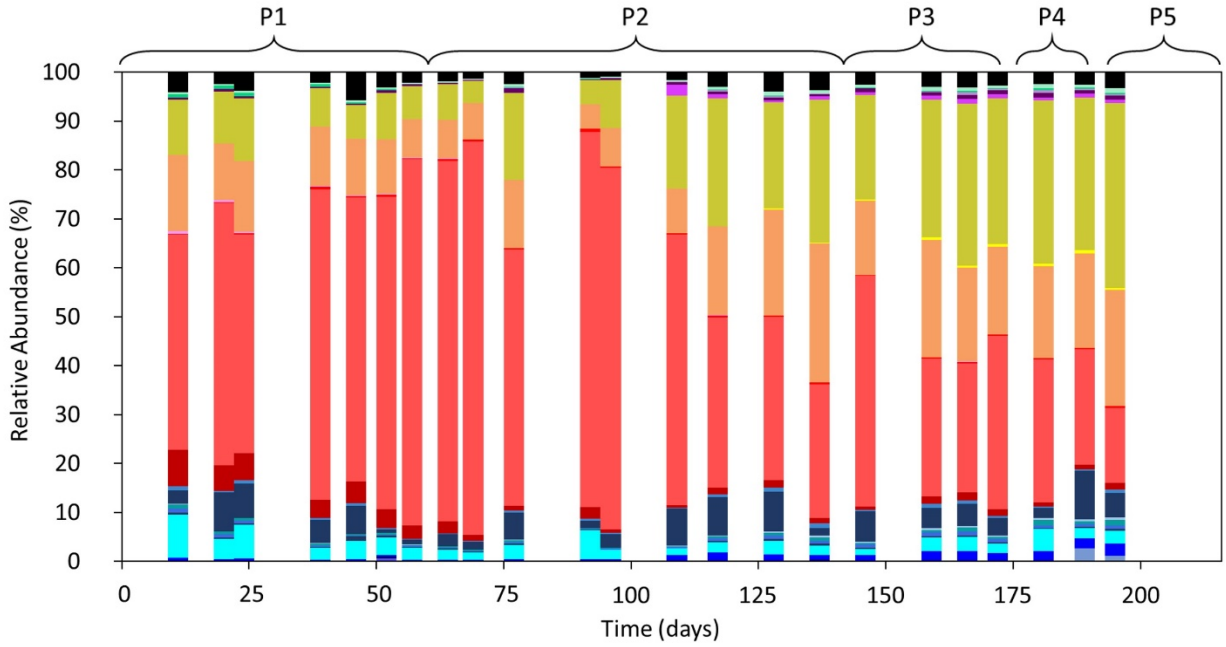

Phylum	Class	Order	Genus
-	-	-	-
Acidobacteria	Acidobacteriia	Solibacterales	-
Acidobacteria	Thermoanaerobaculia	Thermoanaerobaculales	Thermoanaerobaculum
Bacteroidetes	Bacteroidia	Flavobacteriales	Moheibacter
Bacteroidetes	Bacteroidia	Chitinophagales	-
Bacteroidetes	Bacteroidia	Sphingobacteriales	-
Bacteroidetes	Ignavibacteria	-	-
Bacteroidetes	Ignavibacteria	Kryptoniales	-
Chloroflexi	Anaerolineae	-	-
Deinococcus-Thermus	Deinococci	Deinococcales	Truepera
Patescibacteria	Microgenomatia	Pacebacteria	-
Planctomycetes	Brocadiae	Brocadiales	Brocadia
Planctomycetes	Phycisphaerae	Phycisphaerales	-
Proteobacteria	Alphaproteobacteria	Rhizobiales	-
Proteobacteria	Alphaproteobacteria	Rhodospirillales	-
Proteobacteria	Deltaproteobacteria	-	-
Proteobacteria	Deltaproteobacteria	Desulfarculales	-
Proteobacteria	Gammaproteobacteria	-	-
Proteobacteria	Gammaproteobacteria	Betaprotoebacteriales	-
Proteobacteria	Gammaproteobacteria	Betaproteobacteriales	Limnobacter
Proteobacteria	Gammaproteobacteria	Betaproteobacteriales	Denitratisoma
Proteobacteria	Gammaproteobacteria	Oceanospirillales	Oceanobacter
Proteobacteria	Gammaproteobacteria	Xanthomonadales	-
Proteobacteria	Gammaproteobacteria	Xanthomonadales	Stenotrophomonas

Figure 3.5: Relative abundance profiles of bacterial taxa over the lifespan of the MBR. "Others" include taxa that were identified, but their relative abundance profiles never reached 0.5% for any of the sequencing timepoints. The five phases (P) of the experiment are delineated on the secondary x-axis.

3.3.3 Hypothesized dynamics of the anaerobic nitrogen cycling pathways

In this study, the MBR's influent medium was optimized for the anammox bacterium. It contained ammonium, nitrite, and bicarbonate, the main substrates for anammox metabolism. Thus, it was assumed that anammox was the predominant nitrogen removal pathway in the MBR. Additionally, the influent medium did not contain any form of organic carbon, nor did it contain a significant amount of iron. Under these conditions, previous research predicts that nitrate will be reduced to nitrite by denitrifying bacteria, and then further reduced to nitrogen gas by anammox bacteria (Burgin and Hamilton 2007). This recycling of nitrate into nitrite for anammox metabolism has been coined the "nitrite loop" (Winkler et al. 2012).

As a baseline for anaerobic nitrogen cycling dynamics in the MBR, it was assumed that anammox bacteria convert ammonium and nitrite to nitrogen gas, with a small amount of nitrate produced. Denitrifying bacteria convert the produced nitrate back to nitrite, which can then be cycled back into anammox metabolism via the "nitrite loop" (Figure 3.6).

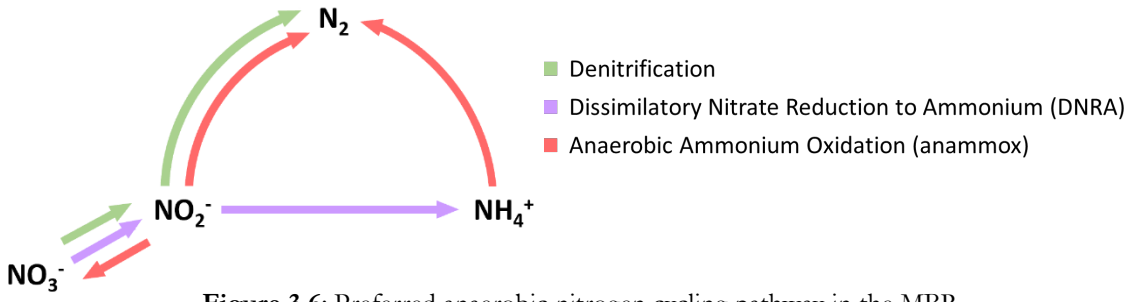

Figure 3.6: Preferred anaerobic nitrogen cycling pathway in the MBR

During phase 1 of experimentation, ammonium and nitrite were supplied to the reactor in a 1:1.32 ratio, and consumed in the reactor in a 1:1.31 ratio. Additionally, 0.31 moles of nitrate were produced per mole of ammonium consumed in the reactor. The observed stoichiometry during phase 1 of experimentation aligned very closely with the stoichiometry proposed by Strous et al. Also during phase 1 of experimentation, *Brocadia* was enriched in the bacterial community. In combination, these two sets of results indicate that the species of anammox bacteria in the MBR follow the model of anammox metabolism proposed by Strous et al. When ammonium and nitrite are supplied in the ratio required for anammox metabolism, anammox bacteria are able to dominate the overall anaerobic nitrogen cycling community in the MBR, leaving little room for denitrifying and DNRA bacteria to flourish.

During phases 2 – 5 of experimentation, ammonium and nitrite were supplied to the reactor in ratios lower than 1:1.32. If the species of anammox bacteria in the MBR were indeed following the metabolism proposed by Strous et al., then excess ammonium was supplied during these phases. The excess ammonium was consumed in the MBR, resulting in an ammonium:nitrite consumption ratio of 1:1.22 – 1.25. Additionally, 0.23 – 0.29 moles of nitrate were produced per mole of ammonium consumed in the reactor. The observed stoichiometry during phases 2 – 5 deviated from the stoichiometry proposed by Strous et al., yet did not align with the stoichiometry proposed by Lotti et al. Also during phases 2 – 5 of experimentation, the relative abundance of *Brocadia* declined in favor of Ignavibacteria and Anaerolineae. In combination, these results indicate that the

"nitrite loop" may be at work. When ammonium is supplied in excess of the requirement for anammox metabolism, not all of it can initially be consumed by anammox bacteria. Dentrifying bacteria must first reduce some of the nitrate produced by anammox bacteria back into nitrite. Then, the excess ammonium can be combined with the nitrite produced by denitrifying bacteria in anammox metabolism. This additional round of anammox produces more nitrate, and the "nitrite loop" continues. Such a loop explains the deviation from the model of anammox metabolism.

Heterotrophic organisms that are capable of reducing nitrate to nitrite are generally able to grow more rapidly than autotrophic organisms (such as anammox) (Madigan et al. 2006). In the MBR, the reduction of nitrate to nitrite was most likely performed by Ignavibacteria and Anaerolineae, as their increases in relative abundances aligned with the instances of increased reliance on the "nitrite loop" for the overall function of the MBR (One previous metagenomic study of unclassified Ignavibacteria found that the genome encoded the respiratory nitrate reductase (Nar) gene, which is responsible for the reduction of nitrate to nitrite (Bhattacharjee et al. 2017). Potentially, the unclassified Ignavibacteria encode the Nar gene here as well.). More work must be done to elucidate Ignavibacteria's and Anaerolineae's roles in nitrogen cycling in an anammox reactor.

3.3.4 Conclusions

The performance and temporal dynamics of an anammox MBR were investigated through several manipulations of the ratio of influent concentrations of ammonium:nitrite. It appears that an influent ammonium:nitrite speciation ratio of 1:1.32 favors the enrichment of the anammox species in the MBR, while lower ammonium:nitrite speciation ratios (1:1.1 – 1:1.2) favor the enrichment of a more diverse bacterial community in the MBR, including the enrichment of bacteria that are potentially capable of heterotrophic nitrogen cycling (i.e., Ignavibacteria and Anaerolineae). Both of these enrichments are capable of robust nitrogen removal performance within the MBR.

Ultimately, the more diverse anammox community with heterotrophic nitrogen cycling bacteria (and a "nitrite loop") has a greater capacity to remove reactive nitrogen species from an influent wastewater stream. Yet, in Chapter 2, results indicated that an over-dominance of heterotrophic nitrogen cycling bacteria can cause the overall performance of the MBR to collapse. So, where is the tipping point between the positive and negative roles of heterotrophic nitrogen cycling bacteria in an anammox reactor? More work must be done to elucidate the precise mechanisms that control the interactions among anammox, denitrifying, and DNRA bacteria within the MBR. Understanding nitrogen cycling (and other metabolic interactions) among anammox, denitrifying, and DNRA microorganisms within an anammox reactor will enable better operation and control of this important process for effective removal of reactive nitrogen in wastewater streams.

Chapter 4:

The Impact of Biomass Retention Strategies on the Performance and Bacterial Community Structure of an Anammox Reactor

4.1 Introduction

The slow growth rate of anammox bacteria is one of the greatest hindrances to the widespread adoption of the anammox technology (Zhu et al. 2014). While efforts have been made to increase anammox growth rates under typical wastewater conditions, advancements in the retention of anammox biomass within a reactor have proven to be more effective at overcoming the challenges associated with the bacteria's slow growth rate (Lotti et al. 2015; Stinson 2018). Most notably, advancements in reactor configuration, such as the moving-bed biofilm reactor (MBBR), the gas-lift or upflow reactor (i.e., the upflow anaerobic sludge blanket (UASB)), the sequencing batch reactor (SBR), and the membrane bioreactor (MBR) have been successful in minimizing anammox bacterial washout (van Dongen et al. 2001; Wett 2007; Jin et al. 2008; van der Star et al. 2008; Tang et al. 2011; Kowalski et al. 2018; Stinson 2018).

Additional research efforts have also revealed that anammox bacteria are capable of attaching to biomass support media, such as inorganic salts and plastic, and developing robust biofilms upon them (Fernandez et al. 2008a; Klaus et al. 2016). Many of the aforementioned reactor configurations have exploited this property of anammox bacteria by including biomass support media within their reactor vessels (Christensson et al. 2013; Veolia 2018). As a result, the surface area for biomass attachment and subsequent biofilm formation within the reactor is dramatically increased, and anammox bacterial washout can be even further reduced.

Currently, new anammox reactors are seeded with 10% of their desired operational biomass concentration (Stinson 2018). As a result, it can take several months for biomass to accumulate within a new reactor and for the reactor's nitrogen removal to reach its desired operational performance. If strategies can be developed to better retain biomass within an anammox reactor, the duration of the startup phase can be decreased. The research presented in this chapter investigates the efficacy of two novel biomass support materials—polyvinyl alcohol-sodium alginate (PVA-SA) and zeolite—to further improve biomass aggregation and retention (and ultimately, performance) within anammox reactors. Particular emphasis is placed on the startup phase.

PVA-SA is a polymer-based material that has been widely used to artificially aggregate biomass (Figure 4.1) (Rouse et al. 2005; Ge et al. 2009). When biomass becomes entrapped within a PVA-SA matrix, the volume occupied by the biomass becomes larger and the biomass becomes less likely to wash out of a reactor. While this technology has been around for several decades, its application has only recently been extended to anammox bacteria within anammox reactors (Zhu et al. 2014; Ali et al. 2015b). As a result, the behavior of anammox bacteria and associated community members in PVA-SA is not yet well understood (Date et al. 2008; Manonmani and Joseph 2018).

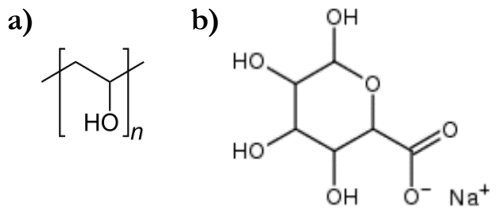

Figure 4.1: Molecular structure of polyvinyl alcohol-sodium alginate (PVA-SA). PVA is depicted in panel (a), while SA is depicted in panel (b).

Zeolites are naturally-occurring, aluminosilicate minerals of a porous structure (Figure 4.2). They are characterized by their ability to lose and gain water reversibly, sorb molecules of appropriate cross-sectional diameter, and exchange their constituent cations without a major change in structure (Tsitsishvili et al. 1992). Because of these unique properties, zeolites are used in a variety of agricultural, industrial, and municipal applications (Chung et al. 2000; Kallo 2001; Wang and Peng 2010; Gupta et al. 2015; Delkash et al. 2015; Zhao 2016; Huang et al. 2018). In the past few years, zeolites' applications have extended to wastewater treatment processes (Fernandez et al. 2008a; Fernandez et al. 2008b; Widiastuti et al. 2008). In particular, clinoptilolite, a type of zeolite with a strong sorption affinity for ammonium, has been used to physically remove ammonium from wastewater streams (Montalvo et al. 2012; KMI Zeolite 2018). While recent research has begun to investigate the ability of clinoptilolite to sorb ammonium in anammox reactors, the research described in this chapter is the first to investigate clinoptilolite's efficacy as a growth support media for the anammox bacterial community in typical sidestream conditions (Grismer and Collison 2017; Collison and Grismer 2018).

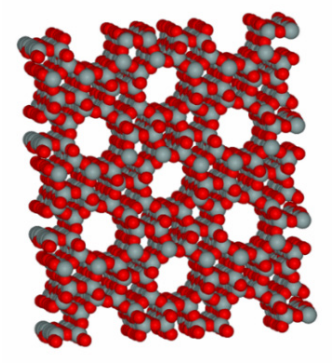

Figure 4.2: Molecular structure of clinoptilolite zeolite. The partial substitution of Al^{3+} for Si^{4+} in the aluminosilicate building block results in a permanent, excess negative charge that can be offset by alkali and earth alkaline cations. The aluminosilicate building blocks are arranged into rings, leaving channels and cavities to accommodate the mineral's sorption and ion exchange capacities (Coldstream Industries 2015; Grismer and Collison 2017).

4.2 Materials and methods

4.2.1 Chemicals and seed biomass

All chemicals used in the synthesis of PVA-SA, as well as the chemicals used in the creation of synthetic wastewater, were obtained from Millipore Sigma (St. Louis, MO) and used as received without further purification. Clinoptilolite zeolite was obtained from KMI Zeolite (Pahrump, NV) as crushed gravel. Concentrated anammox biomass was obtained from the in-house MBR described in Chapters 2 and 3. Prior to all downstream uses, the anammox biomass had been extracted from the MBR and stored anaerobically at 4° C for up to three months.

4.2.2 Synthetic medium preparation

Synthetic medium was designed to mimic sidestream effluent at a municipal wastewater treatment plant (Table 4.1) (van de Graaf et al. 1996; Chen et al. 2014; Liu et al. 2015). In summary, it contained ammonium, nitrite (added as $(NH_4)_2SO_4$ and $NaNO_2$, respectively), bicarbonate, and trace nutrients—the substrates for anammox growth. Concentrations of ammonium and nitrite varied quite dramatically, depending on the synthetic medium's application. The pH was adjusted to 6.8 +/- 0.1 with 1N HCl and 1N NaOH.

Constituent	Concentration	Unit
$(NH_4)_2SO_4$	variable	mg-N/L
$NaNO_2$	variable	mg-N/L
NaCl	1000	mg/L
$MgCl_2 \cdot 6H_2O$	500	mg/L
KH_2PO_4	200	mg/L
KCl	300	mg/L
$CaCl_2 \cdot 2H_2O$	180	mg/L
$KHCO_3$	420	mg/L
$FeCl_2 \cdot 4H_2O$	17.9	mg/L
$CoCl_2 \cdot 6H_2O$	0.24	mg/L
$MnCl_2 \cdot 4H_2O$	0.99	mg/L
$ZnCl_2$	0.20	mg/L
H_3BO_3	0.014	mg/L
$Na_2MoO_4 \cdot 2H_2O$	0.22	mg/L
$NiCl_2 \cdot 6H_2O$	0.19	mg/L
$CuCl_2 \cdot 2H_2O$	0.17	mg/L
$Na_2SeO_3 \cdot 5H_2O$	0.16	mg/L
pH	6.8 +/- 0.1	-

Table 4.1: Synthetic medium composition.

4.2.3 Preparation and characterization of biomass retention materials

4.2.3.1 PVA-SA preparation

Anammox biomass immobilization was carried out as previously described by Zhu et al. 2009, with a few modifications. In summary, a 2% PVA – 6% SA (w/v) solution was prepared by dissolving the PVA and SA powder chemicals into ultrapure water from a Milli-Q system (Millipore Sigma, St. Louis, MO). To ensure full dissolution, the solution was left in a 60° C water bath overnight. Separately, anammox biomass was washed with a 20% (v/v) phosphate buffered saline (PBS) solution and its concentration was measured following standard methods for volatile suspended solids (VSS) quantification (APHA 2005).

Next, the PVA-SA solution was cooled and mixed with the proper amount of washed and quantified anammox biomass to achieve a biomass concentration of 10 g VSS/L within the solution. A peristaltic pump (Cole-Parmer, Vernon Hills, IL) was used to drip the PVA-SA-anammox solution into a 4% (w/v) solution of calcium chloride at a rate of 0.02 mL min^{-1}. Anaerobic conditions were maintained in the calcium chloride solution by constant bubbling with argon gas. Through the dripping process, the PVA-SA-anammox solution crystallized into spherical beads, roughly 4 mm in diameter (Appendix 5). The beads were stored overnight at 4° C to ensure sufficient curing. Finally, the beads were washed with a 20% PBS solution before transferal to downstream experimentation.

4.2.3.2 Zeolite preparation

Zeolites were pulverized via mortar and pestle and sorted into various sizes by sifting through a series of sieves. Particles falling between 0.3 – 1.4 mm were chosen for all downstream analyses. Subsets of the zeolites were subjected to pretreatments previously outlined in Inglezakis et al. 2003, to eliminate any potential contaminants from the zeolites' surfaces. During pretreatments, the subsets of the zeolites were washed three times with deionized (DI) water, 1M NaCl in DI water, or 0.1N HCl in DI water. Then, the subsets of the zeolites were stored overnight on a shaking table at room temperature in their respective pretreatment solutions. Finally, the subsets of zeolites were washed three times with DI water and dried at 100° C before transferal to downstream experimentation.

4.2.3.2.1 Quantification of zeolites' sorption capacity

In order to quantify the ammonium sorption capacity of the zeolites, batch sorption experiments were conducted in 25 mL glass serum bottles that were prepared with an argon headspace, capped with butyl rubber septa, and sealed with aluminum crimp caps. 10 mL of nitrogen-free media and 0.2 g of zeolite were added to each bottle. Concentrated solutions of ammonium and nitrite were added in a 1:1.32 stoichiometric ratio to produce initial concentrations ranging from 0:0 – 2000:2640 mg N L^{-1}, respectively. A series of control bottles without zeolites were also prepared, following the same procedure. The bottles were stored overnight on a shaking table at 37° C. The following morning, samples were withdrawn from the bottles and the aqueous concentrations of ammonium and nitrite were quantified via ion chromatography (IC) (Dionex ICS-1100, Thermo Fisher Scientific, Waltham, MA). The concentrations in the control bottles were used to calculate the amount of ammonium and nitrite that was sorbed onto the zeolites.

4.2.4 Reactor setup and operation

Before moving into longer-term anammox biomass attachment and retention experiments, the biomass support materials were screened for any potential inhibitory effects on anammox bacteria. These initial screening experiments were performed in batch reactors. The biomass support materials that passed the initial screening advanced to the longer-term anammox biomass attachment and retention experiments. These longer-term experiments were performed in UASB reactors.

4.2.4.1 Batch reactors

All batch reactor experiments, including the live anammox microcosms and the support-material-only controls (i.e., no biomass), were conducted in 125 mL glass serum bottles that were prepared with an argon headspace, capped with butyl rubber septa, and sealed with aluminum crimp caps. 100 mL of nitrogen-free media was added to each bottle. Where appropriate, 10 g L^{-1} of support materials and/or anammox biomass were added to achieve final concentrations of 10 g L^{-1} and/or 10 g VSS L^{-1}, respectively, within the bottle. At the beginning of incubations, concentrated solutions of ammonium and nitrite were added to produce initial aqueous concentrations of 100 mg N L^{-1} and 132 N L^{-1}, respectively, within the bottle. When aqueous concentrations of nitrite dipped below 10 mg N L^{-1} within the bottle, ammonium and nitrite were reamended in a 1:1.32 ratio. For the duration of all experiments, all bottles were stored on a stir plate at 37° C. Additionally, neutral pressure was maintained in the bottles by releasing produced nitrogen gas via syringe two or three times per day, and pH was maintained at 6.8 +/- 0.1 with periodic amendments of 1N HCl and 1N NaOH.

4.2.4.2 Upflow anaerobic sludge blanket (UASB) reactors

Two laboratory-scale UASB reactors with working volumes of 1.2 L each were constructed to study the performance of the anammox microbial community with and without zeolite support material during the initial startup phase (Figure 4.3). An electric heating jacket (HTS/Amptek, Stafford, TX) was fitted around each reactor vessel to maintain temperature at 37° C. Media was supplied continuously to the UASBs at a rate of 50 mL hr^{-1}, which corresponds to a 24-hour HRT. Mixed gas ($ArCO_2$ = 95:5) was supplied continuously to the UASBs at a rate of 180 mL min^{-1} +/- 10 mL min^{-1} to eliminate dissolved oxygen and maintain pH at 7.2. Media and gas were mixed prior to their delivery to the reactor vessel. A spherical air stone, 3 cm in diameter, was mounted at the inlet of each reactor vessel to diffuse gas being fed into the UASB.

On day 0, each UASB was inoculated with approximately 1 g VSS L^{-1} of anammox biomass (meant to mimic the initial 10% biomass inoculation in a full-scale anammox reactor) (Stinson 2018). Also on day 0, 10 g L^{-1} of zeolite was added to one of the UASBs as a support material (this concentration was chosen based on literature recommendations) (Fernandez et al. 2008; Wang and Peng 2010). Ammonium and nitrite were fed to the UASBs in a 1:1.2 ratio, in order to maintain nitrite-limiting conditions and prevent performance inhibition from the accumulation of nitrite (Lotti et al. 2012). Initial ammonium and nitrite concentrations were 100 mg N L^{-1} and 120 mg N L^{-1}, respectively. If the effluent concentration of nitrite dipped below 10 mg N L^{-1}, the influent concentrations of ammonium and nitrite were increased by 100 mg N L^{-1} and 120 mg N L^{-1}, respectively. Conversely, if the effluent concentration of nitrite rose above 70 mg N L^{-1}, the influent concentrations of ammonium and nitrite were decreased by 50 mg N L^{-1} and 60 mg N L^{-1}, respectively. This pattern was continued for a minimum of 30 days, the minimum amount of time required for a new, full-scale anammox reactor to reach its desired operational performance (Stinson 2018).

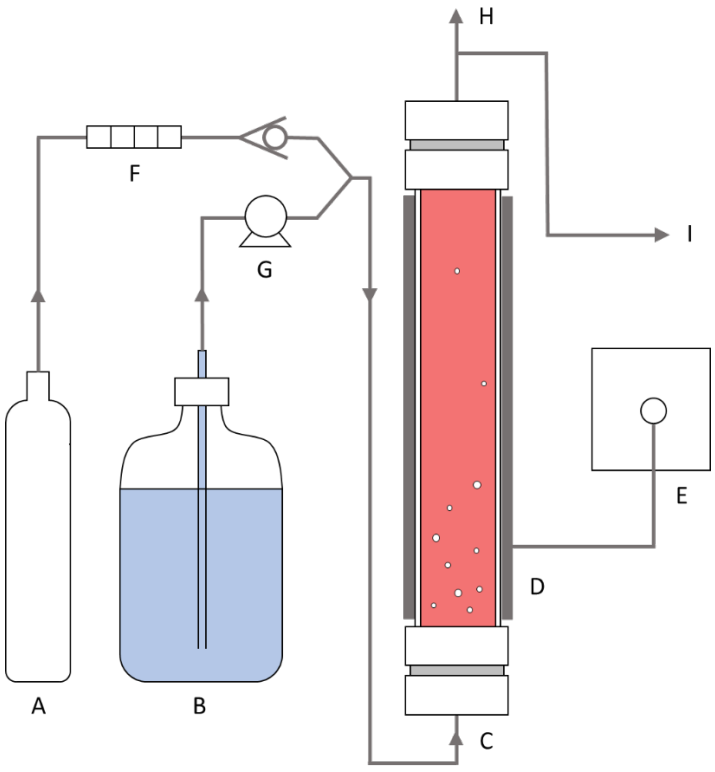

Figure 4.3: Configuration of the laboratory-scale upflow anaerobic sludge blanket (UASB) reactor. Each letter refers to a different component of the UASB: A – influent gas tank, B – influent media tank, C – 1.2L reactor vessel, D – heating jacket, E – heating jacket power source and temperature controller, F – flowmeter, G – influent peristaltic pump, H – phase separator, and I – effluent media line. This figure is not drawn to scale.

4.2.4.3 Chemical analyses

Concentrations of ammonium, nitrite, and nitrate were measured using HACH test kits (HACH, Loveland, CO), as described in the manufacturer's methods 10031, 10019, and 10020, respectively. For the batch reactors, concentrations of the aforementioned compounds were measured immediately before and after infusions of ammonium and nitrite. For the UASB reactors, influent and effluent concentrations of the aforementioned compounds were measured approximately every other day.

4.2.5 Biomass collection and DNA extraction

Biomass samples were extracted via syringe from the bottom third of the UASBs every 2-10 days and stored frozen at -80° C until use. Genomic DNA was extracted from the samples using the DNeasy PowerSoil Kit (Qiagen, Carlsbad, CA), as described in the manufacturer's protocol. The concentration and purity of extracted DNA was measured with a NanoDrop Spectrophotometer (Thermo Fisher Scientific, Waltham, MA). The concentration of genomic DNA in all samples was normalized to 10 ng/μL with nuclease-free water (Thermo Fisher Scientific, Waltham, MA). All genomic DNA samples were stored at -80 ℃ until use.

4.2.6 16S rRNA gene sequencing and analysis

Genomic DNA samples were sent to the California Institute for Quantitative Biosciences (qb3) (Berkeley, CA) for amplification of the variable 4 (V4) region of the 16S rRNA gene, library preparation, and amplicon sequencing. The full protocol was previously described on the qb3 website (qb3 2018). In summary, the V4 region of the bacterial 16S rRNA gene was amplified from DNA samples using revised primers 515FB (5'-GTGYCAGCMGCCGCGGTAA-3') and 806RB (3'-TAATCTWTGGGVNCATCAGG-5'), with barcodes attached to either side of the molecule (A dual unique indexing strategy was employed to reduce the occurrence of data bleed within samples.). Amplicons were pooled at equal molality and purified via solid phase reversible immobilization. Paired-end sequencing was then performed on the barcoded, purified amplicons with the Illumina MiSeq sequencer (Illumina, San Diego, CA).

Subsequent sequence processing and data analysis were performed in-house using mothur v.1.39.5, following the MiSeq standard operating procedure (SOP) (Schloss et al. 2009, Kozish et al. 2013). In summary, sequences were demultiplexed, merged, trimmed, and quality filtered. Unique sequences were aligned against the SILVA v.132 16S rRNA gene reference alignment database (Pruesse et al. 2007). Sequences that did not align to the position of the forward primer were discarded. Chimeras were detected and removed. Remaining sequences were clustered into operational taxonomic units (OTUs) within a 97% similarity threshold using the Phylip-formatted distance matrix. Representative sequences from each OTU were assigned taxonomic identities from the SILVA v.132 16S rRNA gene reference alignment database (Pruesse 2007). Sequences that were not classified as bacteria were removed. Remaining OTUs were counted, and the 150 most abundant OTUs (accounting for up to 99% of sequence reads within individual samples) were transferred to Microsoft Excel (Microsoft Office Professional Plus 2016) for downstream interpretation and visualization of their relative abundances. Phylogenetic distances were generated for the 150 most abundant OTUs using Clearcut (Evans et al. 2006).

4.2.7 Statistical analyses

Statistical analyses were performed in Microsoft Excel (Microsoft Office Professional Plus 2016) and RStudio v1.1.383 (RStudio Team 2015) using the ggplot2 and vegan packages. Average concentrations and amounts are reported as the mean +/- standard deviation (SD) for three replicates, unless noted otherwise. SD was calculated as follows:

$$SD = \sqrt{\frac{\sum_{i=1}^{N}(x_i - M)^2}{N - 1}}$$

where $\{x_1, x_2, \ldots, x_N\}$ are the observed values of the sample items, M is the arithmetic mean of these observations, and N is the number of observations in the sample.

A significance level of $\alpha = 0.05$ was used for all analyses, unless noted otherwise. For all analyses involving multiple comparisons, p-values were adjusted using the Sidak correction to maintain a significance level of $\alpha = 0.05$. The correction is given by:

$$p_{adjusted} = 1 - \left(1 - p_{unadjusted}\right)^{n}$$

where *n* is the number of comparisons performed (Sidak 1967; Brisson 2015). Details of statistical methods used for additional analyses are given below.

4.2.7.1 Microbial diversity

The Shannon index (*H'*) was chosen to quantify microbial diversity within each biological sample. *H'* was calculated as follows:

$$H' = -\sum_{i=1}^{N} p_i \ln p_i$$

Where $\{p_1, p_2, \ldots, p_N\}$ are the relative abundances of the OTUs within the biological sample of interest and *N* is the number of observations in the sample (Hill et al. 2006).

4.3 Results and discussion

4.3.1 Efficacy of biomass retention materials

Before moving into longer-term anammox biomass attachment and retention experiments, the biomass support materials were first screened in attempts to understand their potential interactions with the anammox microbial community in a reactor setting. The results of these initial screenings are detailed in the sections below.

4.3.1.1 Sorption capacity

The capacity of the clinoptilolite zeolite to sorb ammonium and nitrite from the synthetic medium under expected reactor conditions was investigated (PVA-SA was not selected as a biomass support material for its sorption capacity, so its sorption capacity for ammonium and nitrite was not formally investigated) (Papageorgiou et al. 2006; Cheraghali et al. 2013; Yu et al. 2017).

The zeolite's sorption capacity was quantified in its natural state (as received from KMI Zeolite), as well as after various pretreatment conditions. Batch sorption tests revealed that the zeolite was able to sorb ammonium, but not nitrite (Figure 4.4; Appendix 5). In its natural state, the zeolite's sorption capacity was roughly 15 mg NH_4^+ per g zeolite. After all three of the pretreatments (DI washing, NaCl washing, and HCl washing), the zeolite's sorption capacity was increased to roughly 30 mg NH_4^+ per g zeolite. Because clinoptilolite zeolite has such a strong preferential sorption capacity for ammonium (the order of preferential sorption for clinoptilolite is delineated in Equation 4.1), it is likely that the zeolite already contained ammonium in its natural state (Tsitsishvili et al. 1992; KMI Zeolite 2018). All three of the pretreatments successfully exchanged the ammonium ions for other constituent ions (most likely H^+ in the case of the DI washing, Na^+ in the case of the NaCl washing, and H^+ in the case of the HCl washing).

4.1) Cs > Rb > K > **NH_4** > Pb > Ag > Ba > Na > Sr > Ca > Li > Cd > Cu > Zn

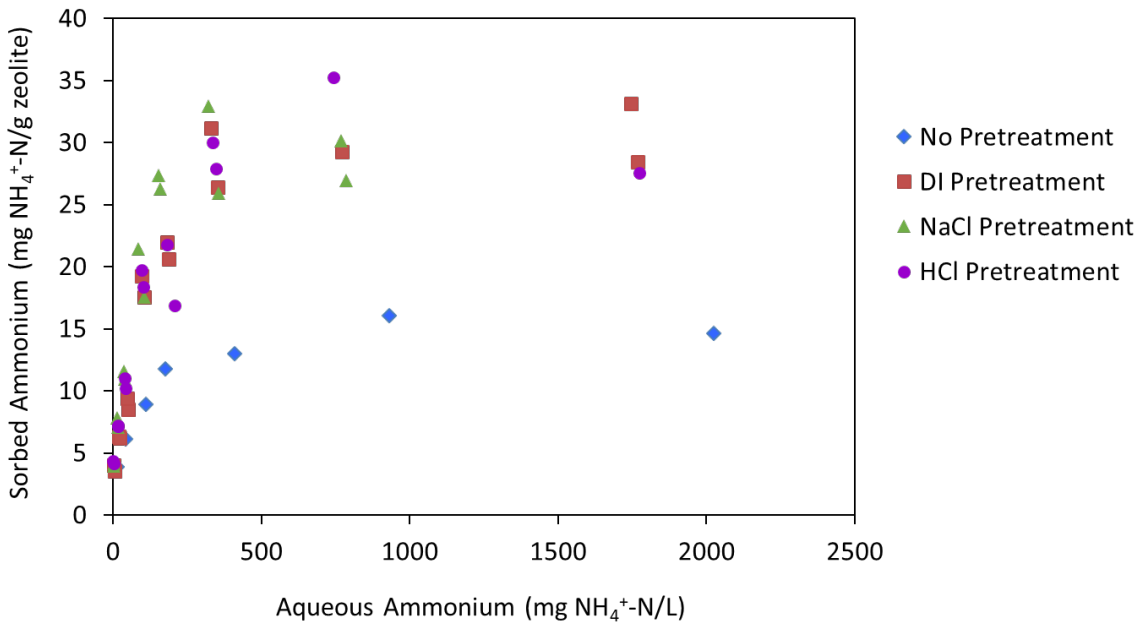

Figure 4.4: Zeolite's ammonium sorption capacity after various pretreatments.

4.3.1.2 Inhibition

The capacity for PVA-SA and zeolite to inhibit anammox performance were investigated in a series of batch anammox reactor experiments. The performances of the reactors were tracked for a period of 10 – 14 days. Differences in influent and effluent concentrations of reactive nitrogen species for each of the batch reactors were then tabulated into the nitrogen removal rate (NRR)—g-N removed, per liter, per day—and used to compare performances across the reactors (Figure 4.5).

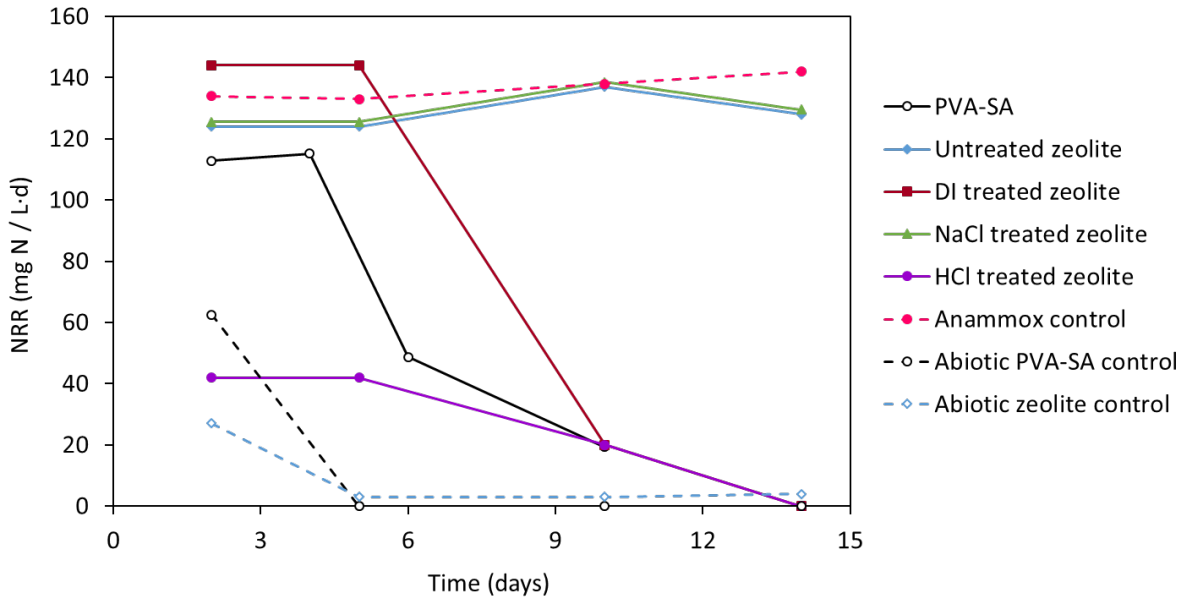

Figure 4.5: Inhibitory effects of biological support materials on anammox performance.

Within the first two days of operation, the anammox control reactor (containing anammox biomass only; no PVA-SA, no zeolite) achieved a NRR of 140 mg N L^{-1} d^{-1}. This NRR was sustained for the duration of the experiment, and was considered the performance baseline for all experimental reactors. The abiotic PVA-SA control reactor (containing biomass-free PVA-SA beads only; no anammox biomass, no zeolite) initially displayed a capacity to remove ammonium and nitrite, but the NRR dropped to zero by the fifth day of the experiment. The abiotic zeolite control reactor (containing zeolite only; no anammox biomass, no PVA-SA) initially displayed a capacity to remove ammonium, but the NRR also dropped to zero by the fifth day of the experiment. The initial nitrogen removal seen in both of these abiotic reactors is most likely due to physical removal from solution: entrapment in the PVA-SA matrix in the case of the abiotic PVA-SA control, and sorption via ion exchange in the case of the abiotic zeolite control.

The PVA-SA experimental reactor (containing anammox biomass entrapped within PVA-SA beads; no zeolite) achieved a NRR of 110 mg N L^{-1} d^{-1} within the first two days of the experiment. However, the NRR dropped to 50 mg N L^{-1} d^{-1} by the sixth day of the experiment, and 25 mg N L^{-1} d^{-1} by the tenth day of the experiment. Within PVA-SA, the diffusion of substrates to microorganisms entrapped within can limit the microorganisms' capacity for growth (Manonmani and Joseph 2018). This factor was expected to be the reason for the limited anammox performance in the PVA-SA experimental reactor. Follow-up experiments were performed to verify that diffusion limitations were indeed the cause of inhibition seen here (Appendix 5). Because the PVA-SA support material did not pass this initial inhibition screening, it did not advance to the longer-term anammox biomass attachment and retention experiments performed in UASB reactors.

The untreated zeolite experimental reactor and the NaCl pretreated reactor (both containing anammox biomass and their respective zeolites; no PVA-SA) achieved and sustained NRRs comparable to the NRR of the anammox control reactor. It appears that zeolite, in its natural form or after the NaCl pretreatment, had no inhibitory effect on anammox performance. The DI pretreated zeolite experimental reactor initially displayed a NRR higher than that of the anammox control reactor, but the DI pretreated zeolite reactor's NRR dropped off quite dramatically by the tenth day of the experiment. The HCl pretreated zeolite experimental reactor displayed a limited NRR from the outset of the experiment. In the case of these two zeolite experimental reactors (i.e., the DI and HCl pretreated zeolites), it is hypothesized that a change in pH was the cause of inhibition seen here.

In summary, NaCl pretreated zeolites not only displayed a higher capacity for ammonium sorption, but they also did not display any inhibitory impacts on anammox performance. As a result, NaCl pretreated zeolites were chosen and the most ideal biomass support material to advance to the longer-term anammox biomass attachment and retention experiments performed in UASB reactors.

4.3.2 UASB reactor performance

The performances of two UASBs, one zeolite-free and another containing 10 g L^{-1} of NaCl pretreated zeolite, were tracked for 50 days to investigate the zeolites' impact on the UASB's startup performance (Figure 4.6a,b). Differences in influent and effluent concentrations of reactive nitrogen species were tabulated into the nitrogen removal rate (NRR)—g-N removed, per liter, per day—and nitrogen speciation ratios (Figure 4.6c).

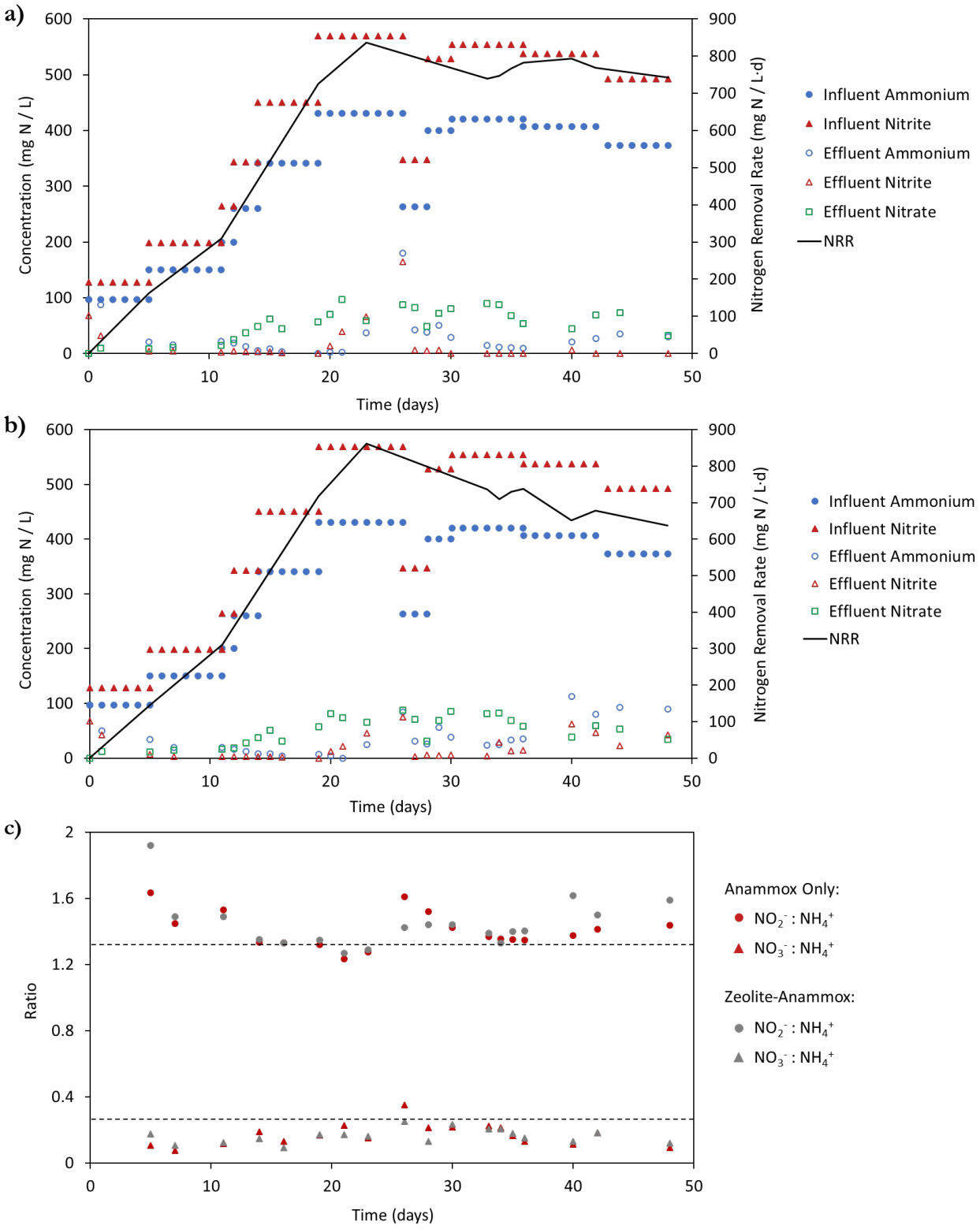

Figure 4.6: Panels (a) and (b) report the influent and effluent concentrations of reactive nitrogen species and the NRR in the zeolite-free and the zeolite-amended UASBs, respectively. Panel (c) reports the nitrogen speciation ratios for both UASBs. The dashed lines represent the stoichiometric nitrogen speciation ratios for anammox.

In summary, the performances of the UASBs steadily improved over the first 26 days of operation. The NRR rose in each UASB, and the ratios of nitrite consumption and nitrate production relative to ammonium consumption converged to the values predicted by anammox stoichiometry (Equation 1.6). The performances of the UASBs over this timespan are practically identical. On day 26, the concentrations of ammonium and nitrite began to rise in the effluents of each of the UASBs, so influent concentrations of ammonium and nitrite were decreased to prevent process failure from nitrite toxicity (Lotti 2012). Process failure was successfully avoided, and the UASBs' performances were quickly restored. After this performance upset, the NRRs of the two UASBs began to diverge. For the last 15 days of the experiment, the UASB without zeolites performed slightly better than the UASB with zeolites. By the conclusion of the experiment, the NRR of the UASB without zeolite was greater than the NRR of the UASB with zeolite by roughly 100 mg N L^{-1} d^{-1}, and the nitrogen speciation ratios had also diverged from the values predicted by anammox stoichiometry (Equation 1.6).

The NRRs of both UASBs declined over the last 15 days of the experiment, indicating that the community may not have fully recovered from the process upset around day 26. Ultimately, it appears that the zeolites had no impact on the UASB's startup performance under the conditions provided in this experiment. Additionally, neither of the reactors reached a NRR of 1 kg N L^{-1} d^{-1} within 30 days—the NRR (and time timeline to achieve it) expected from a full-scale anammox reactor.

This same experiment was repeated again, with one small modification. NaCl was removed from the influent synthetic medium to encourage more sorption of ammonium onto the zeolites. The results from the second iteration of the experiment were similar to the results from the first iteration of the experiment (Appendix 5).

4.3.3 Bacterial community structure

The V4 region of 16S rRNA genes was sequenced at five distinct timepoints over the lifespan of the reactor performance study detailed in Section 4.3.2. These timepoints captured the differences between the zeolite-free and zeolite-amended environments, and also the bacterial community's transition from a controlled washout environment (within the MBR) to an uncontrolled washout environment (within the UASBs).

The resulting OTUs were very similar to those reported in Chapters 2 and 3 (Appendix 6). The few, small discrepancies can be accounted to the use of an updated DNA extraction kit (as the previous kit had been discontinued). Members of the phyla Bacteroidetes, Chlorobi (i.e., Ignavibacteria), Chloroflexi, and Proteobacteria accounted for the majority of the recovered OTUs in the MBR (Gonzalez-Martinez et al. 2015b). These phyla accounted for 19, 13, 23, and 44 of the recovered OTUs, respectively. Members of the genus *Brocadia* were identified as the anammox bacteria within the MBR. 27 OTUs are associated with this genus.

The remainder of the OTUs were classified into the phyla Acidobacteria, Actinobacteria, Cyanobacteria, Firmicutes, Patescibacteria, Planctomycetes, Spirochaetes, and Verrucomicrobia. Due to the current disagreement on the classification of Ignavibacteria as a class of Bacteroidetes, as a class of Chlorobi, or as its own phylum, it has been depicted here as its own phylum (Parks et al. 2018).

4.3.3.1 Temporal community dynamics

The relative abundances of OTUs within each UASB were tabulated into five relative abundance profiles over the lifespan of the reactor performance study detailed in Section 4.3.2 (Figure 4.7; Appendix 6).

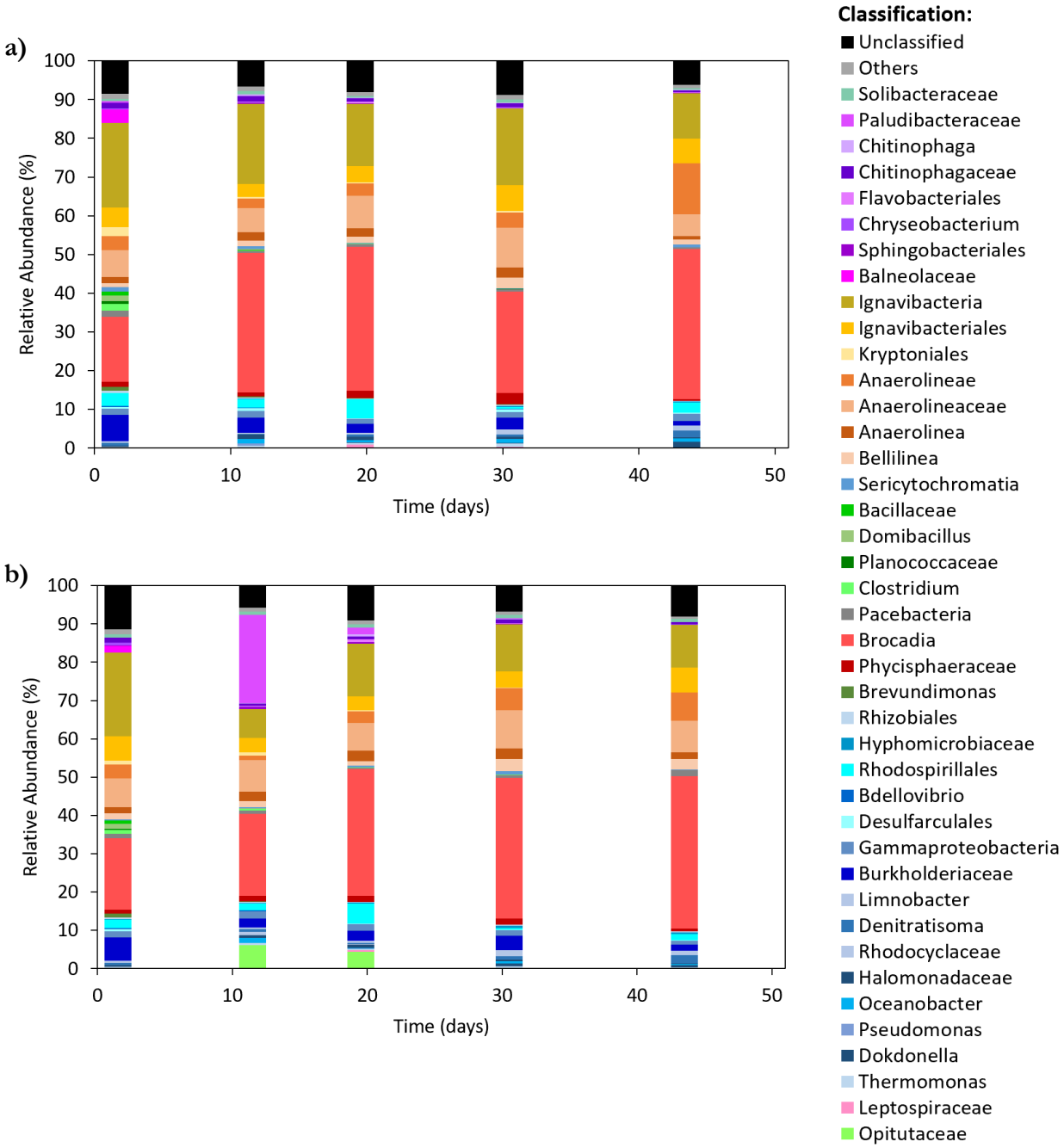

Figure 4.7: Relative abundance profiles of bacterial taxa over the lifespans of the UASBs. Panel (a) refers to the zeolite-free UASB, while Panel (b) refers to the zeolite-amended UASB. "Others" include taxa that were identified, but their relative abundance profiles never reached 0.5% for any of the sequencing timepoints.

At the beginning of experimentation, members of the genus *Brocadia* accounted for 20% of the bacteria in each of the UASB's bacterial communities. Instead, members of the phylum Ignavibacteria were most abundant; they accounted for 30% of the bacteria in each of the UASB's bacterial communities. Over the course of experimentation, the relative abundance profiles of the two UASBs (one zeolite-free, and the other zeolite-amended) evolved fairly similarly. By the end of experimentation, the relative abundance of *Brocadia* rose to 40% in each of the UASB's bacterial communities, and the relative abundance of the phylum Ignavibacteria decreased to 15% in each of the UASB's bacterial communities.

It appears that the addition of zeolite to a UASB anammox reactor had minimal impact on the evolution of the bacterial community. Additionally, it appears that the majority of the bacterial taxa were able to survive the transition from a controlled washout environment (within the MBR) to an uncontrolled washout environment (within the UASBs). The genus *Pseudomonas* was washed out of the zeolite-amended UASB, but all other bacterial taxa that were present at the beginning of experimentation were also present at the end of experimentation.

4.3.4 Conclusions

In Chapter 4, two new support media—PVA-SA and zeolite—were identified to improve biomass retention (and hence, decrease startup time) within an anammox reactor. Their efficacies were investigated through a series of laboratory-scale batch, column, and upflow anaerobic sludge blanket (UASB) reactor experiments. Sodium alginate interfered with the performance of anammox bacteria, so its capacity to enhance anammox reactor performance was not fully investigated here. Only zeolite was amended to UASB reactor experiments. Bacterial community shifts to new lifestyles in a UASB in the presence of zeolite were interpreted through 16S rRNA gene sequencing analyses.

None of the reactors reached a NRR of 1 kg N L^{-1} d^{-1} within 30 days, the NRR (and timeline to achieve it) expected from a full-scale anammox reactor. Additionally, it appears that the zeolites had no impact on the UASB's startup performance under the conditions provided in this experiment, nor the evolution of the bacterial community within the UASB during the startup period. More research must be done to verify the efficacy (or lack, thereof) of zeolite amendments to an anammox UASB reactor. Perhaps a different reactor configuration would allow zeolites to play a more active role in shaping reactor performance and bacterial community structure during the startup of an anammox reactor.

Chapter 5:

Analysis of Co-Occurrence Patterns in Anammox Bacterial Communities

5.1 Introduction

In the past decade, freshwater and groundwater supplies in New Zealand have become increasingly contaminated with reactive nitrogen (Figure 5.1) (NZ ME 2015). The issue has spread across both urban and rural water supplies, with urbanization acting as the main culprit in urban areas and the intensification of dairy farming acting as the main culprit in rural areas (Morton 2017; Shaddad 2017; Wright 2017). As a direct result, 60% of the country's rivers and lakes have become unswimmable, and groundwater supplies have become no longer fit to drink (NZ ME 2015; The Economist 2017).

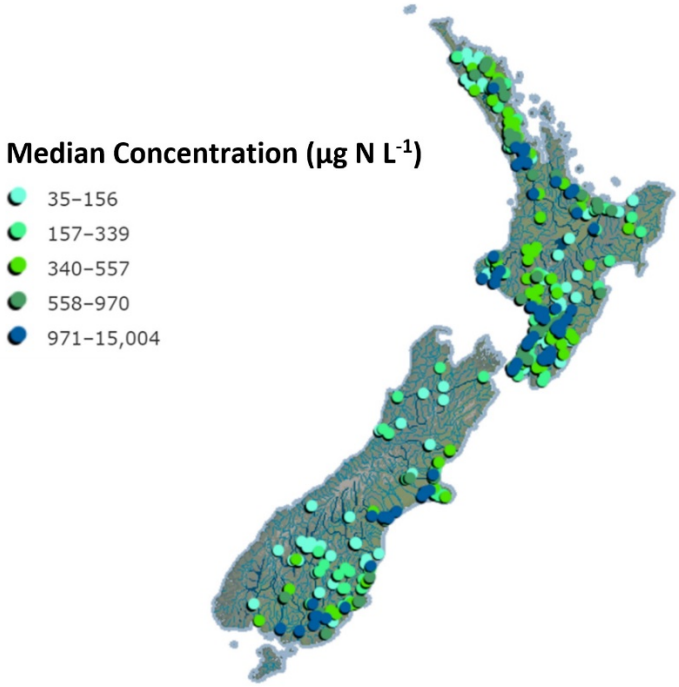

Figure 5.1: Total nitrogen concentrations in New Zealand rivers (adapted from NZ ME 2015).

The anammox technology stands out as a viable option to manage the reactive nitrogen pollution originating from wastewater treatment plants across New Zealand. Unfortunately, current laws ban the import of new organisms into the country: any organism that was not documented to be within New Zealand on or before July 29, 1998 is considered a new organism and cannot be introduced into the country (NZ ME 2017; EPA TMRT 2018). All species of anammox bacteria are considered new organisms under this law, so anammox biomass cannot be purchased and imported from any of the leading anammox technology providers to seed a new reactor. If decision-makers in New Zealand decide to pursue the anammox technology, the anammox biomass for the country's initial reactor must be enriched from an indigenous source (Suneethi et al. 2014).

Across the globe, anammox bacteria have been detected in almost every habitat, from freshwater sediments to marine water columns to geothermal hotsprings to the intestinal tracts of fish (Jaeschke et al. 2009; Sonthiphand et al. 2014; Chan et al. 2016). Their role in some of these natural habitats can be quite extensive: anammox bacteria may be responsible for up to 30% of the reactive nitrogen conversions in marine environments, and up to 36% of the reactive nitrogen conversions in

freshwater environments (Moore et al. 2011; Babbin et al. 2014). Thus, it is extremely likely that anammox bacteria not only exist, but also play crucial roles, in New Zealand's natural habitats. The work presented in this chapter supports the development of the anammox technology within New Zealand by investigating a catalogue of microbial diversity within New Zealand's stream habitats for the presence of indigenous species of anammox bacteria. Once anammox bacteria have been identified, scientists and engineers can begin to enrich an indigenous anammox microbial community to seed New Zealand's first anammox reactor (Perez-Garcia et al. 2018).

As previously discussed in Chapter 2, one opportunity to improve the functionality of anammox reactors lies in the identification of patterns in microbial community structure that support the proliferation of anammox bacteria. The resulting patterns can then be used to inform targeted strategies to improve the performance the anammox reactor. In this chapter, previous analyses of microbial community structure will be extended to include the freshwater habitat samples from New Zealand that contain anammox bacteria. This extended investigation will support the fundamental, community-level understanding of the anammox process, not only within New Zealand, but also across the rest of the globe.

5.2 Materials and methods

5.2.1 Database collation

A catalogue of microbial diversity within New Zealand's stream habitats, recorded as unprocessed 16S rRNA gene sequences and accompanying metadata, was provided for this investigation by Dr. Gavin Lear from the University of Auckland. The samples that comprised this catalogue were collected from biofilms growing on submerged rocks in 244 rivers and streams across New Zealand. The samples spanned a north-south gradient of 1000 km, an elevation gradient of 750 m, and were collected from a variety of catchment types (Appendix 7) (Lear et al. 2013). Additional information regarding sample locations, sample processing, and sequencing can be found in Lear et al. 2013.

5.2.2 16S rRNA gene sequence processing

16S rRNA gene sequence processing and data analysis were performed in-house using mothur v.1.39.5, following the MiSeq standard operating procedure (SOP) (Schloss et al. 2009, Kozish et al. 2013). In summary, sequences were demultiplexed, merged, trimmed, and quality filtered. Unique sequences were aligned against the SILVA v.132 16S rRNA gene reference alignment database (Pruesse et al. 2007). Sequences that did not align to the position of the forward primer were discarded. Chimeras were detected and removed. Remaining sequences were clustered into operational taxonomic units (OTUs) within a 97% similarity threshold using the Phylip-formatted distance matrix. Representative sequences from each OTU were assigned taxonomic identities from the SILVA v.132 16S rRNA gene reference alignment database (Pruesse 2007). Sequences that were not classified as bacteria were removed. Remaining OTUs were counted, and the 2500 most abundant OTUs (accounting for a minimum of 76% of sequence reads within individual samples) were transferred to Microsoft Excel (Microsoft Office Professional Plus 2016) for downstream interpretation and visualization of their relative abundances.

Representative sequences were extracted from each of the 2500 most abundant OTUs. Separately, nine anammox sequences, spanning all five of the currently recognized anammox genera, were identified and downloaded from the National Center for Biotechnology Information (NCBI) database (Appendix 7) (NCBI 2018a). The representative sequences and anammox sequences were combined and re-aligned against the SILVA v.132 16S rRNA gene reference alignment database. Phylogenetic distances were generated using Dendroscope to identify the representative sequences from the OTUs that aligned with the anammox sequences (Huson and Scornavacca 2012). Average nucleotide sequence identities between representative sequences from the OTUs and anammox sequences were calculated using the NCBI average nucleotide identity tool (NCBI 2018b).

5.2.3 Statistical analyses

Statistical analyses were performed in Microsoft Excel (Microsoft Office Professional Plus 2016) and RStudio v1.1.383 (RStudio Team 2015) using the igraph, ggplot2, and vegan packages. A significance level of $\alpha = 0.05$ was used for all analyses, unless noted otherwise. Details of statistical methods used for additional analyses are given below.

5.2.3.1 Nonmetric multidimensional scaling (NMDS)

Relative abundance profiles of bacterial taxa from select samples within the catalogue of microbial diversity in New Zealand's stream habitats were combined with previously reported relative abundance profiles of bacterial taxa within anammox reactors, and nonmetric multidimensional scaling (NMDS) was used to collapse information across all of these samples onto a two-dimensional plot for visualization and interpretation (Oksanen 2018). In summary, the original positions of each sample were defined in multidimensional space based on the rank-order of the relative abundances of bacterial taxa within the sample. If relative abundance data was provided at the OTU-level, OTUs that were assigned identical taxonomies were merged. An initial, random configuration of the bacterial taxa and samples was constructed in two-dimensions. Distances in this initial configuration were regressed against the observed (i.e., measured) distances. The stress (i.e., disagreement) between the initial configuration and predicted values from the regression were determined. Configurations were iterated until the stress value became less than 0.1.

5.2.3.2 Network analysis

Network analysis was used to investigate co-occurrence patterns of bacterial taxa within the samples that contained (potential) anammox sequences, as identified in section 5.2.3.1 (Barberan et al. 2012; Sonthiphand et al. 2014). In summary, Spearman's rank correlations were calculated between all bacterial taxa with a relative abundance of at least 0.5% in one of the samples. Bacterial taxa that did not meet this requirement were excluded from all downstream analyses. A correlation was considered valid if the Spearman's correlation coefficient was both greater than 0.6 and statistically significant ($\alpha < 0.05$) (Junker and Schreiber 2008). Valid correlations were then transferred to Gephi v.0.9.2, where co-occurrence network properties were calculated and visualized in accordance with previous studies (Bastian et al. 2009; Ju et al. 2014; Ma et al. 2016; Shu et al. 2018).

5.3 Results and discussion

5.3.1 Potential anammox bacterial taxa within New Zealand

A phylogenetic tree was constructed using Dendroscope to identify OTUs within New Zealand's stream habitat samples that aligned with anammox sequences (Appendix 7) (Huson and Scornavacca 2012). One OTU—number 262—was clustered with the anammox sequences on the resulting phylogenetic tree. Average nucleotide sequence identities between OTU 262 and the anammox sequences were calculated using the NCBI average nucleotide identity tool (Table 5.1) (NCBI 2018b). Thresholds for bacterial taxonomic boundaries, based on the identities of 16S rRNA gene sequences (97% for species, 94.5% for genus, 86.5% for family, 82.0% for order, 78.5% for class, and 75% for phylum), were used to classify OTU 262 against the known anammox genera (Fox et al. 2012; Yarza et al. 2014). OTU 262 fell just below the threshold for the family Brocadiaceae, but within the threshold for the order Brocadiales. Currently, all of the species identified within this order are capable of anammox metabolism (van Niftrik and Jetten 2012). Of course, deeper analyses are required to verify this particular OTU's capacity for anammox metabolism.

Genus	Average nucleotide identity	Shared classification level
Anammoxoglobus	83%	Order
Brocadia	85%	Order
Jettenia	83%	Order
Kuenenia	85%	Order
Scalindua	79%	Class

Table 5.1: Classification of OTU 262.

OTU 262 was identified in 48% of the samples analyzed in this study. The magnitude of its relative abundance was greatest within sample AKD2.10, at 0.5% (Figure 5.2; Appendix 7). AKD2.10 was collected from a grassland catchment area near Auckland, New Zealand, 20 m above sea level (Appendix 7). At the time of sampling, the stream's pH at sample site AKD2.10 was 6.1, and the total nitrogen concentration was 1.9 mg L^{-1}.

Members of the phylum Proteobacteria accounted for the majority of the recovered OTUs in AKD2.10. The remainder of the OTUs were classified into the phyla Acidobacteria, Actinobacteria, Bacteroidetes, Chlorobi, Chloroflexi, Cyanobacteria, Firmicutes, Gemmatimonadetes, Nitrospirae, Planctomycetes, and Verrucomicrobia.

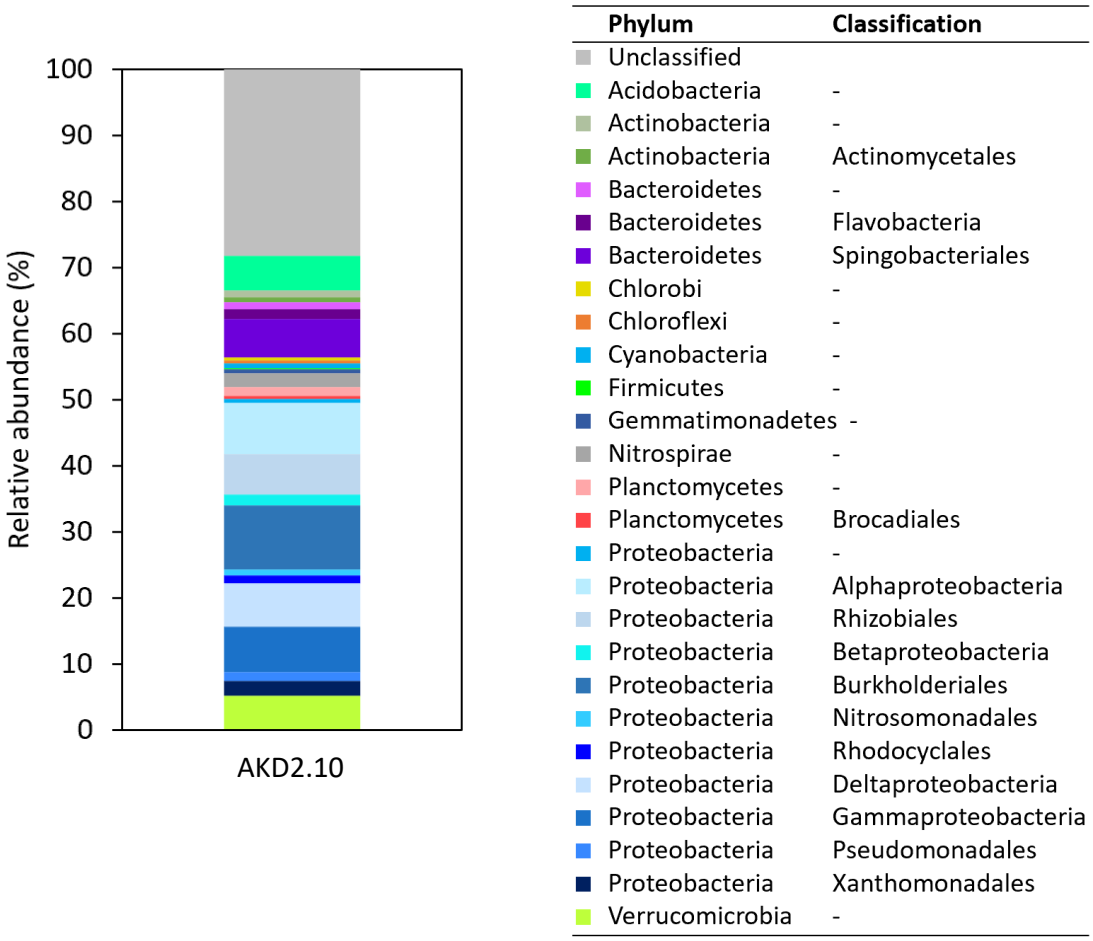

Figure 5.2: Relative abundance profiles of bacterial taxa within AKD2.10 (the select New Zealand habitat sample).

5.3.2 Database structure

In order to draw correlations between the bacterial community structure in New Zealand habitat samples and the bacterial community structure in established anammox bacterial communities, previously reported relative abundance profiles of bacterial taxa from anammox reactors were collected and synthesized, along with their supporting metadata (Figure 5.3; Table 5.2; Appendix 7) (Gonzalez-Martinez et al. 2014; Chu et al. 2015; Gonzalez-Gil et al. 2015; Gonzalez-Martinez et al. 2015a; Bagchi et al. 2016; Gonzalez-Martinez et al. 2016; Agrawal et al. 2017; Liu et al. 2017; Wang et al. 2017; Ding et al. 2018; He et al. 2018; Tang et al. 2018; Xu et al. 2018).

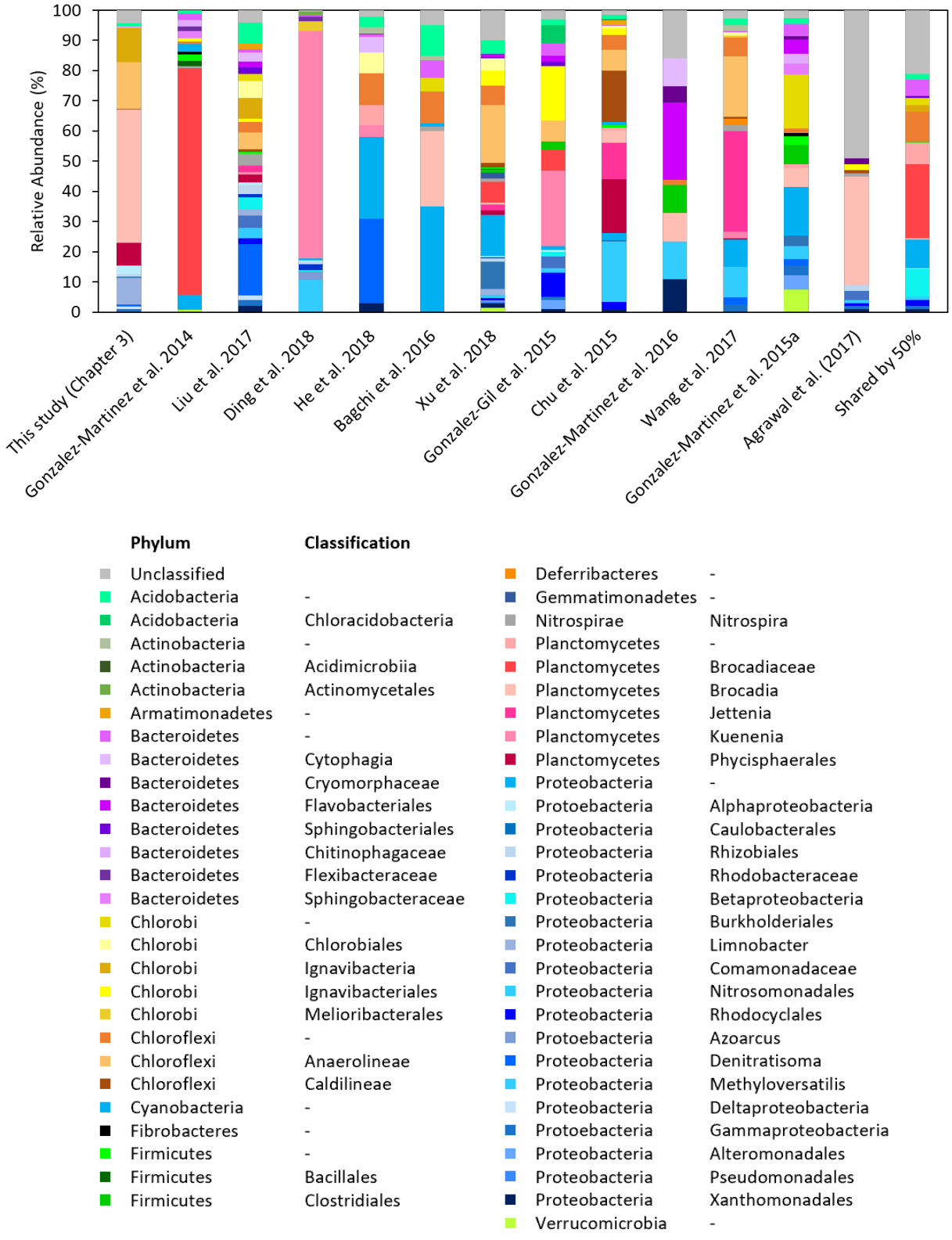

Figure 5.3: Relative abundance profiles of bacterial taxa within anammox reactors. Bacterial taxa that were found in at least 50% of the reactors are plotted in the last column, "Shared by 50%."

Only members of the phyla Bacteroidetes, Planctomycetes, and Proteobacteria were found in all of the anammox reactor samples. Aside from the order Brocadiales, no other higher classifications were found in all of the anammox reactor samples. The majority of the reactors (i.e., > 50%) contained members of the phylum Acidobacteria, the order Sphingobacteriales within the phylum Bacteroidetes, the phylum Chlorobi and the class Ignavibacteria within it, the phylum Chloroflexi, the phylum Firmicutes, the genus *Brocadia* within the phylum Planctomycetes, the classes Alphaproteobacteria, Betaproteobacteria, and Gammaproteobacteria within the phylum Proteobacteria, the orders Burkholderiales, Nitrosomonadales, and Rhodocyclales within the class Alphaproteobacteria, and the order Xanthomonadales within the class Gammaproteobacteria.

Aside from the class Ignavibacteria within the phylum Chlorobi and the genus *Brocadia* within the phylum Planctomycetes, all of the aforementioned bacterial taxa were also found in AKD2.10.

Reporting Authors	Configuration	Vessel Size (L)	Temperature (°C)	pH	HRT (hrs)
This study (Chapter 3)	MBR	1	37	7.2	12
Gonzalez-Martinez et al. 2014	MBR	10	30	7	40
Liu et al. 2017	stirred-tank	2.4	15 - 17	7.5 - 7.8	2
Ding et al. 2018	stirred-tank	2.4	30	7.3 - 7.6	72
He et al. 2018	UASB	2.5	33	7.5 - 7.9	24
Bagchi et al. 2016	SBR	4	21	6.8 - 7.2	16
Tang et al. 2018	SBR	3	37	6.8 - 7.0	18
Xu et al. 2018	SBR	6	35	7.5 - 8.3	24
Gonzalez-Gil et al. 2015	SHARON	70,000	31 - 37	7.5 - 8	19.4
Chu et al. 2015	SBR	2	33	7.5	24
Gonzalez-Martinez et al. 2016	SBR	2.7	21	7.1 - 7.5	7
Wang et al. 2017	SBR	2	33	7.8 - 8.2	16
Gonzalez-Martinez et al. 2015a	DEMON	24,000	30	6.7	8
Agrawal et al. 2017	MBBR	10	10	7 – 7.6	36

Reporting Authors	Medium Source	Nitritation Included?	Influent TN (mg N/L)	NH4 : NO2
This study (Chapter 3)	synthetic	no	1260	1:1.1
Gonzalez-Martinez et al. 2014	synthetic	no	1680	1:1
Liu et al. 2017	synthetic	no	50	1:1
Ding et al. 2018	synthetic	no	700	1.5:1
He et al. 2018	synthetic	no	600	1:1.32
Bagchi et al. 2016	synthetic	no	220	1:1.3
Tang et al. 2018	synthetic	no	600	1:1
Xu et al. 2018	synthetic	no	138	1:1.3
Gonzalez-Gil et al. 2015	digested sludge liquor	no	1200	1:1
Chu et al. 2015	synthetic	yes	250	N/A
Gonzalez-Martinez et al. 2016	synthetic	yes	160	N/A
Wang et al. 2017	synthetic	yes	200	N/A
Gonzalez-Martinez et al. 2015a	digested sludge liquor	yes	1208	N/A
Agrawal et al. 2017	synthetic	yes	50	N/A

Table 5.2: Metadata for the anammox reactors. "SHARON" and "DEMON" are both propriety names of full-scale anammox reactor configurations (van Dongen et al. 2001; WWW 2015).

Aside from the SHARON and DEMON full-scale reactors, all of the reactors were laboratory-scale. The full-scale reactors were fed digested sludge liquor from municipal wastewater treatment plants, while the laboratory-scale reactors were fed synthetic medium. In general, the anammox reactors were maintained at mesophilic temperatures and circumneutral pH.

5.3.2.1 Community grouping

To examine overall similarities in bacterial community structure between the New Zealand stream samples that contained (potential) anammox sequences and established anammox reactors, NMDS analyses were applied to the relative abundance profiles of the New Zealand stream samples that contained (potential) anammox sequences and the anammox reactor samples collected from the literature (Figure 5.4; Appendix 7). The resulting NMDS projection shows that AKD2.10 falls right in the center of the anammox reactor samples. While the bacterial community structure of AKD2.10 is not identical to any of the bacterial community structures within the anammox reactor samples, it does share a significant number of similarities with all of the anammox reactor samples. Ultimately, these similarities suggest that the anammox bacterial community typical of a successful anammox reactor may be successfully enriched from New Zealand's stream habitat.

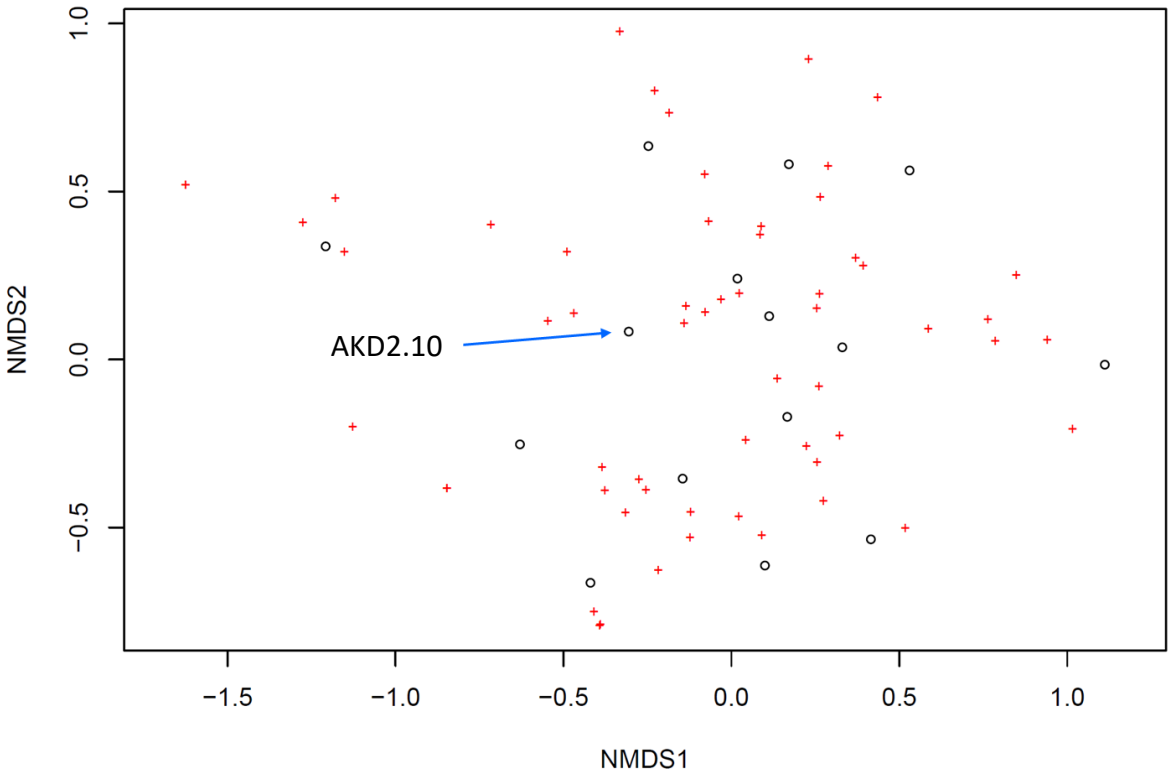

Figure 5.4: Nonmetric multidimensional scaling (NMDS) projection of bacterial taxa and biological samples. Bacterial taxa are represented by red crosses, and biological samples are represented by open, black circles. AKD2.10, the New Zealand stream sample, has been highlighted.

5.3.2.2 Co-occurrence patterns

To identify co-occurrence patterns among bacterial taxa within anammox-containing microbial communities, network analyses were applied to the relative abundance profiles of the New Zealand stream samples that contained (potential) anammox sequences and the anammox reactor samples collected from the literature (Figure 5.5; Appendix 7). The resulting co-occurrence projection shows that the majority of bacterial taxa within these samples do not have statistically significant connections to other taxa. A few connections can be seen between a handful of the minor taxa, but none of these connections included any of the anammox bacteria. A lack of input data may potentially be responsible for the lack of statistically significant connections among bacterial taxa (Berry and Widder 2014).

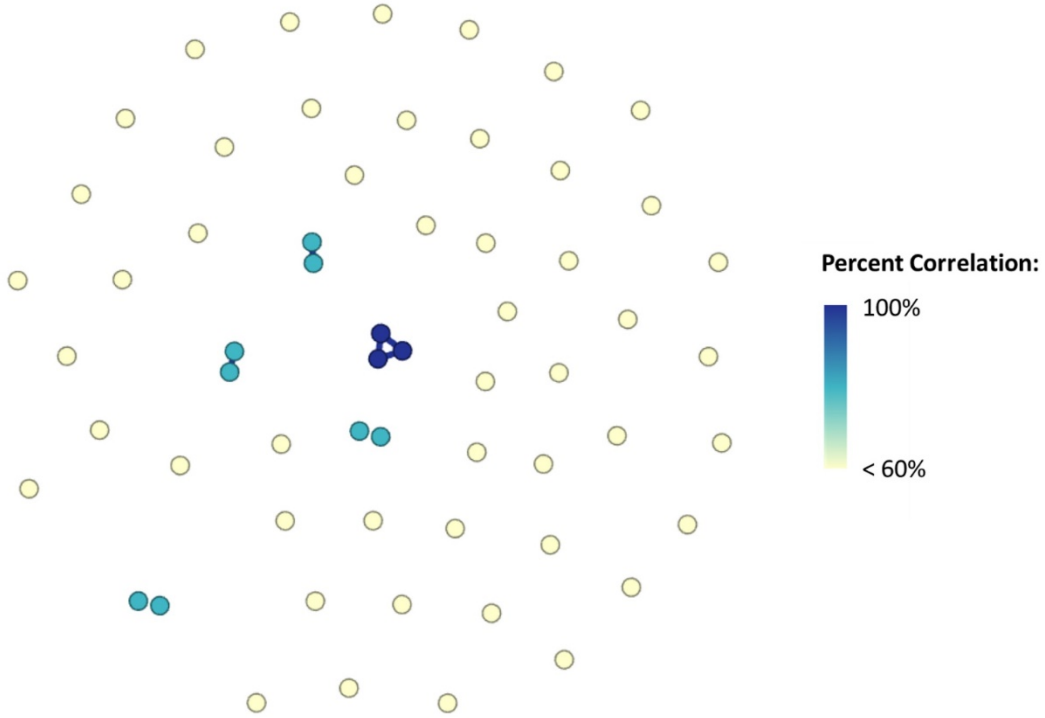

Figure 5.5: Co-occurrence patterns among bacterial taxa within the biological samples. Each circle represents a bacterial taxon. Bacterial taxa that do not have any statistically significant connections to other taxa are colored in yellow, and are disconnected from neighboring taxa. Bacterial taxa that do have statistically significant connections to other taxa are colored in varying shades of green/blue, and are connected to their co-occurring taxon(a).

5.3.3 Conclusions

The anammox technology stands out as a viable option to sustainably manage the rising levels of reactive nitrogen pollution across New Zealand. Because national laws prohibit the import of new microorganisms (including anammox) into the country, anammox-containing biomass for New Zealand's initial anammox reactor must be enriched from an indigenous source (Suneethi et al. 2014). This initial investigation into a catalogue of microbial diversity within New Zealand's stream habitats revealed that anammox bacteria may indeed be present within the country. Further

investigations into the overall bacterial community structure of a select New Zealand stream habitat sample revealed that the sample's bacterial community structure shared many similarities with the overall bacterial community structure of established anammox reactors.

Ultimately, the results of these investigations suggest that the bacterial community typical of an anammox reactor may be successfully enriched from New Zealand's stream habitats. Moving forward, more experimentation must be done to verify the capacity for anammox metabolism within New Zealand's stream habitats. If these experiments are successful, then scientists and engineers can begin to enrich an indigenous anammox microbial community to seed New Zealand's first anammox reactor.

Chapter 6:

Conclusions and Suggestions for Future Work

Since the inception of the Haber-Bosch Process, the global rate of nitrogen gas fixation into reactive nitrogen has doubled (UNEP 2007). Excess concentrations of reactive nitrogen are escaping into aquatic environments surrounding all of the inhabited continents, primarily through agricultural runoff and wastewater effluent (UNSD 2018). As world populations continue to grow, these excess concentrations of reactive nitrogen will grow as well. If left unchecked, these rising concentrations of reactive nitrogen will wreak havoc on the health of aquatic environments and the communities that depend upon them. Moving forward, it will only become more important for municipalities and industries to protect the health of their nearby aquatic environments by removing reactive nitrogen from their wastewater streams before they are discharged to the environment. A new technology, anammox, shows promise as energy-efficient treatment process that removes reactive nitrogen from wastewater. Unfortunately, the bacteria responsible for anammox have very low growth rates within engineered conditions, and are easily inhibited by a variety of factors including temperature, pH, and variable substrate and metabolite concentrations. These problems are compounded by what is now only a cursory understanding of the microbial communities that are responsible for the stable and robust performance of the anammox treatment process.

While there is a substantial body of literature describing the performance of the anammox treatment process in response to various perturbations and operational conditions, very few studies have examined anammox bacteria's performance on a molecular level or the roles of other bacteria within anammox reactors. The work presented in this dissertation seeks to fill this gap by investigating the temporal dynamics of the anammox bacterial community during the start-up and continued operation of laboratory-scale treatment processes, as well as the spatial dynamics of the anammox bacterial community across a nitrogen-contaminated environment. The results of this work have bolstered the fundamental, community-level understanding of the anammox treatment process. This, in turn, will enable more comprehensive control of this promising technology and help facilitate its widespread adoption at municipal wastewater treatment plants across the globe.

Chapter 2 began with a review of previous literature that supports the idea of a core microbial community within anammox treatment process reactors. This review was combined with temporal-scale data from 440 days of continuous operation of a laboratory-scale anammox reactor to identify trends in bacterial community composition and associated reactor performance. Results indicate that anammox, denitrifying, and DNRA bacteria are omnipresent in the laboratory-scale anammox reactor. Results also suggest that these bacteria may cooperate and maximize nitrogen removal under desirable conditions, but that they may compete and sabotage nitrogen removal under undesirable conditions (primarily because they share an electron acceptor—nitrite). More research must be done to understand and control the conditions that support cooperation versus competition between these three groups of nitrogen-cycling bacteria in an anammox reactor. Moving forward, more in-depth metagenomic and metatranscriptomic analyses of the microbial community within anammox reactors are recommended. These analyses will provide insight into the actual nitrogen-cycling capabilities of individual microorganisms within the anammox community, and the conditions that support and suppress their metabolic functions.

Chapter 3 built off Chapter 2 and dug more deeply into the relationship between anammox, denitrifying, and DNRA bacteria. The performance and temporal dynamics of these three groups of nitrogen-cycling bacteria was investigated through manipulations of the ratio of ammonium to nitrite concentrations in the influent wastewater stream provided to a laboratory-scale anammox reactor. Results indicate that an influent ammonium to nitrite concentration ratio of 1 to 1.32 favors

the enrichment of the anammox species in the laboratory-scale anammox reactor, while lower ammonium to nitrite concentration ratios (1 to 1.1 – 1 to 1.2) favor the enrichment of a more diverse bacterial community (that may include denitrifying and DNRA bacteria) in the laboratory-scale anammox reactor. Results also suggest that a more diverse bacterial community (containing denitrifying and DNRA bacteria alongside anammox bacteria) has a greater capacity to remove reactive nitrogen species from wastewater, as it is capable of removing not only ammonium and nitrite, but also nitrate—the product of anammox metabolism—from wastewater. Nevertheless, still more research must be done to elucidate the precise mechanisms that control the interactions among these three groups of nitrogen-cycling bacteria within an anammox reactor. Again, more in-depth metagenomic and metatranscriptomic analyses of the microbial community within anammox reactors are recommended. These analyses will provide insight into the actual nitrogen-cycling capabilities of individual microorganisms within the anammox community, and the conditions that support and suppress their metabolic functions.

In Chapter 4, the capacity of two new support media—PVA-SA and clinoptilolite zeolite—to improve biomass retention (and hence, decrease startup time) within an anammox reactor was investigated through a series of laboratory-scale batch, column, and UASB reactor experiments. Corresponding bacterial community shifts to new lifestyles in the presence of these support media were also interpreted through 16S rRNA gene sequencing analyses. Results indicated that neither of the support media were able to improve the performance of the laboratory-scale anammox reactors under the conditions provided in this study. Moreover, results indicated that the amendment of zeolite to a laboratory-scale UASB reactor had no impact on the structure of the bacterial community within it (again, under the conditions provided in this study). More research must be done to rule out the capacity of PVA-SA and clinoptilolite zeolite to improve the performance of the anammox treatment process. Perhaps these support media were not prepared and supplied to the reactors in the appropriate ways. Moving forward, more efficient ways to combine anammox bacteria and PVA-SA are recommended. Since diffusion of substrates through the PVA-SA matrix was identified as a barrier to the success of anammox bacteria within the PVA-SA matrix, more care should be taken to ensure that the anammox bacteria fall near the exterior of the PVA-SA matrix. Additionally, more efficient ways to combine anammox bacteria and zeolite are recommended. Because the zeolite particles were significantly denser than the synthetic wastewater media, the majority of them fell to the bottom of the UASBs during experimentation. Strategies should be identified to allow the zeolites to become more buoyant with the reactor of choice. In future iterations of experimentation, perhaps the zeolite could also be entrapped within the PVA-SA matrix.

Chapter 5 investigated the abundance and distribution of anammox bacteria across nitrogen-contaminated stream habitats in New Zealand. The results of these investigations suggested that the bacterial community typical of an anammox reactor may be successfully enriched from New Zealand's stream habitats. Moving forward, more experimentation must be done to verify the capacity for anammox metabolism within select locations in New Zealand's stream habitats. To achieve this, metagenomic analyses of the microbial communities within select locations in New Zealand's stream habitats are recommended. These analyses will provide insight into the actual nitrogen-cycling capabilities of individual microorganisms within the anammox community, and the conditions that support and suppress their metabolic functions. If these experiments successfully verify the presence of anammox activity within select locations in New Zealand's stream habitats,

scientists and engineers can begin to enrich an indigenous anammox microbial community to seed New Zealand's first anammox reactor.

Ultimately, the results of the research described in this dissertation bolster the fundamental understanding of the bacterial communities that exist within the anammox treatment process. These results, in turn, should enable the more comprehensive control of the promising anammox technology and help facilitate its widespread adoption at municipal and industrial wastewater treatment plants across the globe.

References

S. Agrawal, S. Karst, E. Gilbert, H. Horn, P. Nielsen, S. Lackner (2017) "The role of inoculum and reactor configuration for microbial community composition and dynamics in mainstream partial nitritation anammox reactors." *MicrobiologyOpen* 6 (4) 1 – 11.

L. Alejo-Alvarez, V. Guzman-Fierro, K. Fernandez, M. Roeckel (2016) "Technical and economical optimization of a full-scale poultry manure treatment process: Total ammonia nitrogen balance." *Environmental Technology* 37 (22) 2865 – 2878.

M. Ali, S. Okabe (2015a) "Anammox-based technologies for nitrogen removal: Advances in process start-up and remaining issues." *Chemosphere* 141 144 – 153.

M. Ali, M. Oshiki, L. Rathnayake, S. Ishii, H. Satoh, S. Okabe (2015b) "Rapid and successful start-up of anammox process by immobilizing the minimal quantity of biomass in PVA-SA gel beads." *Water Research* 79 147 – 157.

American Public Health Association (APHA) (2005) "Standard methods for the examination of water and wastewater, 21st edition." American Public Health Association, Washington, DC 20005.

K. Arrigo (2005) "Marine microorganisms and global nutrient cycles." *Nature* 437 (7057) 349 – 355.

R. Babbin, G. Keil, H. Devol, B. Ward (2014) "Organic matter stoichiometry, flux, and oxygen control nitrogen loss in the ocean." *Science* 344 406 – 408.

S. Bagchi, R. Lamendella, S. Strutt, M. van Loosdrecht, P. Saikaly (2016) "Metatranscriptomics reveals the molecular mechanism of large granule formation in granular anammox reactor." *Scientific Reports* 6 28327.

A. Barberan, S. Bates, E. Casamayor, N. Fierer (2012) "Using network analysis to explore co-occurrence patterns in soil microbial communities." *The ISME Journal* 6 343 – 351.

M. Bastian, S. Heymann, M. Jacomy (2009) "Gephi: an open source software for exploring and manipulating networks." *International Association for the Advancement of Artificial Intelligence Conference on Weblogs and Social Media*, San Jose, Californa.

D. Berry, S. Widder (2014) "Deciphering microbial interactions and detecting keystone species with co-occurrence networks." *Frontiers in Microbiology* 5 (219) 1 – 14.

A. Bhattacharjee, S. Wu, C. Lawson, M. Jetten, V. Kapoor, J. Santo Domingo, K. McMahon, D. Noguera, R. Goel (2017) "Whole-community metagenomics in two different anammox configurations: Process performance and community structure." *Environmental Science and Technology* 51 (8) 4317 – 4327.

V. Brisson (2015) "Utilizing "omics" based approaches to investigate targeted microbial practices." ProQuest Dissertation Number 3720393.

A. Burgin, S. Hamilton (2007) "Have we overemphasized the role of denitrification in aquatic ecosystems? A review of nitrate removal pathways." *Frontiers in Ecology and the Environment* 5 (2) 89 – 96.

P. Cabello, M. Roldan, C. Moreno-Vivian (2004) "Nitrate reduction and the nitrogen cycle in archaea." *Microbiology* 150 (11) 3527 – 3546.

California Institute for Quantitative Biosciences (qb3) (2018) " iTag library generation and sequencing." http://qb3.berkeley.edu/gsl/itag-library-generation-and-sequencing/. Accessed 10/11/18 at 6:00pm.

J. Camargo, Á. Alonso (2006) "Ecological and toxicological effects of inorganic nitrogen pollution in aquatic ecosystems: A global assessment." *Environment International* 32 831 – 849.

D. Canfield, A. Glazer, P. Falkowski (2010) "The evolution and future of Earth's nitrogen cycle." *Science* 330 (6001) 192 – 196.

S. Cao, R. Du, B. Li, N. Ren, Y. Peng (2016) "High-throughput profiling of microbial community structures in an ANAMMOX-UASB reactor treating high-strength wastewater." *Applied Microbiology and Biotechnology* 100 (14) 6457 – 6467.

J. Carvajal-Arroyo, W. Sun, R. Sierra-Alvarez, J. Field (2013) "Inhibition of anaerobic ammonium oxidizing (anammox) enrichment cultures by substrates, metabolites, and common wastewater constituents." *Chemosphere* 91 22 – 27.

C. Castro-Barros, M. Jia, M. van Loosdrecht, E. Volcke, M. Winkler (2017) "Evaluating the potential for dissimilatory nitrate reduction by anammox bacteria for municipal wastewater treatment." *Bioresource Technology* 233 363 – 372.

H. Chan, H. Meng, J. Gu (2016) "Anammox bacteria detected in fish intestinal tract systems." *Applied Environmental and Biotechnology* 1 13 – 18.

H. Chen, J. Yu, X. Jia, R. Jin (2014) "Enhancement of anammox performance by Cu(II), Ni(II), and Fe(III) supplementation." *Chemosphere* 117 610 – 616.

R. Cheraghali, H. Tavakoli, H. Sepehrian (2013) "Preparation, characterization, and lead sorption performance of alginate-SBA-15 composite as a novel adsorbent." *Scientia Iranica* 20 (3) 1028 – 1034.

K. Cho, M. Choi, S. Lee, H. Bae (2018) "Negligible seeding source effect on the final ANAMMOX community under steady and high nitrogen loading rate after enrichment using poly(vinyl alcohol) gel carriers." *Chemosphere* 208 21 – 30.

S. Cho, Y. Takahashi, N. Fujii, Y. Yamada, H. Satoh (2010) "Nitrogen removal performance and microbial community analysis of an anaerobic up-flow granular bed anammox reactor." *Chemosphere* 78 1129 – 1135.

M. Christensson, S. Ekstrom, A. Andersson Chan, E. Le Vaillant, R. Lemaire (2012) "Experience from start-ups of the first ANITA Mox plants." *Water Science and Technology* 67 (12) 2677 – 2684.

Z. Chu, K. Wang, X. Li, M. Zhu, L. Yang, J. Zhang (2015) "Microbial characterization of aggregates within a one-stage nitritation-anammox system using high-throughput amplicon sequencing." *Chemical Engineering Journal* 262 41 – 48.

Y. Chung, D. Son, D. Ahn (2000) "Nitrogen and organics removal from industrial wastewater using natural zeolite media." *Water Science and Technology* 42 (5 – 6) 127 – 134.

Coldstream Industries (2015) "Zeolite – top 10 uses for this mighty mineral." http://blog.coldstreamoutdoor.com/top-10-uses-for-zeolite/. Accessed 10/09/18 at 5:00pm.

R. Collison, M. Grismer (2018) "Upscaling the zeolite-anammox process: Treatment of secondary effluent." *Water* 10 (3) 236.

R. Connan, P. Dabert, H. Khalil, G. Bridoux, F. Beline, A. Magri (2016) "Batch enrichment of anammox bacteria and study of the underlying microbial community dynamics." *Chemical Engineering Journal* 297 217 – 228.

J. Cornwell, W. Kemp, T. Kana (1999) "Denitrification in coastal ecosystems: Methods, environmental controls, and ecosystem level controls, a review." *Aquatic Ecology* 33 41 – 54.

A. Dapena-Mora, I. Fernandez, J. Campos, A. Mosquera-Corral, R. Mendez, M. Jetten (2007) "Evaluation of activity and inhibition effects on anammox process by batch tests based on the nitrogen gas production." *Enzyme and Microbial Technology* 40 (4) 859 – 865.

Y. Date, K. Isaka, T. Sumino, S. Tsuneda, Y. Inamori (2008) "Microbial community of anammox bacteria immobilized in polyethylene glycol gel carrier." *Water Science and Technology* 58 (5) 1121 – 1128.

M. de Graaff, N. Vieno, K. Kujawa-Roeleveld, G. Zeeman, H. Temmink, C. Buisman (2011) "Fate of hormones and pharmaceuticals during combined anaerobic treatment and nitrogen removal by partial nitritation-anammox in vacuum collected black water." *Water Research* 45 (1) 375 – 383.

M. Delkash, B. Bakhshayesh, H. Kazemian (2015) "Using zeolitic adsorbents to cleanup special wastewater streams: A review." *Microporous and Mesoporous Materials* 214 224 – 241.

C. Ding, E. Francis, L. Adrian (2018) "Anaerobic ammonium oxidation (anammox) with planktonic cells in a redox-stable semicontinuous stirred-tank reactor." *Environmental Science and Technology* 52 5671 – 5681.

W. Dodds, W. Bouska, J. Fitzmann, T. Pilger, K. Pitts, A. Riley, J. Schloesser, D. Thornbrugh (2009) "Eutrophication of U.S. freshwaters: Analysis of potential economic damages." *Environmental Science and Technology* 43 (1) 12 – 39.

J. Dosta, J. Vila, I. Sancho, N. Basset, M. Griffoll, J. Mata-Alvarez (2015) "Two-step partial nitritation/anammox process in granulation reactors: Start-up, operation, and microbial characterization." *Journal of Environmental Management* 164 196 – 205.

Earth Microbiome Project (2018) "16S Illumina Amplicon Protocol." http://press.igsb.anl.gov/earthmicrobiome/protocols-and-standards/16s/. Accessed 9/26/18 at 4:00pm.

The Economist (2017) "Dairy farming is polluting New Zealand's water." https://www.economist.com/asia/2017/11/16/dairy-farming-is-polluting-new-zealands-water. Accessed 10/31/18 at 5:00pm.

Environmental Protection Agency (EPA) (2007) "Biological nutrient removal processes and costs." https://www.epa.gov/sites/production/files/documents/criteria_nutrient_bioremoval.pdf. Accessed 9/4/18 at 2:00pm.

Environmental Protection Agency (EPA) (2016) "Status of nutrient requirements for NPDES-permitted facilities." https://www.epa.gov/npdes/status-nutrient-requirements-npdes-permitted-facilities. Accessed 9/4/18 at 2:00pm.

Environmental Protection Agency (EPA) (2017) "Aquatic life criteria – ammonium." https://www.epa.gov/wqc/aquatic-life-criteria-ammonia. Accessed 10/02/18 at 10:00am.

Environmental Protection Agency Te Mana Rauhi Taiao (EPA TMRT) (2018) "About new organisms." https://www.epa.govt.nz/industry-areas/new-organisms/about-new-organisms/. Accessed 10/18/18 at 5:00pm.

J. Evans, L. Sheneman, J. Foster (2006) "Relaxed-neighbor joining: A fast distance-based phylogenetic tree construction method." *Journal of Molecular Evolution* 62 785 – 792.

I. Fernandez, J. Vasquez-Padin, A. Mosquera-Corral, J. Campos, R. Mendez (2008a) "Biofilm and granular systems to improve anammox biomass retention." *Biochemical Engineering Journal* 42 (3) 308 – 313.

N. Fernandez, S. Montalvo, R. Borja, L. Guerrero, E. Sanchez, I. Cortes, M. Colmenarejo, L. Travieso, F. Raposo (2008b) "Performance evaluation of an anaerobic fluidized bed reactor with natural zeolite as support material when treating high-strength distillery wastewater." *Renewable Energy* 33 2458 – 2466.

B. Fernandez-Gomez, M. Richter, M. Schuler, J. Pinhassi, S. Acinas, J. Gonzalez, C. Pedros-Alio "Ecology of marine Bacteroidetes: A comparative genomics approach." *The ISME Journal* 7 1026 – 1037.

G. Fox, J. Wisotzkey, P. Jurtshuk, Jr. (1992) "How close is close: 16S rRNA sequence identity may not be sufficient to guarantee species identity." *International Journal of Systematic Bacteriology* 42 (1) 166 – 170.

Y. Ge, A. Yamaguchi, H. Sakuma (2009) "Study on the performance of anaerobic ammonium oxidation treatment using PVA gel as a carrier." *Water Science and Technology* 59 1037 – 1041.

G. Gonzalez-Gil, R. Sougrat, A. Behzad, P. Lens, P. Saikaly (2015) "Microbial community composition and ultrastructure of granules from a full-scale anammox reactor." *Microbial Ecology* 70 (1) 118 – 131.

A. Gonzalez-Martinez, F. Osorio, A. Rodriguez-Sanchez, M. Martinez-Toledo, J. Gonzalez-Lopez, T. Lotti, M. van Loosdrecht (2014) "Bacterial community structure of a lab-scale anammox membrane bioreactor." *Biotechnology Progress* 31 186 – 193.

A. Gonzalez-Martinez, A. Rodriguez-Sanchez, B. Munoz-Palazon, M. Garcia-Ruiz, R. Osorio, M. van Loozdrecht, J. Gonzalez-Lopez (2015a) "Microbial community analysis of a full-scale DEMON bioreactor." *Bioprocess and Biosystems Engineering* 38 (3) 499 – 508.

A. Gonzalez-Martinez, F. Osorio, J. Morillo, A. Rodriguez-Sanchez, J. Gonzalez-Lopez, B. Abbas, M. van Loosdrecht (2015b) "Comparison of bacterial diversity in full scale anammox bioreactors operated under different conditions." *Applied Cellular Physiology and Metabolic Engineering* 31 (6) 1464 – 1472.

A. Gonzalez-Martinez, J. Purswani, T. Lotti, P. Maza-Marquez, M. van Loosdrecht, R. Vahala (2016) "Distribution and microbial community structure analysis of a single-stage partial nitritation/anammox granular sludge bioreactor operating at low temperature." *Environmental Technology* 37 (18) 2281 – 2291.

M. Grismer, R. Collison (2017) "The zeolite-anammox treatment process for nitrogen removal from wastewater—a review." *Water* 9 (11) 901.

P. Grow, D. Graham (2018) "EPA grant-funded regional sidestream nutrient removal study." *Mainstream and Sidestream Nutrient Removal Workshop,* Berkeley, California.

V. Gupta, H. Sadegh, M. Yari, R. Ghoshekandi, B. Maazinejad, M. Chahardori (2015) "Removal of ammonium ions from wastewater: A short review in development of efficient methods." *Global Journal of Environmental Science and Management* 1 (2) 149 – 158.

S. He, Y. Chen, M. Qin, Z. Mao, L. Yuan, Q. Niu, X. Tan (2018) "Effects of temperature on anammox performance and community structure." *Bioresource Technology* 260 186 – 195.

T. Hill, K. Walsh, J. Harris, B. Moffett (2006) "Using ecological diversity measures with bacterial communities." *FEMS Microbiology Ecology* 43 (1) 1 – 11.

J. Hiras, Y. Wu, S. Eichorst, B. Simmons, S. Singer (2016) Refining the phylum Chlorobi by resolving the phylogeny and metabolic potential of the representative of a deeply branching, uncultivated lineage." *The ISME Journal* 10 833 – 845.

X. Hou, S. Liu, Z. Zhang (2015) "Role of extracellular polymeric substance in determining the high aggregation ability of anammox sludge." *Water Research* 75 51 – 62.

Z. Hu, D. Houweling, P. Dold (2012) "Biological nutrient removal in municipal wastewater treatment: New directions in sustainability." *Journal of Environmental Engineering* 138 (3) 307 – 317.

J. Huang, N. Kankanamge, C. Chow, D. Welsh, T. Li, P. Teasdale (2018) "Removing ammonium from water and wastewater using cost-effective adsorbents: A review." *Journal of Environmental Sciences* 63 174 – 197.

D. Huson, C. Scornavacca (2012) "Dendroscope 3: An interactive tool for rooted phylogenetic trees and networks." *Systematic Biology* 61 (6) 1061 – 1067.

V. Inglezakis, M. Loizidou, H. Grigoropoulou (2003) "Studies on the pretreatment of zeolite clinoptilolite in packed beds." *Environmental Technology* 25 (2) 133 – 139.

A. Jaeschke, H. Op en den Camp, H. Harhangi, A. Klimiuk, E. Hopmans, M. Jetten, S. Schouten, J. Damste (2009) "16S rRNA gene and lipid biomarker evidence for anaerobic ammonium-oxidizing bacteria (anammox) in California and Nevada hot springs." *FEMS Microbiology and Ecology* 67 343 – 350.

Y. Jeanningros, S. Vlaeminck, A. Kaldate, W. Verstraete, L. Graveleau (2010) "Fast start-up of a pilot-scale deammonification sequencing batch reactor from an activated sludge inoculum." *Water Science and Technology* 61 (6) 1393 – 1400.

R. Jin, B. Hu, P. Zheng, M. Qaisar, A. Hu, E. Islam (2008) "Quantitative comparison of stability of anammox process in different reactor configurations." *Bioresource Technology* 99 1603 – 1609.

R. Jin, G. Yang, J. Yu, P. Zheng (2012) "The inhibition of the anammox process: A review." *Chemical Engineering Journal* 197 67 – 79.

F. Ju, Y. Xia, F. Guo, Z. Wang, T. Zhang (2014) "Taxonomic relatedness shapes bacterial assembly in activated sludge of globally distributed wastewater treatment plants." *Environmental Microbiology* 16 (8) 2421 – 2432.

B. Junker, F. Shreiber (2008) "Analysis of biological networks." John Wiley and Sons, Inc., Hoboken, New Jersey 07030.

A. Kallistova, A. Dorofeev, Y. Nikoaev, M. Kozlov, M. Kevbrina, N. Pimenov (2016) "Role of anammox bacteria in removal of nitrogen compounds from wastewater." *Microbiology* 85 (2) 140 – 156.

D. Kallo (2001) "Applications of natural zeolites in water and wastewater treatment." *Reviews in Mineralogy and Geochemistry* 45 519 – 550.

B. Kartal, L. van Niftrik, O. Sliekers, M. Schmid, I. Schmidt, K. van de Pas-Schoonen, I. Cirpus, W. van der Star, M. van Loosdrecht, W. Abma, J. Kuenen, J. Mulder, M. Jetten (2004) "Application, eco-physiology, and biodiversity of anaerobic ammonium-oxidizing bacteria." *Reviews in Environmental Science and Biotechnology* 3 (3) 255 – 264.

B. Kartal, J. Kuenen, M. van Loosdrecht (2010) "Sewage treatment with anammox." *Science* 7;328 (5979) 702 – 703.

B. Kartal, L. van Niftrik, J. Keltjens, H. Op den Camp, M. Jetten (2012) "Anammox – Growth, physiology, cell biology, and metabolism." *Advances in Microbial Physiology* 60 211 – 262.

B. Kartal, N. de Almeida, W. Maalcke, H. Op den Camp, M. Jetten, J. Keltjens (2013) "How to make a living from anaerobic ammonium oxidation." *FEMS Microbiology Reviews* 3 (1) 428 – 461.

Y. Ke, M. Azari, P. Han, I. Gortz, J. Gu, M. Denecke (2015) "Microbial community of nitrogen-converting bacteria in anammox granular sludge." *International Biodeterioration and Biodegradation* 103 105 – 115.

A. Kielak, C. Barreto, G. Kowalchuk, J. van Veen, E. Kuramae (2016) "The ecology of Acidobacteria: Moving beyond genes and genomes." *Frontiers in Microbiology* 7 (744) 1 – 16.

T. Kindaichi, S. Yuri, N. Ozaki, A. Ohashi (2012) "Ecophysiological role and function of uncultured Chloroflexi in an anammox reactor." *Water Science and Technology* 66 2556 – 2561.

E. Kirton (2017) "iTag sequencing protocol updates." https://jgi.doe.gov/jgi-itag-primer-sequences-v1-0/. Accessed 9/26/18 at 4:00pm.

S. Klaus, P. McLee, A. Schuler, C. Bott (2016) "Methods for increasing the rate of anammox attachment in a sidestream deammonification MBBR." *Water Science and Technology* 74 (1) 110 – 117.

KMI Zeolite (2018) "KMI Zeolite mines and processes the purest naturally occurring clinoptilolite zeolite." https://www.kmizeolite.com/about/. Accessed 10/11/18 at 4:00pm.

M. Kowalski, T. Devlin, J. Oleszkiewicz (2018) "Startup and long-term performance of anammox moving bed biofilm reactor seeded with granular biomass." *Chemosphere* 200 481 – 486.

J. Kozich, S. Westcott, N. Baxter, S. Highlander, P. Schloss (2013) "Development of a dual-index sequencing strategy and curation pipeline for analyzing amplicon sequence data on the MiSeq Illumina sequencing platform." *Applied and Environmental Microbiology* 79 (17) 5112 – 5120.

J. Kuenen (2008) "Anammox bacteria: from discovery to application." *Nature Reviews in Microbiology* 6 320 – 327.

S. Lackner, E. Gilbert, S. Vlaeminck, A, H. Horn, M. van Loosdrecht (2014) "Full-scale partial nitritation/anammox experiences – An application survey." *Water Research* 55 292 – 303.

M. Laureni, P. Falas, O. Robin, A. Wick, D. Weissbrodt, J. Neilsen, T. Ternes, E. Morgenroth, A. Joss (2016) "Mainstream partial nitritation and anammox: Long-term process stability and effluent quality as low temperatures." *Water Research* 101 628 – 639.

C. Lawson, S. Wu, A. Bhattacharjee, J. Hamilton, K. McMahon, R. Goel, D. Noguera (2016) "Metabolic network analysis reveals microbial community interactions in anammox granules." *Nature Communications* 15416.

G. Lear, V. Washington, M. Neale, B. Case, H. Buckley, G. Lewis (2013) "The biogeography of stream bacteria." *Global Ecology and Biogeography* 22 544 – 554.

J. Lefcheck (2012) "NMDS tutorial in R." https://jonlefcheck.net/2012/10/24/nmds-tutorial-in-r/. Accessed 9/21/18 at 7:00pm.

I. Letunic, P, Bork (2016) "Interactive tree of life (iTOL) v3: an online tool for the display and annotation of phylogenetic and other trees. *Nucleic Acids Research* 8 (44) 242 – 245.

X. Li, B. Du, H. Fu, R. Wang, J. Shi, Y. Wang, M. Jetten, Z. Quan (2009) "The bacterial diversity in an anaerobic ammonium-oxidizing (anammox) reactor community." *Systematic and Applied Microbiology* 32 (4) 278 – 289.

X. Li, S. Klaus, C. Bott, Z. He (2018) "Status, challenges, and perspectives of mainstream nitritation-anammox for wastewater treatment." *Water Environment Research* 90 634 – 649.

W. Liu, D. Yang, W. Chen, X. Gu (2017) "High-throughput sequencing-based microbial characterization of size fractionated biomass in an anoxic anammox reactor for low-strength wastewater at low temperatures." *Bioresource Technology* 231 45 – 52.

Y. Liu, B. Ni (2015) "Appropriate Fe(II) addition significantly enhances anaerobic ammonium oxidation (anammox) activity through improving bacterial growth rate." *Scientific Reports* 5 (8204) 1 – 7.

T. Lotti, W. van der Star, R. Kleerebezem, C. Rubello, M. van Loosdrecht (2012) "The effect of nitrite inhibition on the anammox process." *Water Research* 15 (46) 2559 – 2569.

T. Lotti, R. Kleerebezem, C. Lubello, M. van Loosedrecht (2014) "Physiological and kinetic characterization of a suspended cell anammox culture." *Water Research* 60 1 – 14.

T. Lotti, R. Kleerebezem, J. Abelleira-Pereira, B. Abbas, M. van Loosdrecht (2015) "Faster through training: The anammox case." *Water Research* 81 261 – 268.

B. Ma, H. Wang, M. Dsouza, J. Lou, Y. He, Z. Dai, P. Brookes, J. Xu, J. Gilbert (2016) "Geographic patterns of co-occurrence network topological features for soil microbiota at continental scale in eastern China." *The ISME Journal* 10 1891 – 1901.

M. Madigan, J. Martinko, P. Dunlap, D. Clark (2006) "Biology of Microorganisms." Pearson Benjamin Cummings, San Francisco, CA 94111.

U. Manonmani, K. Joseph (2018) "Research advances and challenges in anammox immobilization for autotrophic nitrogen removal." *Journal of Chemical Technology and Biotechnology* 93 (9) 2486 – 2497.

Y. Miura, Y. Watanabe, S. Okabe (2007) "Significance of Chloroflexi in performance of submerged membrane bioreactors (MBR) treating municipal wastewater." *Environmental Science and Technology* 41 (22) 7787 – 7794.

B. Molinuevo, M. Garcia, D. Karakashev, I. Angelidaki (2009) "Anammox for ammonia removal from pig manure effluents: Effect of organic matter content on process performance." *Bioresource Technology* 100 (7) 2171 – 2175.

S. Montalvo, L. Guerrero, R. Borja, E. Sanchez, Z. Milan, I. Cortes, M. Angeles de la Rubia (2012) "Application of natural zeolites in anaerobic digestion processes: A review." *Applied Clay Science* 58 125 – 133.

T. Moore, Y. Xing, B. Lazenby, M. Lynch, S. Schiff, W. Roberston, R. Timlin, S. Lanza, M. Ryan, R. Aravena, D. Fortin, I. Clarke, J. Neufeld (2011) "Prevalence of anaerobic ammonium-oxidizing bacteria in contaminated groundwater." *Environmental Science and Technology* 45 7217 – 7225.

J. Morton (2017) "Damning rivers and lakes report: Nitrogen levels rising, fish threatened." https://www.nzherald.co.nz/nz/news/article.cfm?c_id=1&objectid=11846084. Accessed 10/31/18 at 5:00pm.

National Center for Biotechnology Information (NCBI) (2018a) "RefSeq: NCBI reference sequence database." https://www.ncbi.nlm.nih.gov/refseq/. Accessed 10/29/18 at 12:00pm.

National Center for Biotechnology Information (NCBI) (2018b) "Needleman-Wunsch global align nucleotide sequences." https://blast.ncbi.nlm.nih.gov/Blast.cgi?PAGE_TYPE=BlastSearch&PROG_DEF=blastn&BLAST_PROG_DEF=blastn&BLAST_SPEC=GlobalAln&LINK_LOC=BlastHomeLink. Accessed 10/29/18 at 12:00pm.

New Zealand Ministry for the Environment (NZ ME) (2015) "Geographic pattern of nitrogen in river water." http://archive.stats.govt.nz/browse_for_stats/environment/environmental-reporting-series/environmental-indicators/Home/Fresh%20water/river-water-quality-nitrogen/geographic-pattern-nitrogen-river-water-archived-27-04-2017.aspx. Accessed 10/29/18 at 4:00 pm.

New Zealand Ministry for the Environment (NZ ME) (2017) "Hazardous substances and new organisms act 1996." http://www.legislation.govt.nz/act/public/1996/0030/93.0/DLM381222.html. Accessed 10/18/18 at 5:00pm.

B. Ni, M. Ruscalleda, B. Smets (2012) "Evaluation of the microbial interactions of anaerobic ammonium oxidizers and heterotrophs in anammox biofilm." *Water Research* 46 4645 – 4652.

R. Nielsen (2005) "Can we feed the world?" http://home.iprimus.com.au/nielsens/nitrogen.html. Accessed 8/2/18 at 6:00pm.

J. Oksanen (2018) "Vegan: an introduction to ordination." https://cran.r-project.org/web/packages/vegan/vignettes/intro-vegan.pdf. Accessed 9/18/18 at 12:00pm.

S. Papageorgiou, F. Katsaros, E. Kouvelos, J. Nolan, H. Deit, N. Kanellopoulos (2006) "Heavy metal sorption by calcium alginate beads from Laminaria digitata." *Journal of Hazardous Materials* 137 (3) 1765 – 1772.

Paques (2018) "ANAMMOX." https://en.paques.nl/products/featured/anammox. Accessed 9/4/18 at 3:00pm.

H. Park, A. Rosenthal, K. Ramalingam, J. Filos, K. Chandran (2010) "Linking community profiles, gene expression, and N-removal in anammox bioreactors treating municipal anaerobic digestion reject water." *Environmental Science and Technology* 44 6110 – 6116.

D. Parks, M. Chuvochina, D. Waite, C. Rinke, A. Sharshewski, P. Chaumeil, P. Hugenholtz (2018) "A proposal for a standardized bacterial taxonomy based on genome phylogeny." https://www.biorxiv.org/content/biorxiv/early/2018/01/30/256800.full.pdf. Accessed 9/19/18 at 11:00am.

A. Pereira, A. Cabezas, C. Etchebehere, C. Chernicharo, J. Araujo (2017) "Microbial communities in anammox reactors: a review." *Environmental Technology Reviews* 6 (1) 74 – 93.

O. Perez-Garcia, F. Ng, N. Singhal, P. Bickers (2018) "A utilities guide to starting up anammox." *Water New Zealand Conference and Expo*, Hamilton, New Zealand.

A. Preisler, D. de Beer, A. Lichtschlag, G. Lavik, A. Boetius, B. Jorgensen (2007) "Biological and chemical sulfide oxidation in a Beggiatoa inhabited marine sediment." *The ISME Journal* 1 341 – 353.

E. Pruesse, C. Quast, K. Knittel, B. Fuchs, W. Ludwig, J. Peplies, F. Glockner (2007) "SILVA: A comprehensive online resource for quality checked and aligned ribosomal RNA sequence data compatible with ARB." *Nucleic Acids Research* 35 (21) 7188 – 7186.

L. Pugh (2012) "Sustainable approaches to sidestream nutrient removal and recovery." http://www.mi-wea.org/docs/Lucy%20%20PP%201-19-12.pdf. Accessed 10/13/2015 at 5:00pm.

D. Puyol, J. Caravajal-Arroyo, B. Garcia, R. Sierra-Alvarez, J. Field (2013) "Kinetic characterization of *Brocadia* spp.-dominated anammox cultures." *Bioresource Technology* 139 94 – 100.

P. Regmi, M. Miller, B. Holgate, R. Bunch, H. Park, K. Chandran, B. Wett, S. Murthy, C. Bott (2014) "Control of aeration, aerobic SRT, and COD input for mainstream nitritation/ denitritation." *Water Research* 57 162 – 171.

B. Rittmann, P. McCarty (2001) "Environmental Biotechnology: Principles and Applications." McGraw-Hill Companies Inc., 1221 Avenue of the Americas, New York, NY 10020.

J. Rouse, T. Fujii, H. Sugino, H. Tran, K. Furukawa (2005) "PVA-gel beads as a biomass carrier for anaerobic oxidation of ammonium in a packed-bed reactor." *Proceedings of the HELECO '05 Conference*, Session 16, Athens, Greece.

RStudio Team (2015) "RStudio: Open source and enterprise-ready professional software for R." https://www.rstudio.com/. Accessed 9/18/18 at 11:00am.

D. Scaglione, E. Ficara, V. Corbellini, G. Tornotti, A. Teli, R. Canziani, R. Malpei (2015) "Autotrophic nitrogen removal by a two-step SBR process applied to mixed agro-digestate." *Bioresource Technology* 176 98 – 105.

P. Schloss, S. Westcott, T. Ryabin, J. Hall, M. Hartmann, E. Hollister, R. Lesniewski, B. Oakley, D. Parks, C. Robinson, J. Sahl, B. Stres, G. Thallinger, D. Van Horn, C. Weber (2009) "Introducing mothur: Open-source, platform-independent, community-supported software for describing and comparing microbial communities." *Applied and Environmental Microbiology* 75 (23) 7537 – 7541.

S. Seitzinger (1988) "Denitrification in freshwaterand coastal marine ecosystems: Ecological and geochemical significance." *Limnology and Oceanography* 33 702 – 724.

R. Shaddad (2017) "What is the problem with New Zealand's water sources?" https://www.aljazeera.com/indepth/features/2017/08/problem-zealand-water-sources-170831090704101.html. Accessed 10/31/18 at 5:00pm.

S. Shalini, K. Joseph (2012) "Nitrogen management in landfill leachate: Application of SHARON, ANAMMOX, and combined SHARON-ANAMMOX processes. *Waste Management* 32 (12) 2385 – 2400.

D. Shu, Y. He, H. Yue, J. Gao, Q. Wang, S. Yang (2016) "Enhanced long-term nitrogen removal by organotrophic anammox bacteria under different C/N ratio constraints: quantitative molecular mechanism and microbial community dynamics." *RSC Advances* 6 87593 – 87606.

D. Shu, B. Zhang, Y. He, G. Wei (2018) "Abundant and rare microbial sub-communities in anammox granules present contrasting assemblage patterns and metabolic functions in response to inorganic carbon stresses." *Bioresource Technology* 265 299 – 309.

Z. Sidak (1967) "Rectangular confidence regions for the means of multivariate normal distributions." *Journal of the American Statistical Association* 62 (318) 626 – 633.

P. Sonthiphand, M. Hall, J. Neufeld (2014) "Biogeography of anaerobic ammonium-oxidizing bacteria." *Frontiers in Microbiology* 5 (399) 1 – 14.

D. Speth, M. Zandt, S. Guerrero-Cruz, B. Dutilh, M.Jetten (2016) "Genome-based microbial ecology of anammox granules in a full-scale wastewater treatment system." *Nature Communications* 7 (11172) 1 – 10.

B. Stinson (2018) "Introduction, technologies, and theory on sidestream and mainstream nitrogen removal." *Mainstream and Sidestream Nutrient Removal Workshop,* Berkeley, California.

S. Suneethi, S. Sri Shalini, J. Kurian (2014) "State of the art strategies for successful anammox startup and development: A review." *International Journal of Waste Resources* 4 (4) 1 – 14.

D. Sylvia, J. Fuhrman, P. Hartel, D. Zuberer (2005) "Principles and Applications of Soil Microbiology." Pearson Education Inc., Upper Saddle River, New Jersey 07458.

C. Tang, P. Zheng, C. Wang, Q. Mahmood, J. Zhang, X. Chen, L. Zhang, J. Chen (2011) "Performance of high-loaded anammox UASB reactors containing granular sludge." *Water Research* 45 135 – 144.

X. Tang, Y. Guo, B. Jiang, S. Liu (2018) "Metagenomic approaches to understanding bacterial communication during the anammox reactor start-up." *Water Research* 136 95 – 103.

G. Tsitsishvili, T. Andronikashvili, G. Kirov, L. Filizova (1992) "Natural Zeolites." Ellis Horwood Limited, Chichester, West Sussex, PO19 1EB, England.

Q. Tu, Z. He, L. Wu, K. Xue, G. Xie, P. Chain, P. Reich, S. Hobbie, J. Zhou (2017) "Metagenomic reconstruction of nitrogen cycling pathways in a CO_2-enriched grassland ecosystem." *Soil Biology and Biochemistry* 106 99 – 108.

United Nations Environment Programme (UNEP) (2007) "Reactive nitrogen in the environment." http://www.unep.org/pdf/dtie/Reactive_Nitrogen.pdf. Accessed 10/26/2015 at 5:00pm.

United Nations Statistics Division (UNSD) (2018) "Sustainable development goals." https://unstats.un.org/sdgs/report/2016/goal-14/. Accessed 8/2/18 at 5:00pm.

A. van de Graaf, P. de Bruijn, L. Robertson, M. Jetten, J. Kuenen (1996) "Autotrophic growth of anaerobic ammonium-oxidizing micro-organisms in a fluidized bed reactor." *Microbiology* 142 2187 – 2196.

I. van de Leemput, A. Veraart, V. Dakos, J. de Klein, M. Strouss, M. Scheffer (2014) "Predicting microbial nitrogen pathways from basic principles." *Environmental Microbiology* 13 (6) 1477 – 1487.

W. van der Star, W. Abma, D. Biommers, J. Mulder, T. Tokutomi, M. Strous, C. Picioreanu, M. van Loosdrecht (2007) "Startup of reactors for anoxic ammonium oxidation: Experiences from the first full-scale anammox reactor in Rotterdam." *Water Research* 41 (18) 4149 – 4163.

W. van der Star, A. Miclea, U. van Dongen, G. Muyzer, C. Picioreanu, M. van Loosdrecht (2008) "The membrane bioreactor: A novel tool to grow anammox as free cells." *Biotechnololgy and Bioengineering* 101 (2) 286 – 294.

U. van Dongen, M. Jetten, M. van Loosdrecht (2001) "The SHARON-Anammox process for treatment of ammonium rich wastewater." *Water Science and Technology* 44 (1) 153 – 160.

L. van Niftrik, M. Jetten (2012) "Anaerobic ammonium-oxidizing bacteria: Unique microorganisms with exceptional properties." *Microbiology and Molecular Biology Reviews* 76 (3) 585 – 596.

Veolia (2018) "AnoxKaldnes ANITA Mox." http://technomaps.veoliawatertechnologies.com/anita/en/anita_mox.htm. Accessed 10/10/18 at 1:00pm.

S. Vlaemink, A. Terada, B. Smets, H. de Clippeleir, T. Shaubroeck, S. Bolca, L. Demeestere, J. Mast, N. Boon, M. Carballa, W. Verstraete (2010) "Aggregate size and architecture determine microbial activity balance for one-stage partial nitritation and anammox." *Applied and Environmental Microbiology* 76 900 – 909.

S. Wang, Y. Peng (2010) "Natural zeolites as effective adsorbents in water and wastewater treatment." *Chemical Engineering Journal* 156 (1) 11 – 24.

Y. Wang, J. Chen, S. Zhou, X. Wang, Y. Chen, X. Lin, Y. Yan, X. Ma, M. Wu H. Han (2017) "16S rRNA gene high-throughput sequencing reveals shift in nitrogen conversion related microorganisms in a CANON system in response to salt stress." *Chemical Engineering Journal* 317 512 – 531.

N. Ward, J. Challacombe, P. Janssen, B. Henrissat, P. Coutinho, M. Wu, G. Xie, D. Haft, M. Sait, J. Badger, R. Barabote, B. Bradley, T. Brettin, L. Brinkac, D. Bruce, T. Creasy, S. Daugherty, T. Davidsen, R. DeBoy, J. Detter, R. Dodson, A. Durkin, A. Ganapathy, M. Gwinn-Giglio, C. Han, H. Khouri, H. Kiss, S. Kothari, R. Madupu, K. Nelson, W. Nelson, I. Paulsen, K. Penn, Q. Ren, M. Rosovitz, J. Selengut, S. Shriviastava, S. Sullivan, R. Tapia, L. Thompson, K. Watkins, Q. Yang, C. Yu, N. Zafar, L. Zhou, C. Kuske (2009) "Three genomes from the Phylum Acidobacteria provide insight into the lifestyles of these microorganisms in soils." *Applied and Environmental Microbiology* 75 2046 – 2056.

B. Wett (2007) "Development and implementation of a robust deammonification process." *Water Science and Technology* 56 (7) 81 – 88.

N. Widiastuti, H. Wu, M. Ang, D. Zhang (2008) "The potential application of natural zeolite for greywater treatment." *Desalination* 218 271 – 280.

M. Winkler, J. Bassin, R. Kleerebezem, D. Sorokin, M. van Loosdrecht (2012) "Unravelling the reasons for disproportion in the ratio of AOB and NOB in aerobic granular sludge." *Applied Microbiology and Biotechnology* 94 1657 – 1666.

World Resources Institute (WRI) (2018) "Sources of eutrophication." https://www.wri.org/our-work/project/eutrophication-and-hypoxia/sources-eutrophication. Accessed 9/3/18 at 12:00pm.

World Water Works (WWW) (2015) "The anammox based DEMON process." http://www.worldwaterworks.com/slides/demon. Accessed 10/27/2015 at 3:30pm.

T. Wright (2017) "Special report: How polluted are New Zealand's rivers?" https://www.newshub.co.nz/home/new-zealand/2017/02/special-report-how-polluted-are-new-zealand-s-rivers.html. Accessed 10/31/18 at 5:00pm.

L. Wu, C. Wen, Y. Qin, H. Yin, Q. Tu, J. van Nostrand, T. Yuan, M. Yuan, Y. Deng, J. Zhou (2015) "Phasing amplicon sequencing on Illumina Miseq for robust environmental microbial community analysis." *BMC Microbiology* 15 (125) 1 – 12.

X. Xu, G. Liu, Y. Wang, Y. Zhang, H. Wang, L. Qi, H. Wang (2018) "Analysis of key microbial community during the start-up of anaerobic ammonium oxidation process with paddy soil as inoculated sludge." *Journal of Environmental Sciences* 64 317 – 327.

Y. Yang, J. Zho, Z. Quan, S. Lee, P. Shen, X. Gu (2006) "Study on performance of granular ANAMMOX process and characterization of the microbial community in sludge." *Water Science and Technology* 54 (8) 197 – 207.

Z. Yao, P. Lu, D. Zhang, X. Wan, Y. Li, S. Peng (2015) "Stoichiometry and kinetics of the anaerobic ammonium oxidation (anammox) with trace hydrazine addition." *Bioresource Technology* 198 70 – 76.

P. Yarza, P. Yilmaz, E. Pruesse, F. Glockner, W. Ludwig, K. Schleifer, W. Whitman, J. Euzeby, R. Amann, R. Rossello-Mora (2014) "Uniting the classification of cultured and uncultured bacteria and archaea using 16S rRNA gene sequences." *Nature Reviews Microbiology* 12 635 – 645.

J. Yu, J. Wang, Y. Jiang (2017) "Removal of uranium from aqueous solution by alginate beads." *Nuclear Engineering and Technology* 49 534 – 540.

Y. Zhao (2016) "Review of the natural, modified, and synthetic zeolites for heavy metals removal from wastewater." *Environmental Engineering Science* 33 (7) 443 – 454.

B. Zheng, L. Zhang, J. Guo, S. Zhang, A. Yang, Y. Peng (2016) "Suspended sludge and biofil shaped different anammox communities in two pilot-scale one-stage anammox reactors." *Bioresource Technology* 211 273 – 279.

G. Zhu, Y. Hu, Q. Wang (2009) "Nitrogen removal performance of anaerobic ammonia oxidation co-culture immobilized in different gel carriers." *Water Science and Technology* 9 (12) 2379 – 2386.

G. Zhu, J. Yan, Y. Hu (2014) "Anaerobic ammonium oxidation in polyvinyl alcohol and sodium alginate immobilized biomass system: a potential tool to maintain anammox biomass in application." *Water Science and Technology* 69 (4) 718 – 726.

W. Zhu, P. Zhang, D. Yu, H. Dong, J. Li (2017) "Nitrogen removal performance of ammonia oxidation (anammox) in presence of organic matter." *Biodegradation* 28 (2 – 3) 159 – 170.

Appendices

Appendix 1:

Full taxonomic classifications of all recovered operational taxonomic units (OTUs) in the anaerobic membrane bioreactor (MBR)

Phylum	Class	Order	Family	Genus
-	-	-	-	-
Acidobacteria	Acidobacteriia	Solibacterales	Solibacteraceae	-
Acidobacteria	Acidobacteriia	Solibacterales	Solibacteraceae	-
Acidobacteria	Acidobacteriia	Solibacterales	Solibacteraceae	-
Acidobacteria	Acidobacteriia	Solibacterales	Solibacteraceae	-
Acidobacteria	Acidobacteriia	Solibacterales	Solibacteraceae	-
Acidobacteria	Acidobacteriia	Solibacterales	Solibacteraceae	Bryobacter
Acidobacteria	Acidobacteriia	Solibacterales	Solibacteraceae	Bryobacter
Acidobacteria	Blastocatellia	Blastocatellales	Blastocatellaceae	-
Acidobacteria	Thermoanaeronaculia	Thermoanaerobaculales	Thermoanaerobaculace	-
Acidobacteria	Thermoanaeronaculia	Thermoanaerobaculales	Thermoanaerobaculace	Thermoanaerobaculum
Actinobacteria	Acidimicrobiia	-	-	-
Actinobacteria	Acidimicrobiia	Actinomarinales	-	-
Actinobacteria	Thermoleophilia	Gaiellales	Gaiellaceae	Gaiella
Armatimonadetes	-	-	-	-
Armatimonadetes	Fibriimonadia	Fibriimonadales	Fibriimonadales	-
Bacteroidetes	Bacteroidia	-	-	-
Bacteroidetes	Bacteroidia	Chitinophagales	Chitinophagaceae	-
Bacteroidetes	Bacteroidia	Chitinophagales	Chitinophagaceae	-
Bacteroidetes	Bacteroidia	Chitinophagales	Chitinophagaceae	-
Bacteroidetes	Bacteroidia	Chitinophagales	Saprospiraceae	Phaeodactylibacter
Bacteroidetes	Bacteroidia	Flavobacteriales	-	-

Bacteroidetes	Bacteroidia	Sphingobacteriales	-	-
Bacteroidetes	Bacteroidia	Sphingobacteriales	-	-
Bacteroidetes	Bacteroidia	Sphingobacteriales	-	-
Bacteroidetes	Bacteroidia	Sphingobacteriales	-	-
Bacteroidetes	Ignavibacteria	-	-	-
Bacteroidetes	Ignavibacteria	-	-	-
Bacteroidetes	Ignavibacteria	-	-	-
Bacteroidetes	Ignavibacteria	Ignavibacteriales	-	-
Bacteroidetes	Ignavibacteria	Ignavibacteriales	-	-
Bacteroidetes	Ignavibacteria	Ignavibacteriales	-	-
Bacteroidetes	Ignavibacteria	Ignavibacteriales	Ignavibacteriaceae	Ignavibacterium
Chloroflexi	-	-	-	-
Chloroflexi	-	-	-	-
Chloroflexi	-	-	-	-
Chloroflexi	-	-	-	-
Chloroflexi	-	-	-	-
Chloroflexi	Anaerolineae	-	-	-
Chloroflexi	Anaerolineae	-	-	-
Chloroflexi	Anaerolineae	-	-	-
Chloroflexi	Anaerolineae	-	-	-
Chloroflexi	Anaerolineae	-	-	-
Chloroflexi	Anaerolineae	-	-	-
Chloroflexi	Anaerolineae	-	-	-

Chloroflexi	Anaerolineae	-	-	-
Chloroflexi	Anaerolineae	-	-	-
Chloroflexi	Anaerolineae	-	-	-
Chloroflexi	Anaerolineae	-	-	-
Chloroflexi	Anaerolineae	-	-	-
Chloroflexi	Anaerolineae	-	-	-
Chloroflexi	Anaerolineae	-	-	-
Chloroflexi	Anaerolineae	-	-	-
Chloroflexi	Anaerolineae	-	-	-
Chloroflexi	Anaerolineae	-	-	-
Chloroflexi	Anaerolineae	-	-	-
Chloroflexi	Anaerolineae	-	-	-
Chloroflexi	Anaerolineae	-	-	-
Chloroflexi	Anaerolineae	Anaerolineales	Anaerolineaceae	-
Chloroflexi	Anaerolineae	Anaerolineales	Anaerolineaceae	-
Chloroflexi	Anaerolineae	Anaerolineales	Anaerolineaceae	-
Chloroflexi	Anaerolineae	Anaerolineales	Anaerolineaceae	-
Chloroflexi	Anaerolineae	Anaerolineales	Anaerolineaceae	-
Chloroflexi	Anaerolineae	Anaerolineales	Anaerolineaceae	-
Chloroflexi	Anaerolineae	Anaerolineales	Anaerolineaceae	-
Chloroflexi	Anaerolineae	Anaerolineales	Anaerolineaceae	-
Chloroflexi	Anaerolineae	Ardenticatenales	-	-
Chloroflexi	Anaerolineae	Caldilineales	Caldilineaceae	-

Cyanobacteria	Sericytochromatia	-	-	-
Dadabacteria	Dadabacteriia	Dadabacteriales	-	-
Deinococcus-Thermus	Deinococci	Deinococcales	Trueperaceae	Truepera
Gemmatimonadetes	Gemmatimonadetes	Gemmatimonadales	Gemmatimonadaceae	-
Nitrospirae	Nitrospira	Nitrospirales	Nitrospiraceae	Nitrospria
Patescibacteria	Microgenomatia	Collierbacteria	-	-
Patescibacteria	Microgenomatia	Pacebacteria	-	-
Patescibacteria	Microgenomatia	Pacebacteria	-	-
Patescibacteria	Microgenomatia	Pacebacteria	-	-
Planctomycetes	-	-	-	-
Planctomycetes	Brocadiae	Brocadiales	Brocadiaceae	Brocadia
Planctomycetes	Brocadiae	Brocadiales	Brocadiaceae	Brocadia
Planctomycetes	Brocadiae	Brocadiales	Brocadiaceae	Brocadia
Planctomycetes	Brocadiae	Brocadiales	Brocadiaceae	Brocadia
Planctomycetes	Brocadiae	Brocadiales	Brocadiaceae	Brocadia
Planctomycetes	Brocadiae	Brocadiales	Brocadiaceae	Brocadia
Planctomycetes	Brocadiae	Brocadiales	Brocadiaceae	Brocadia
Planctomycetes	Phycisphaerae	Phycisphaerales	Phycisphaeraceae	-
Planctomycetes	Phycisphaerae	Phycisphaerales	Phycisphaeraceae	-
Planctomycetes	Phycisphaerae	Phycisphaerales	Phycisphaeraceae	-
Planctomycetes	Planctomycetacia	Pirellulales	Pirellulaceae	Anammoximicrobium
Planctomycetes	Planctomycetacia	Pirellulales	Pirellulaceae	Thermogutta
Proteobacteria	Alphaproteobacteria	-	-	-

Proteobacteria	Alphaproteobacteria	Rhizobiales	Rhizobiaceae	-
Proteobacteria	Alphaproteobacteria	Rhizobiales	Xanthobacteraceae	-
Proteobacteria	Alphaproteobacteria	Rhizobiales	Xanthobacteraceae	-
Proteobacteria	Alphaproteobacteria	Rhizobiales	Xanthobacteraceae	Bradyrhizobium
Proteobacteria	Alphaproteobacteria	Rhodobacterales	Rhodobacteraceae	-
Proteobacteria	Alphaproteobacteria	Rhodospirillales	-	-
Proteobacteria	Deltaproteobacteria	-	-	-
Proteobacteria	Deltaproteobacteria	-	-	-
Proteobacteria	Deltaproteobacteria	-	-	-
Proteobacteria	Deltaproteobacteria	Desulfarculales	Desulfarulaceae	-
Proteobacteria	Deltaproteobacteria	Desulfarculales	Desulfarulaceae	
Proteobacteria	Deltaproteobacteria	Oligoflexales	-	-
Proteobacteria	Deltaproteobacteria	Syntrophobacterales	Syntrophaceae	-
Proteobacteria	Gammaproteobacteria	-	-	-
Proteobacteria	Gammaproteobacteria	-	-	-
Proteobacteria	Gammaproteobacteria	-	-	-
Proteobacteria	Gammaproteobacteria	-	-	-
Proteobacteria	Gammaproteobacteria	-	-	-
Proteobacteria	Gammaproteobacteria	Betaproteobacteriales	-	-
Proteobacteria	Gammaproteobacteria	Betaproteobacteriales	-	-
Proteobacteria	Gammaproteobacteria	Betaproteobacteriales	Burkholderiaceae	-
Proteobacteria	Gammaproteobacteria	Betaproteobacteriales	Burkholderiaceae	-
Proteobacteria	Gammaproteobacteria	Betaproteobacteriales	Burkholderiaceae	-

Proteobacteria	Gammaproteobacteria	Betaproteobacteriales	Burkholderiaceae	-
Proteobacteria	Gammaproteobacteria	Betaproteobacteriales	Burkholderiaceae	-
Proteobacteria	Gammaproteobacteria	Betaproteobacteriales	Burkholderiaceae	-
Proteobacteria	Gammaproteobacteria	Betaproteobacteriales	Burkholderiaceae	-
Proteobacteria	Gammaproteobacteria	Betaproteobacteriales	Burkholderiaceae	Castellaneilla
Proteobacteria	Gammaproteobacteria	Betaproteobacteriales	Burkholderiaceae	Lautropia
Proteobacteria	Gammaproteobacteria	Betaproteobacteriales	Burkholderiaceae	Limnobacter
Proteobacteria	Gammaproteobacteria	Betaproteobacteriales	Hydrogenophilaceae	Thiobacillus
Proteobacteria	Gammaproteobacteria	Betaproteobacteriales	Nitrosomonadaceae	Nitrosomonas
Proteobacteria	Gammaproteobacteria	Betaproteobacteriales	Nitrosomonadaceae	Nitrosomonas
Proteobacteria	Gammaproteobacteria	Betaproteobacteriales	Nitrosomonadaceae	Nitrosomonas
Proteobacteria	Gammaproteobacteria	Betaproteobacteriales	Rhodocyclaceae	-
Proteobacteria	Gammaproteobacteria	Betaproteobacteriales	Rhodocyclaceae	Denitratisoma
Proteobacteria	Gammaproteobacteria	Betaproteobacteriales	Rhodocyclaceae	Denitratisoma
Proteobacteria	Gammaproteobacteria	Oceanospirillales	-	-
Proteobacteria	Gammaproteobacteria	Xanthomonadales	-	-
Proteobacteria	Gammaproteobacteria	Xanthomonadales	-	-
Proteobacteria	Gammaproteobacteria	Xanthomonadales	Xanthomonadaceae	-
Proteobacteria	Gammaproteobacteria	Xanthomonadales	Xanthomonadaceae	-
Proteobacteria	Gammaproteobacteria	Xanthomonadales	Xanthomonadaceae	Thermomonas
Spirochaetes	Leptospirae	Leptospirales	Leptospiraceae	Leptonema
Spirochaetes	Leptospirae	Leptospirales	Leptospiraceae	Turneriella
Verrucomicrobia	Verrucomicrobiae	Pedosphaerales	Pedosphaeraceae	-

Appendix 2:

Supplementary materials for Chapter 2

Comparison between the nitrogen removal rate (NRR) and the Shannon index of microbial diversity (*H'*) over the lifespan of the membrane bioreactor (MBR).

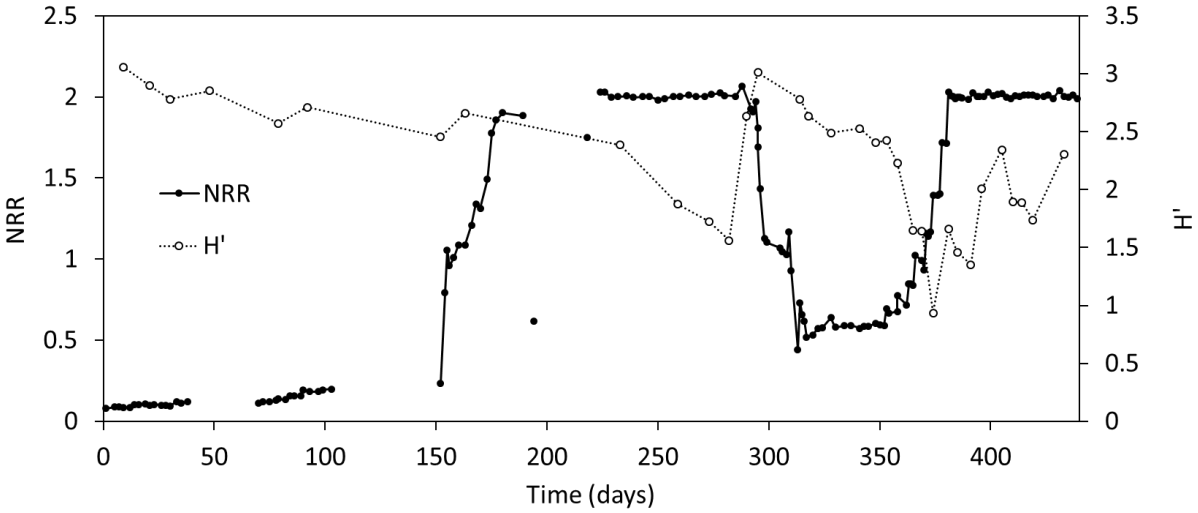

Correlation (or, lack thereof) between the NRR and *H'* over the lifespan of the MBR.

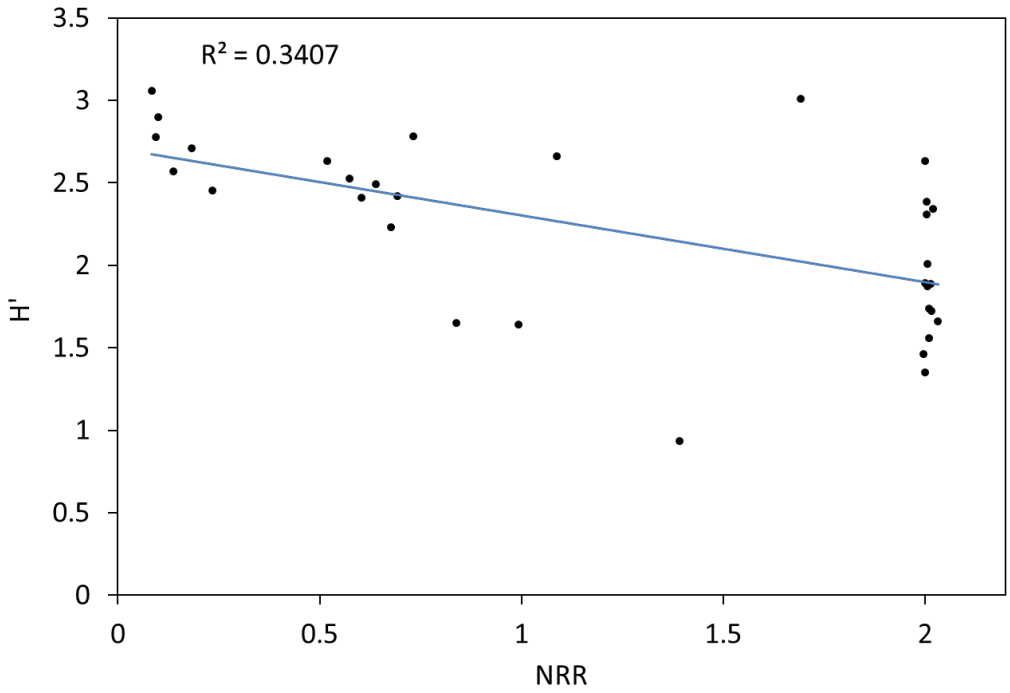

Shepard's plot for Figure 2.6 (Lefcheck 2012).

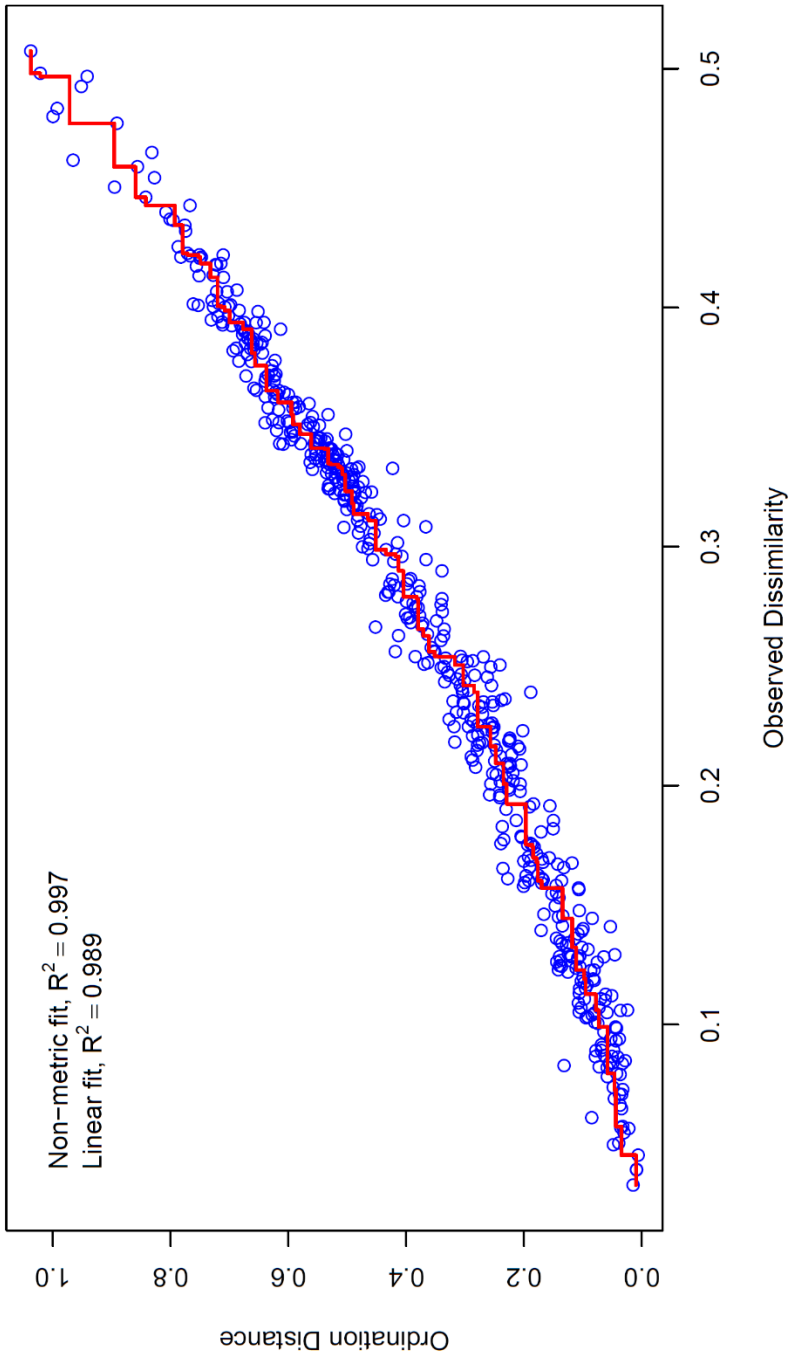

Figure 2.6, with bacterial taxa's names ascribed.

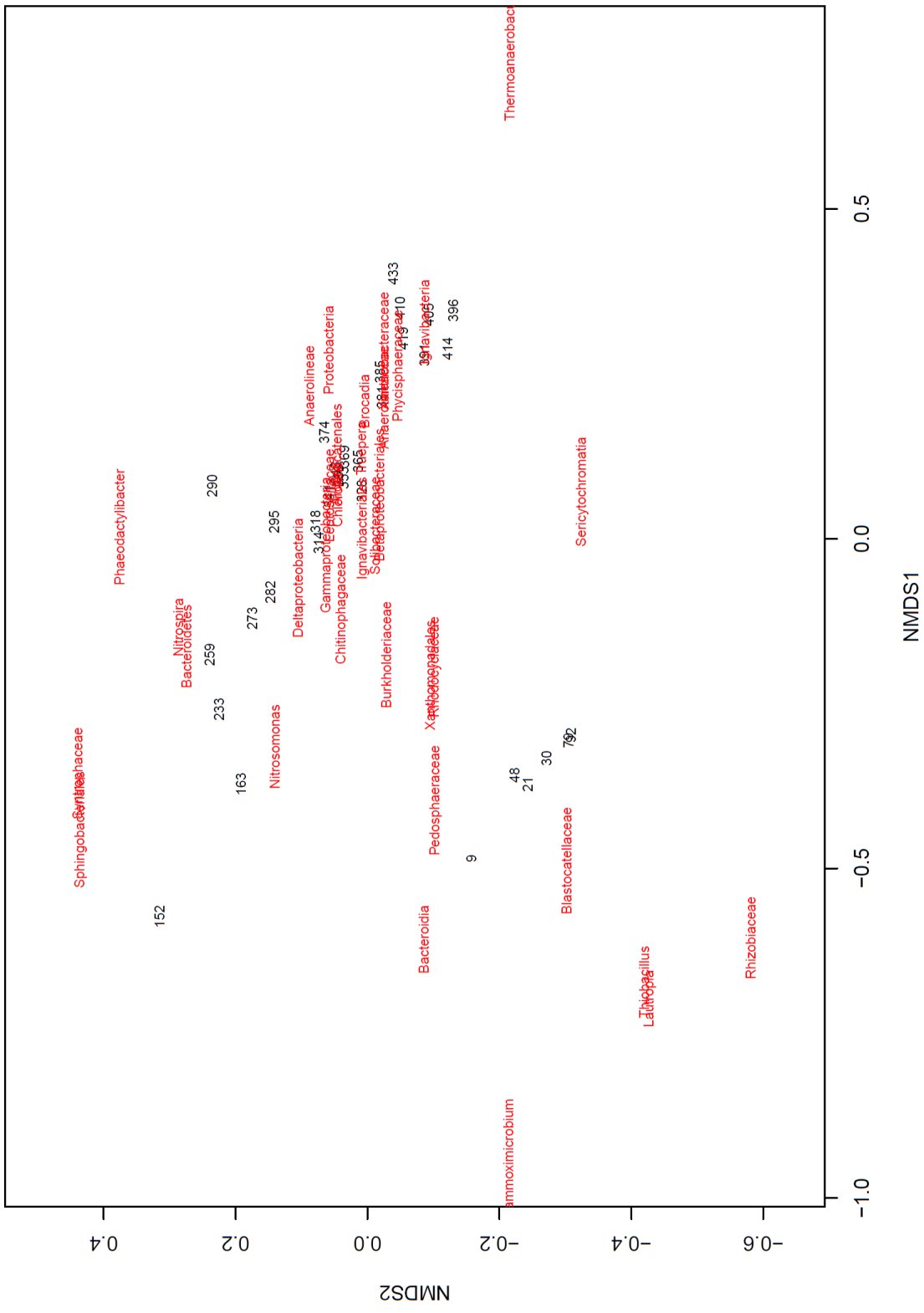

Appendix 3:

Supplementary materials for Chapter 3

Figure 3.3a, with all data averaged over each phase of experimentation.

Influent and effluent concentrations of reactive nitrogen species are plotted against the primary y-axis, and corresponding nitrogen removal rates (NRR) are plotted against the secondary y-axis. Error bars indicate standard deviation over respective phases.

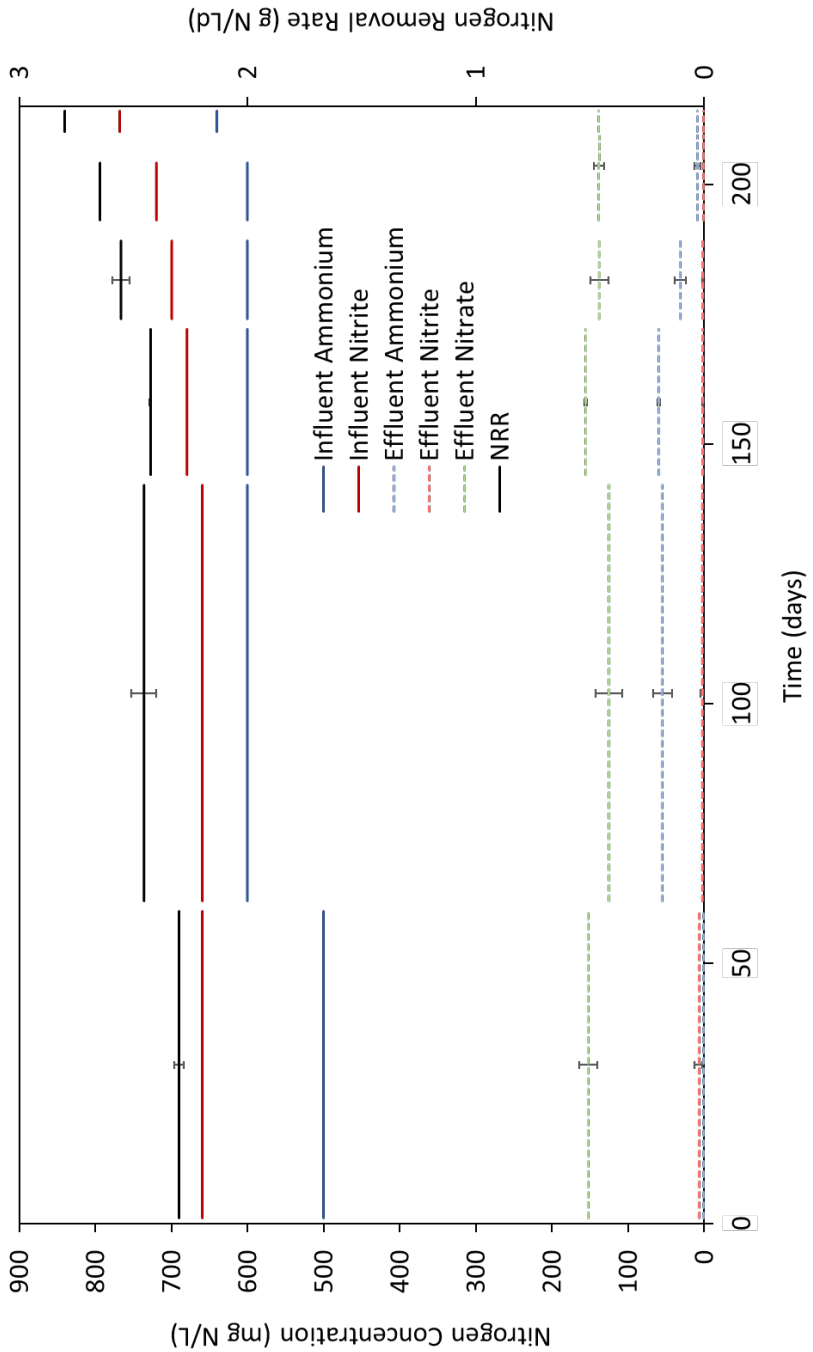

Comparison between the nitrogen removal rate (NRR) and the Shannon index of microbial diversity (*H'*) over the lifespan of the membrane bioreactor (MBR).

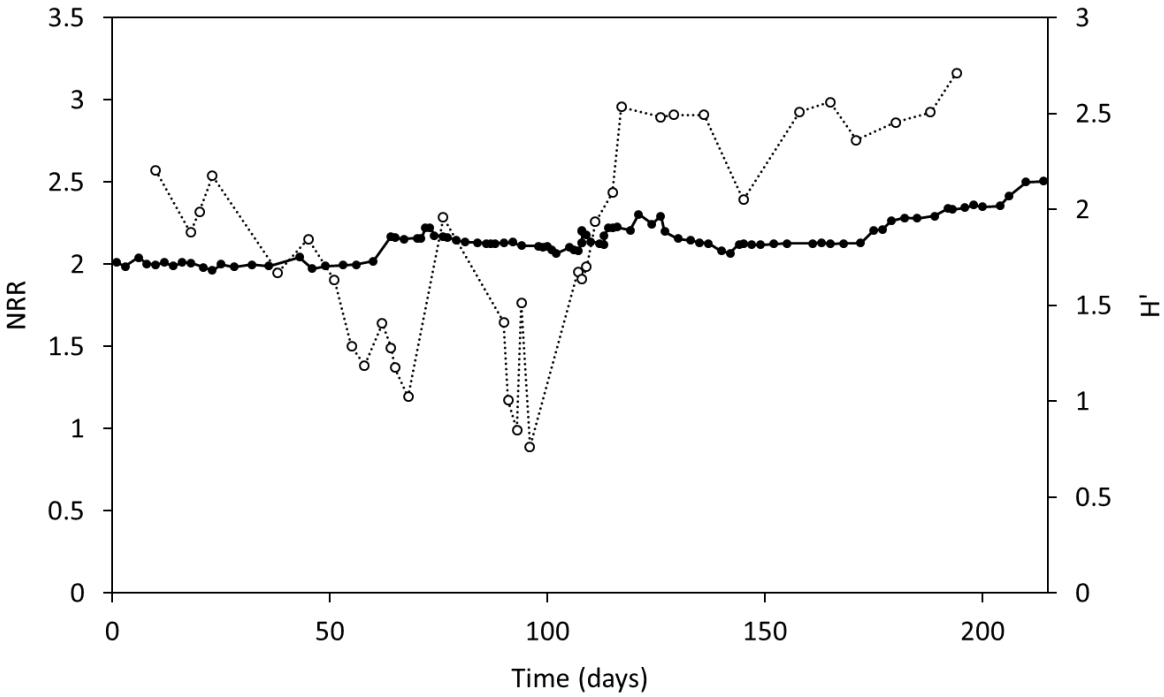

Correlation (or, lack thereof) between the NRR and *H'* over the lifespan of the MBR.

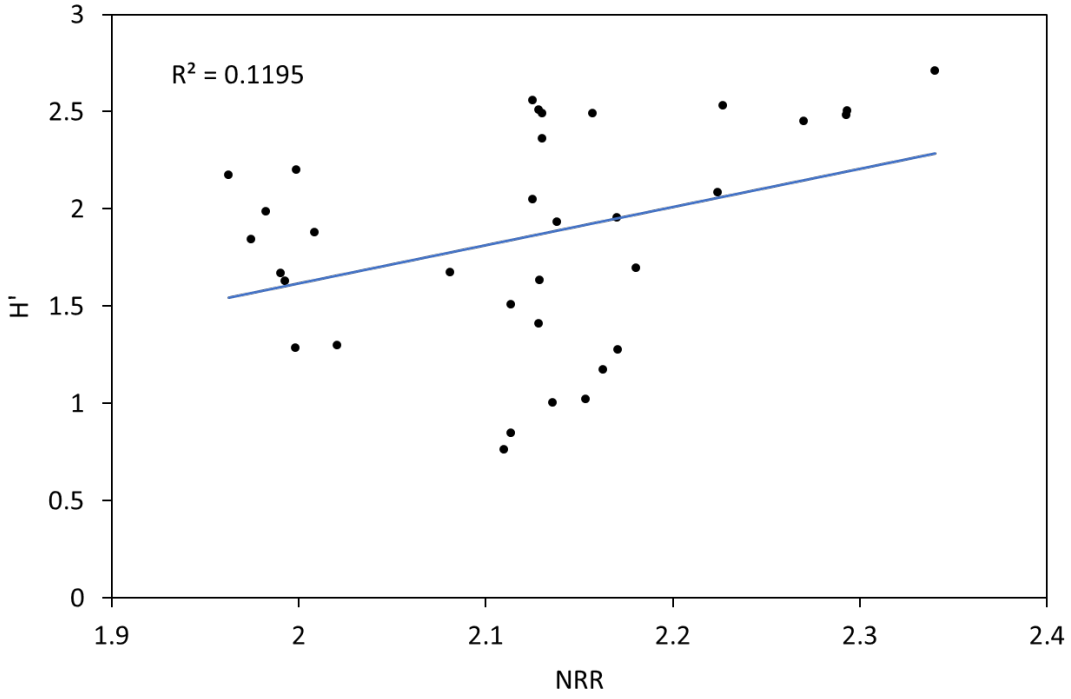

Appendix 4:

Full taxonomic classifications of all recovered operational taxonomic units (OTUs) in the anaerobic membrane bioreactor (MBR)

Phylum	Class	Order	Family	Genus
-	-	-	-	-
-	-	-	-	-
Acidobacteria	Acidobacteriia	Solibacterales	Solibacteraceae	-
Acidobacteria	Acidobacteriia	Solibacterales	Solibacteraceae	-
Acidobacteria	Acidobacteriia	Solibacterales	Solibacteraceae	-
Acidobacteria	Acidobacteriia	Solibacterales	Solibacteraceae	Bryobacter
Acidobacteria	Acidobacteriia	Solibacterales	Solibacteraceae	Paludibaculum
Acidobacteria	Blastocatellia	Blastocatellales	Blastocatellaceae	-
Acidobacteria	Thermoanaerobaculia	Thermoanaerobaculales	Thermoanaerobaculace	Thermoanaerobaculum
Actinobacteria	Acidimicrobiia	-	-	-
Actinobacteria	Actinobacteria	Micrococcales	Cellulomonadaceae	Actinotalea
Actinobacteria	Thermoleophilia	Gaiellales	Gaielaceae	Gaiella
Armatimonadetes	-	-	-	-
Armatimonadetes	Chthonomonadetes	Chthonomonadales	-	-
Bacteroidetes	Bacteroidia	Bacteroidales	Paludibacteraceae	-
Bacteroidetes	Bacteroidia	Bacteroidales	Paludibacteraceae	Paludibacter
Bacteroidetes	Bacteroidia	Chitinophagales	Chitinophagaceae	-
Bacteroidetes	Bacteroidia	Chitinophagales	Chitinophagaceae	-
Bacteroidetes	Bacteroidia	Chitinophagales	Chitinophagaceae	-
Bacteroidetes	Bacteroidia	Chitinophagales	Chitinophagaceae	-
Bacteroidetes	Bacteroidia	Flavobacteriales	-	-
Bacteroidetes	Bacteroidia	Flavobacteriales	Weeksellaceae	Moheibacter

Bacteroidetes	Bacteroidia	Sphingobacteriales	-	-
Bacteroidetes	Bacteroidia	Sphingobacteriales	-	-
Bacteroidetes	Bacteroidia	Sphingobacteriales	-	-
Bacteroidetes	Bacteroidia	Sphingobacteriales	Lentimicrobiaceae	-
Bacteroidetes	Ignavibacteria	-	-	-
Bacteroidetes	Ignavibacteria	-	-	-
Bacteroidetes	Ignavibacteria	-	-	-
Bacteroidetes	Ignavibacteria	-	-	-
Bacteroidetes	Ignavibacteria	Ignavibacteriales	-	-
Bacteroidetes	Ignavibacteria	Ignavibacteriales	-	-
Bacteroidetes	Ignavibacteria	Ignavibacteriales	-	-
Bacteroidetes	Ignavibacteria	Ignavibacteriales	-	-
Bacteroidetes	Ignavibacteria	Ignavibacteriales	-	-
Bacteroidetes	Ignavibacteria	Ignavibacteriales	-	-
Bacteroidetes	Ignavibacteria	Ignavibacteriales	-	-
Bacteroidetes	Ignavibacteria	Ignavibacteriales	-	-
Bacteroidetes	Ignavibacteria	Kryptoniales	-	-
Chlamydiae	Chlamydiae	Chlamydiales	-	-
Chloroflexi	-	-	-	-
Chloroflexi	-	-	-	-
Chloroflexi	-	-	-	-
Chloroflexi	Anaerolineae	-	-	-

Chloroflexi	Anaerolineae	-	-	-
Chloroflexi	Anaerolineae	-	-	-
Chloroflexi	Anaerolineae	-	-	-
Chloroflexi	Anaerolineae	-	-	-
Chloroflexi	Anaerolineae	-	-	-
Chloroflexi	Anaerolineae	-	-	-
Chloroflexi	Anaerolineae	-	-	-
Chloroflexi	Anaerolineae	-	-	-
Chloroflexi	Anaerolineae	-	-	-
Chloroflexi	Anaerolineae	-	-	-
Chloroflexi	Anaerolineae	-	-	-
Chloroflexi	Anaerolineae	-	-	-
Chloroflexi	Anaerolineae	Anaerolineales	Anaerolineaceae	-
Chloroflexi	Anaerolineae	Anaerolineales	Anaerolineaceae	-
Chloroflexi	Anaerolineae	Anaerolineales	Anaerolineaceae	-
Chloroflexi	Anaerolineae	Anaerolineales	Anaerolineaceae	-
Chloroflexi	Anaerolineae	Anaerolineales	Anaerolineaceae	-
Chloroflexi	Anaerolineae	Anaerolineales	Anaerolineaceae	-
Chloroflexi	Anaerolineae	Anaerolineales	Anaerolineaceae	-
Chloroflexi	Anaerolineae	Anaerolineales	Anaerolineaceae	-
Chloroflexi	Anaerolineae	Anaerolineales	Anaerolineaceae	-
Chloroflexi	Anaerolineae	Anaerolineales	Anaerolineaceae	-
Chloroflexi	Anaerolineae	Anaerolineales	Anaerolineaceae	-

Chloroflexi	Anaerolineae	Anaerolineales	Anaerolineaceae	-
Chloroflexi	Anaerolineae	Anaerolineales	Anaerolineaceae	-
Chloroflexi	Anaerolineae	Anaerolineales	Anaerolineaceae	-
Chloroflexi	Anaerolineae	Anaerolineales	Anaerolineaceae	Anaerolinea
Chloroflexi	Anaerolineae	Ardenticatenales	-	-
Chloroflexi	Anaerolineae	Ardenticatenales	-	-
Chloroflexi	Anaerolineae	Caldilineales	Caldilineaceae	-
Chloroflexi	Anaerolineae	Caldilineales	Caldilineaceae	-
Cyanobacteria	Melainabacteria	Obscuribacterales	-	-
Cyanobacteria	Sericytochromatia	-	-	-
Deinococcus-Thermus	Deinococci	Deinococcales	Trueperaceae	Truepera
Dependentiae	Babeliae	Babeliales	Babeliaceae	-
Patescibacteria	Microgenomatia	Collierbacteria	-	-
Patescibacteria	Microgenomatia	Pacebacteria	-	-
Planctomycetes	Brocadiae	Brocadiales	Brocadiaceae	Brocadia
Planctomycetes	Brocadiae	Brocadiales	Brocadiaceae	Brocadia
Planctomycetes	Brocadiae	Brocadiales	Brocadiaceae	Brocadia
Planctomycetes	Brocadiae	Brocadiales	Brocadiaceae	Brocadia
Planctomycetes	Brocadiae	Brocadiales	Brocadiaceae	Brocadia
Planctomycetes	Brocadiae	Brocadiales	Brocadiaceae	Brocadia
Planctomycetes	Phycisphaerae	Phycisphaerales	Phycisphaeraceae	-
Planctomycetes	Planctomycetacia	Pirellulales	Pirellulaceae	Thermogutta
Proteobacteria	Alphaproteobacteria	-	-	-

Proteobacteria	Alphaproteobacteria	-	-	-
Proteobacteria	Alphaproteobacteria	-	-	-
Proteobacteria	Alphaproteobacteria	Acetobacterales	Elioraeaceae	Elioraea
Proteobacteria	Alphaproteobacteria	Parvibaculales	Parvibaculaceae	Parvibaculum
Proteobacteria	Alphaproteobacteria	Rhizobiales	-	-
Proteobacteria	Alphaproteobacteria	Rhizobiales	-	-
Proteobacteria	Alphaproteobacteria	Rhizobiales	-	-
Proteobacteria	Alphaproteobacteria	Rhizobiales	-	-
Proteobacteria	Alphaproteobacteria	Rhizobiales	-	-
Proteobacteria	Alphaproteobacteria	Rhizobiales	Hyphomicrobiaceae	-
Proteobacteria	Alphaproteobacteria	Rhizobiales	Hyphomicrobiaceae	Pedomicrobium
Proteobacteria	Alphaproteobacteria	Rhizobiales	Rhizobiaceae	-
Proteobacteria	Alphaproteobacteria	Rhizobiales	Rhizobiales Incertae	Bauldia
Proteobacteria	Alphaproteobacteria	Rhizobiales	Xanthobacteraceae	-
Proteobacteria	Alphaproteobacteria	Rhizobiales	Xanthobacteraceae	-
Proteobacteria	Alphaproteobacteria	Rhizobiales	Xanthobacteraceae	Nitrobacter
Proteobacteria	Alphaproteobacteria	Rhizobiales	Xanthobacteraceae	Pseudorhodoplanes
Proteobacteria	Alphaproteobacteria	Rhodobacterales	Rhodobacteraceae	-
Proteobacteria	Alphaproteobacteria	Rhodobacterales	Rhodobacteraceae	-
Proteobacteria	Alphaproteobacteria	Rhodospirillales	-	-
Proteobacteria	Alphaproteobacteria	Rhodospirillales	-	-
Proteobacteria	Alphaproteobacteria	Sphingomonadales	Sphingomonadaceae	Sphingopyxis
Proteobacteria	Deltaproteobacteria	-	-	-

Proteobacteria	Deltaproteobacteria	Bdellovibrionales	Bdellovibrionaceae	Bdellovibrio
Proteobacteria	Deltaproteobacteria	Desulfarculales	Desulfarculaceae	-
Proteobacteria	Deltaproteobacteria	Myxococcales	Phaselicystidaceae	Phaselicystis
Proteobacteria	Deltaproteobacteria	Oligoflexales	-	-
Proteobacteria	Gammaproteobacteria	-	-	-
Proteobacteria	Gammaproteobacteria	-	-	-
Proteobacteria	Gammaproteobacteria	-	-	-
Proteobacteria	Gammaproteobacteria	-	-	-
Proteobacteria	Gammaproteobacteria	-	-	-
Proteobacteria	Gammaproteobacteria	-	-	-
Proteobacteria	Gammaproteobacteria	Betaproteobacteriales	-	-
Proteobacteria	Gammaproteobacteria	Betaproteobacteriales	-	-
Proteobacteria	Gammaproteobacteria	Betaproteobacteriales	-	-
Proteobacteria	Gammaproteobacteria	Betaproteobacteriales	-	-
Proteobacteria	Gammaproteobacteria	Betaproteobacteriales	-	-
Proteobacteria	Gammaproteobacteria	Betaproteobacteriales	Burkholderiaceae	-
Proteobacteria	Gammaproteobacteria	Betaproteobacteriales	Burkholderiaceae	-
Proteobacteria	Gammaproteobacteria	Betaproteobacteriales	Burkholderiaceae	-
Proteobacteria	Gammaproteobacteria	Betaproteobacteriales	Burkholderiaceae	-
Proteobacteria	Gammaproteobacteria	Betaproteobacteriales	Burkholderiaceae	-
Proteobacteria	Gammaproteobacteria	Betaproteobacteriales	Burkholderiaceae	Castellaniella
Proteobacteria	Gammaproteobacteria	Betaproteobacteriales	Burkholderiaceae	Limnobacter
Proteobacteria	Gammaproteobacteria	Betaproteobacteriales	Nitrosomonadaceae	Nitrosomonas

Proteobacteria	Gammaproteobacteria	Betaproteobacteriales	Rhodocyclaceae	-
Proteobacteria	Gammaproteobacteria	Betaproteobacteriales	Rhodocyclaceae	Denitratisoma
Proteobacteria	Gammaproteobacteria	Betaproteobacteriales	Rhodocyclaceae	Denitratisoma
Proteobacteria	Gammaproteobacteria	Oceanospirillales	-	-
Proteobacteria	Gammaproteobacteria	Oceanospirillales	Saccharospirillaceae	Oceanobacter
Proteobacteria	Gammaproteobacteria	Xanthomonadales	Rhodanobacteraceae	Dokdonella
Proteobacteria	Gammaproteobacteria	Xanthomonadales	Xanthomonadaceae	-
Proteobacteria	Gammaproteobacteria	Xanthomonadales	Xanthomonadaceae	-
Proteobacteria	Gammaproteobacteria	Xanthomonadales	Xanthomonadaceae	-
Proteobacteria	Gammaproteobacteria	Xanthomonadales	Xanthomonadaceae	Stenotrophomonas
Spirochaetes	Leptospirae	Leptospirales	Leptospiraceae	Leptonema
Spirochaetes	Leptospirae	Leptospirales	Leptospiraceae	Turneriella
Verrucomicrobia	Verrucomicrobiae	Pedosphaerales	Pedosphaeraceae	-

Appendix 5:

Supplementary materials for Chapter 4

Photograph of PVA-SA beads.

The bottle on the left contains PVA-SA beads with anammox biomass entrapped, while the bottle on the right contains PVA-SA beads with anammox biomass and zeolite entrapped. (The beads in the bottle on the right were not used in any of the experiments reported in this dissertation.)

Nitrite sorption capacity of NaCl-treated zeolites (or, lack thereof).

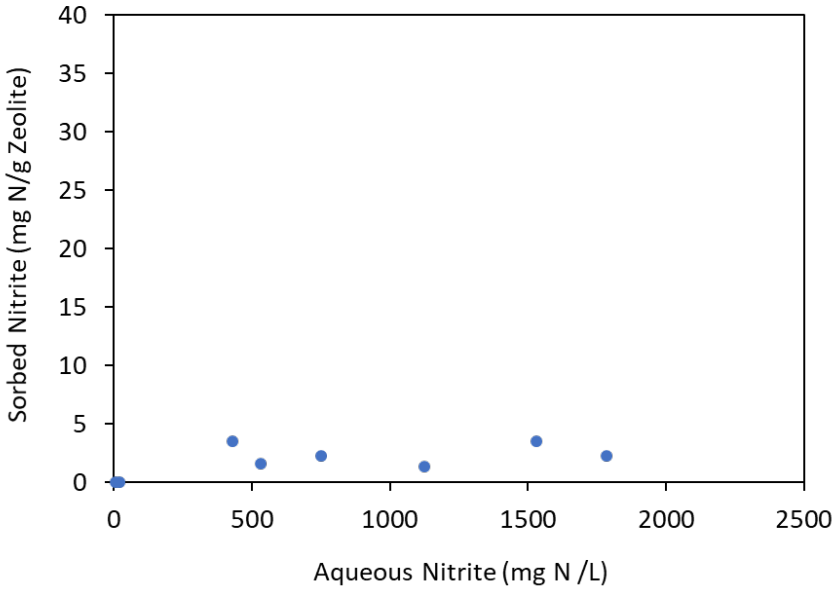

Impact of substrate diffusion through PVA-SA beads on anammox performance.

The initial consumption of ammonium and nitrite by the anammox microbial community within three batch reactor conditions is plotted in panels (a) and (b), respectively. All three conditions, prepared in triplicate, were initially inoculated with the same concentrations of ammonium, nitrite, and anammox biomass. The relationship between anammox biomass and PVA-SA beads was investigated by varying the application of the PVA-SA beads across the three conditions:

1) No PVA-SA beads were supplied; anammox biomass was amended independently of the PVA-SA beads (grey),
2) PVA-SA beads were prepared without biomass and supplied; anammox biomass was amended independently of the PVA-SA beads (blue), and
3) PVA-SA beads were prepared following the standard procedure (i.e., all anammox biomass added to the batch reactor was entrapped within the PVA-SA beads) (orange).

There was little difference between conditions 1 and 2. However, ammonium and nitrite were consumed at a slower rate in condition 3. This indicates that there is no inhibitory impact from the PVA-SA beads themselves, but a diffusion limitation of substrates through the beads impedes anammox performance.

a)

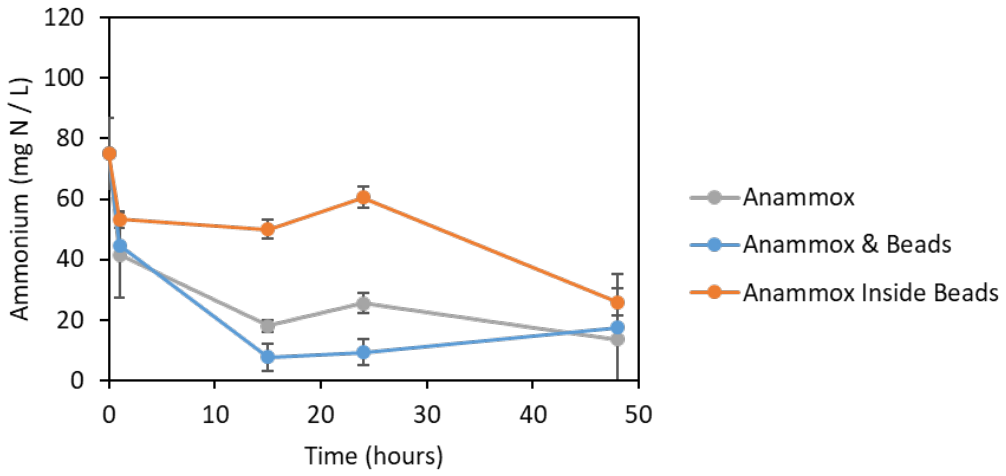

b)

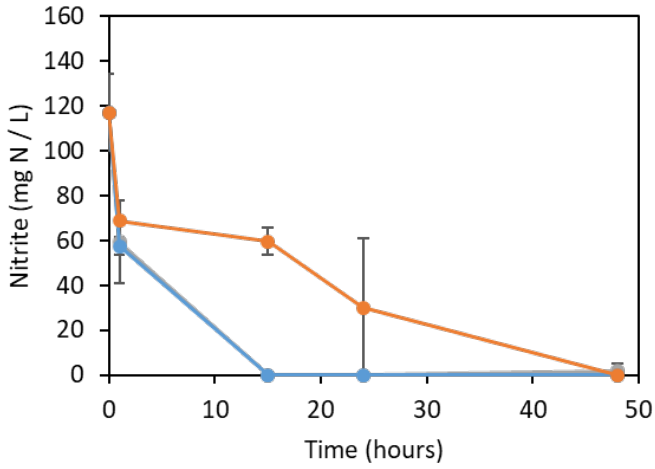

UASB Performance, reproduced with lower influent concentrations of Na^+ and Cl^-.

Panels (a) and (b) report the influent and effluent concentrations of reactive nitrogen species (primary y-axis) and the NRR (secondary y-axis) over time in the zeolite-free and the zeolite-amended UASBs, respectively (influent nitrate concentrations were negligible, so they were not plotted). Panel (c) reports the nitrogen speciation ratios for both UASBs over time. The dashed lines represent the stoichiometric nitrogen speciation ratios for anammox (Equation 1.6).

NaCl was removed from the influent synthetic medium for this iteration of the UASB startup experiment (to encourage more sorption of ammonium onto the zeolites). This iteration was only performed once, but from the results below it appears that the addition of zeolites had a negative impact on anammox performance in a UASB.

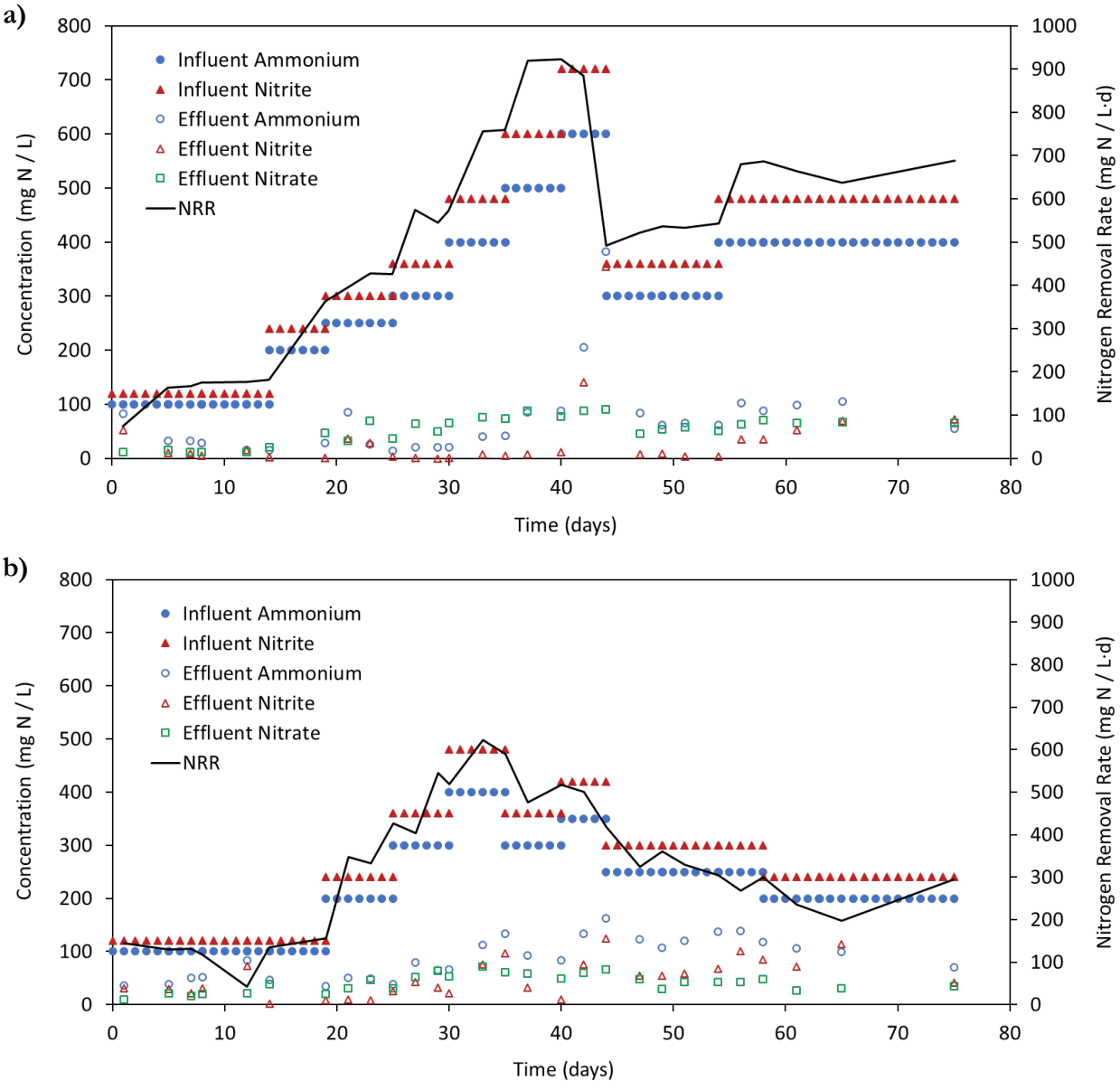

c)

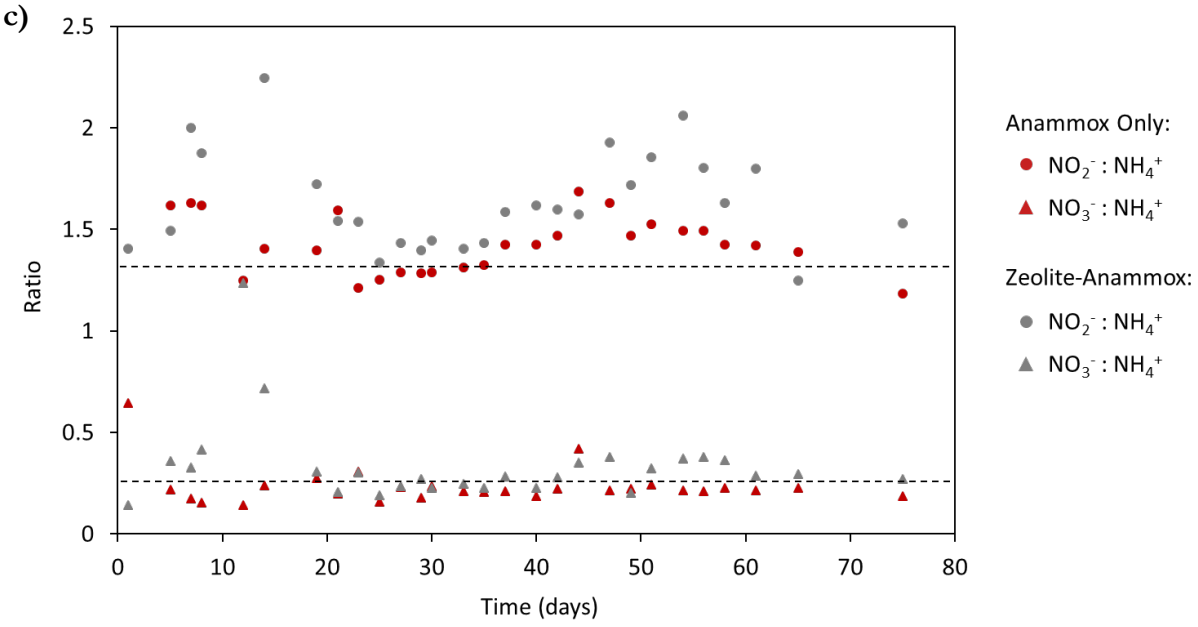
2.5
2
1.5
1
0.5
0
Ratio
0
10
20
30
40
50
60
70
80
Time (days)
Anammox Only:
NO2- : NH4+
NO3- : NH4+
Zeolite-Anammox:
NO2- : NH4+
NO3- : NH4+

Appendix 6:

Full taxonomic classifications of all recovered operational taxonomic units (OTUs) in the upflow anaerobic sludge blanket (UASB) reactors

Phylum	Class	Order	Family	Genus
Acidobacteria	Acidobacteriia	Solibacterales	Solibacteraceae	-
Acidobacteria	Acidobacteriia	Solibacterales	Solibacteraceae	-
Acidobacteria	Acidobacteriia	Solibacterales	Solibacteraceae	-
Acidobacteria	Thermoanaerobaculia	Thermoanaerobaculales	Thermoanaerobaculace	Thermoanaerobaculum
Actinobacteria	-	-	-	-
Bacteroidetes	Bacteroidia	-	-	-
Bacteroidetes	Bacteroidia	Bacteroidales	Paludibacteraceae	-
Bacteroidetes	Bacteroidia	Chitinophagales	Chitinophagaceae	-
Bacteroidetes	Bacteroidia	Chitinophagales	Chitinophagaceae	-
Bacteroidetes	Bacteroidia	Chitinophagales	Chitinophagaceae	-
Bacteroidetes	Bacteroidia	Chitinophagales	Chitinophagaceae	-
Bacteroidetes	Bacteroidia	Chitinophagales	Chitinophagaceae	-
Bacteroidetes	Bacteroidia	Chitinophagales	Chitinophagaceae	-
Bacteroidetes	Bacteroidia	Chitinophagales	Chitinophagaceae	-
Bacteroidetes	Bacteroidia	Chitinophagales	Chitinophagaceae	Chitinophaga
Bacteroidetes	Bacteroidia	Cytophagales	Microscillaceae	-
Bacteroidetes	Bacteroidia	Flavobacteriales	-	-
Bacteroidetes	Bacteroidia	Flavobacteriales	-	-
Bacteroidetes	Bacteroidia	Flavobacteriales	Crocinitomicaceae	Fluviicola
Bacteroidetes	Bacteroidia	Flavobacteriales	Weeksellaceae	Chryseobacterium
Bacteroidetes	Bacteroidia	Sphingobacteriales	-	-
Bacteroidetes	Bacteroidia	Sphingobacteriales	Sphingobacteriaceae	-

Bacteroidetes	Bacteroidia	Sphingobacteriales	Sphingobacteriaceae	-
Bacteroidetes	Ignavibacteria	-	-	-
Bacteroidetes	Ignavibacteria	-	-	-
Bacteroidetes	Ignavibacteria	-	-	-
Bacteroidetes	Ignavibacteria	-	-	-
Bacteroidetes	Ignavibacteria	-	-	-
Bacteroidetes	Ignavibacteria	-	-	-
Bacteroidetes	Ignavibacteria	-	-	-
Bacteroidetes	Ignavibacteria	-	-	-
Bacteroidetes	Ignavibacteria	-	-	-
Bacteroidetes	Ignavibacteria	-	-	-
Bacteroidetes	Ignavibacteria	Ignavibacteriales	-	-
Bacteroidetes	Ignavibacteria	Ignavibacteriales	-	-
Bacteroidetes	Ignavibacteria	Kryptoniales	-	-
Bacteroidetes	Rhodothermia	Balneolales	Balneolaceae	-
Chloroflexi	-	-	-	-
Chloroflexi	Anaerolineae	-	-	-
Chloroflexi	Anaerolineae	-	-	-
Chloroflexi	Anaerolineae	-	-	-
Chloroflexi	Anaerolineae	-	-	-
Chloroflexi	Anaerolineae	-	-	-
Chloroflexi	Anaerolineae	-	-	-
Chloroflexi	Anaerolineae	-	-	-

Chloroflexi	Anaerolineae	-	-	-
Chloroflexi	Anaerolineae	-	-	-
Chloroflexi	Anaerolineae	-	-	-
Chloroflexi	Anaerolineae	Anaerolineales	Anaerolineaceae	-
Chloroflexi	Anaerolineae	Anaerolineales	Anaerolineaceae	-
Chloroflexi	Anaerolineae	Anaerolineales	Anaerolineaceae	-
Chloroflexi	Anaerolineae	Anaerolineales	Anaerolineaceae	-
Chloroflexi	Anaerolineae	Anaerolineales	Anaerolineaceae	-
Chloroflexi	Anaerolineae	Anaerolineales	Anaerolineaceae	-
Chloroflexi	Anaerolineae	Anaerolineales	Anaerolineaceae	-
Chloroflexi	Anaerolineae	Anaerolineales	Anaerolineaceae	-
Chloroflexi	Anaerolineae	Anaerolineales	Anaerolineaceae	Anaerolinea
Chloroflexi	Anaerolineae	Anaerolineales	Anaerolineaceae	Bellilinea
Chloroflexi	Anaerolineae	Anaerolineales	Anaerolineaceae	Bellilinea
Chloroflexi	Anaerolineae	Caldilineales	Caldilineaceae	Caldilinea
Cyanobacteria	Sericytochromatia	-	-	-
Firmicutes	Bacilli	Bacillales	-	-
Firmicutes	Bacilli	Bacillales	Bacillaceae	-
Firmicutes	Bacilli	Bacillales	Planococcaceae	-
Firmicutes	Bacilli	Bacillales	Planococcaceae	Domibacillus
Firmicutes	Clostridia	Clostridiales	Clostridiaceae	Clostridium
Firmicutes	Clostridia	Clostridiales	Clostridiaceae	Proteiniclasticum
Patescibacteria	-	-	-	-

Patescibacteria	Microgenomatia	Collierbaceria	-	-
Patescibacteria	Microgenomatia	Pacebacteria	-	-
Patescibacteria	Microgenomatia	Pacebacteria	-	-
Planctomycetes	-	-	-	-
Planctomycetes	Brocadiae	Brocadiales	Brocadiaceae	Brocadia
Planctomycetes	Brocadiae	Brocadiales	Brocadiaceae	Brocadia
Planctomycetes	Brocadiae	Brocadiales	Brocadiaceae	Brocadia
Planctomycetes	Brocadiae	Brocadiales	Brocadiaceae	Brocadia
Planctomycetes	Brocadiae	Brocadiales	Brocadiaceae	Brocadia
Planctomycetes	Brocadiae	Brocadiales	Brocadiaceae	Brocadia
Planctomycetes	Brocadiae	Brocadiales	Brocadiaceae	Brocadia
Planctomycetes	Brocadiae	Brocadiales	Brocadiaceae	Brocadia
Planctomycetes	Brocadiae	Brocadiales	Brocadiaceae	Brocadia
Planctomycetes	Brocadiae	Brocadiales	Brocadiaceae	Brocadia
Planctomycetes	Brocadiae	Brocadiales	Brocadiaceae	Brocadia
Planctomycetes	Brocadiae	Brocadiales	Brocadiaceae	Brocadia
Planctomycetes	Brocadiae	Brocadiales	Brocadiaceae	Brocadia
Planctomycetes	Brocadiae	Brocadiales	Brocadiaceae	Brocadia
Planctomycetes	Brocadiae	Brocadiales	Brocadiaceae	Brocadia
Planctomycetes	Brocadiae	Brocadiales	Brocadiaceae	Brocadia
Planctomycetes	Brocadiae	Brocadiales	Brocadiaceae	Brocadia
Planctomycetes	Brocadiae	Brocadiales	Brocadiaceae	Brocadia
Planctomycetes	Brocadiae	Brocadiales	Brocadiaceae	Brocadia

Planctomycetes	Brocadiae	Brocadiales	Brocadiaceae	Brocadia
Planctomycetes	Brocadiae	Brocadiales	Brocadiaceae	Brocadia
Planctomycetes	Brocadiae	Brocadiales	Brocadiaceae	Brocadia
Planctomycetes	Brocadiae	Brocadiales	Brocadiaceae	Brocadia
Planctomycetes	Brocadiae	Brocadiales	Brocadiaceae	Brocadia
Planctomycetes	Brocadiae	Brocadiales	Brocadiaceae	Brocadia
Planctomycetes	Brocadiae	Brocadiales	Brocadiaceae	Brocadia
Planctomycetes	Brocadiae	Brocadiales	Brocadiaceae	Brocadia
Planctomycetes	Phycisphaerae	-	-	-
Planctomycetes	Phycisphaerae	Phycisphaerales	Phycisphaeraceae	-
Planctomycetes	Planctomycetacia	Pirellulales	Pirellulaceae	Thermogutta
Proteobacteria	-	-	-	-
Proteobacteria	Alphaproteobacteria	-	-	-
Proteobacteria	Alphaproteobacteria	-	-	-
Proteobacteria	Alphaproteobacteria	Caulobacterales	Caulobacteraceae	Brevundimonas
Proteobacteria	Alphaproteobacteria	Parvibaculales	Parvibaculaceae	Parvibaculum
Proteobacteria	Alphaproteobacteria	Parvibaculales	Parvibaculaceae	Parvibaculum
Proteobacteria	Alphaproteobacteria	Rhizobiales	Hyphomicrobiaceae	-
Proteobacteria	Alphaproteobacteria	Rhizobiales	Rhizobiaceae	-
Proteobacteria	Alphaproteobacteria	Rhizobiales	Xanthobacteraceae	-
Proteobacteria	Alphaproteobacteria	Rhodobacterales	Rhodobacteraceae	-
Proteobacteria	Alphaproteobacteria	Rhodobacterales	Rhodobacteraceae	-
Proteobacteria	Alphaproteobacteria	Rhodobacterales	Rhodobacteraceae	-

Proteobacteria	Alphaproteobacteria	Rhodospirillales	-	-
Proteobacteria	Deltaproteobacteria	Bdellovibrionales	Bdellovibrionaceae	Bdellovibrio
Proteobacteria	Deltaproteobacteria	Bdellovibrionales	Bdellovibrionaceae	Bdellovibrio
Proteobacteria	Deltaproteobacteria	Desulfarculales	Desulfarculaceae	-
Proteobacteria	Gammaproteobacteria	-	-	-
Proteobacteria	Gammaproteobacteria	-	-	-
Proteobacteria	Gammaproteobacteria	Betaproteobacteriales	-	-
Proteobacteria	Gammaproteobacteria	Betaproteobacteriales	Burkholderiaceae	-
Proteobacteria	Gammaproteobacteria	Betaproteobacteriales	Burkholderiaceae	-
Proteobacteria	Gammaproteobacteria	Betaproteobacteriales	Burkholderiaceae	-
Proteobacteria	Gammaproteobacteria	Betaproteobacteriales	Burkholderiaceae	-
Proteobacteria	Gammaproteobacteria	Betaproteobacteriales	Burkholderiaceae	-
Proteobacteria	Gammaproteobacteria	Betaproteobacteriales	Burkholderiaceae	-
Proteobacteria	Gammaproteobacteria	Betaproteobacteriales	Burkholderiaceae	-
Proteobacteria	Gammaproteobacteria	Betaproteobacteriales	Burkholderiaceae	-
Proteobacteria	Gammaproteobacteria	Betaproteobacteriales	Burkholderiaceae	-
Proteobacteria	Gammaproteobacteria	Betaproteobacteriales	Burkholderiaceae	-
Proteobacteria	Gammaproteobacteria	Betaproteobacteriales	Burkholderiaceae	Castellaniella
Proteobacteria	Gammaproteobacteria	Betaproteobacteriales	Burkholderiaceae	Limnobacter
Proteobacteria	Gammaproteobacteria	Betaproteobacteriales	Rhodocyclaceae	-
Proteobacteria	Gammaproteobacteria	Betaproteobacteriales	Rhodocyclaceae	-
Proteobacteria	Gammaproteobacteria	Betaproteobacteriales	Rhodocyclaceae	Denitratisoma
Proteobacteria	Gammaproteobacteria	Betaproteobacteriales	Rhodocyclaceae	Denitratisoma

Proteobacteria	Gammaproteobacteria	Oceanospirillales	Halomonadaceae	-
Proteobacteria	Gammaproteobacteria	Oceanospirillales	Saccharospirillaceae	Oceanobacter
Proteobacteria	Gammaproteobacteria	Pseudomonadales	Pseudomonadaceae	Pseudomonas
Proteobacteria	Gammaproteobacteria	Pseudomonadales	Pseudomonadaceae	Pseudomonas
Proteobacteria	Gammaproteobacteria	Xanthomonadales	Rhodanobacteraceae	Rhodanobacter
Proteobacteria	Gammaproteobacteria	Xanthomonadales	Rhodanobacteraceae	Dokdonella
Proteobacteria	Gammaproteobacteria	Xanthomonadales	Xanthomonadaceae	-
Proteobacteria	Gammaproteobacteria	Xanthomonadales	Xanthomonadaceae	-
Proteobacteria	Gammaproteobacteria	Xanthomonadales	Xanthomonadaceae	Thermomonas
Spirochaetes	Leptospirae	Leptospirales	Leptospiraceae	Leptonema
Spirochaetes	Leptospirae	Leptospirales	Leptospiraceae	Turneriella
Verrucomicrobia	Verrucomicrobiae	Opitutales	Opitutaceae	Diplosphaera
Verrucomicrobia	Verrucomicrobiae	Opitutales	Opitutaceae	Lacunisphaera

Appendix 7:

Supplementary materials for Chapter 5

Stream sampling locations within New Zealand (Lear et al. 2013).

Here, only samples from the "AK" region were investigated.

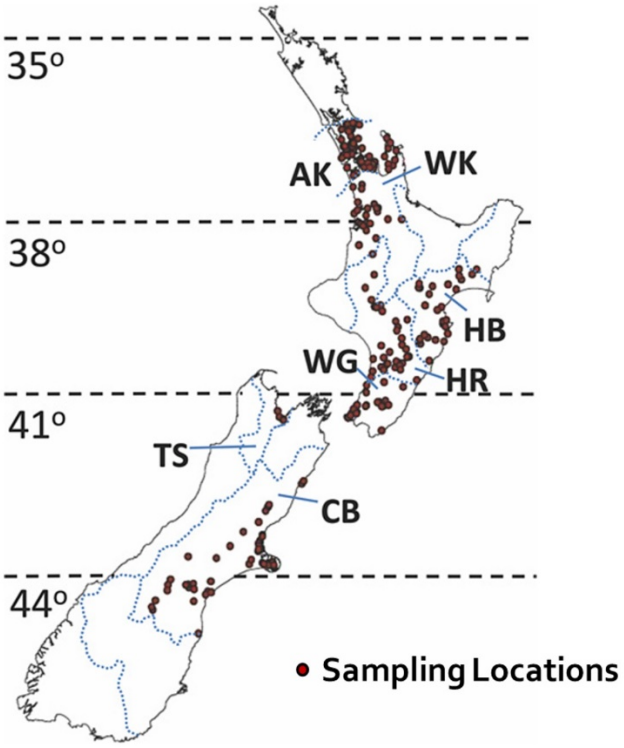

Anammox sequences downloaded from the National Center for Biotechnology Information (NCBI) database.

Bacterium (genus, species)	NCBI accession number
Anammoxoglobus propionicus	DQ317601.1
Brocadia caroliniensis	KF810110.1
Brocadia fulgida	DQ459989.1
Brocadia sinica	KT023578.1
Jettenia asiatica	KF810104.1
Jettenia caeni	AB057453.1
Kuenenia stuttgartiensis	KP663624.1
Scalindua marina	EF602039.1
Scalindua wagneri	AY254882.1

Phylogenetic tree of the 2500 most abundant OTUs within the stream sample database.

The alignment of OTU 262 with the anammox sequences has been highlighted.

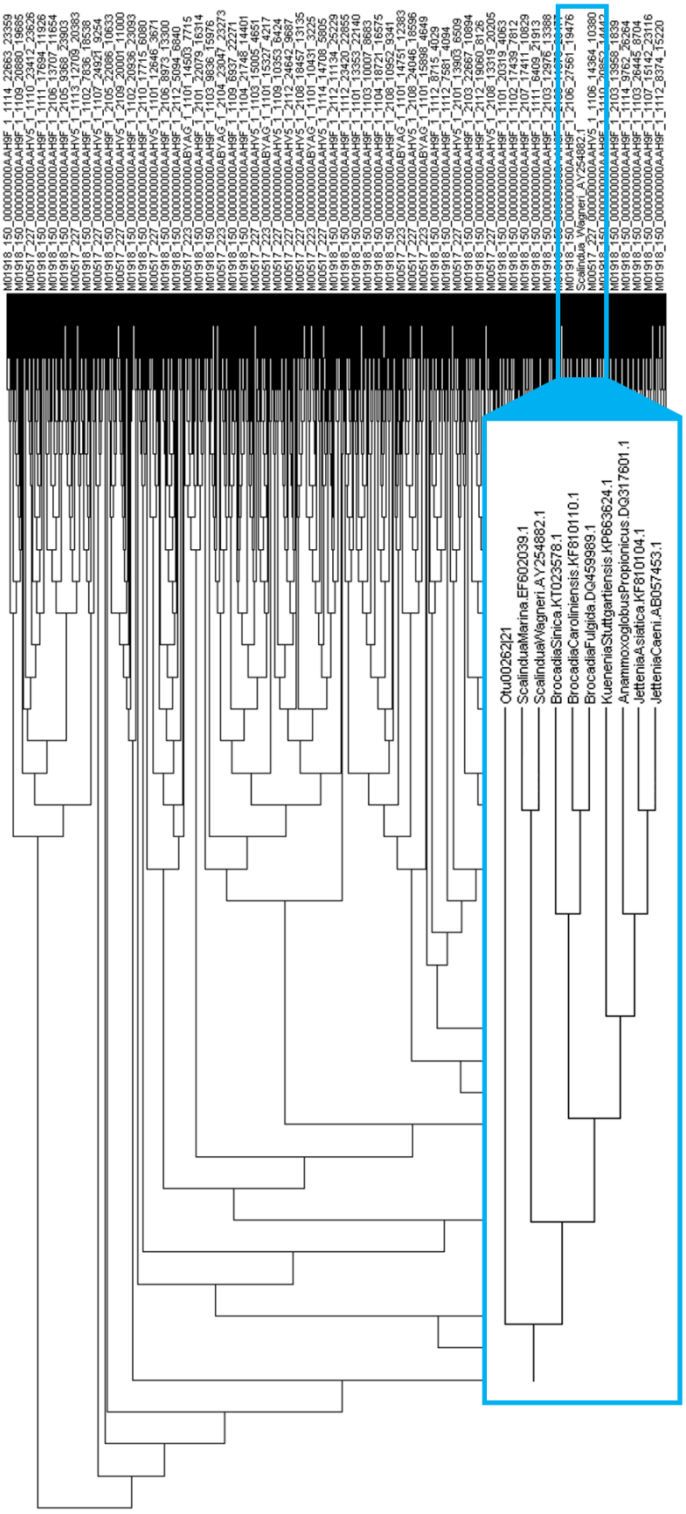

Geographic location of sample AKD2.10

Full classifications of bacterial taxa plotted in Figures 5.2 and 5.3.

Phylum	Class	Order	Family	Genus
Unclassified				
Acidobacteria	-	-	-	-
Acidobacteria	Chloracidobacteria	-	-	-
Actinobacteria	-	-	-	-
Actinobacteria	Acidimicrobiia	-	-	-
Actinobacteria	Actinobacteria	Actinomycetales	-	-
Armatimonadetes	-	-	-	-
Bacteroidetes	-	-	-	-
Bacteroidetes	Cytophagia	-	-	-
Bacteroidetes	Flavobacteria	Cryomorphaceae	-	-
Bacteroidetes	Flavobacteria	Flavobacteriales	-	-
Bacteroidetes	Sphingobacteria	Sphingobacteriales	-	-
Bacteroidetes	Sphigobacteria	Sphingobacteriales	Chitinophagaceae	-
Bacteroidetes	Sphingobacteria	Sphingobacteriales	Flexibacteraceae	-
Bacteroidetes	Sphingobacteria	Sphingobacteriales	Sphingobacteraceae	-
Chlorobi	-	-	-	-
Chlorobi	Chlorobia	Chlorobiales	-	-
Chlorobi	Ignavibacteria	-	-	-
Chlorobi	Ignavibacteria	Ignavibacteriales	-	-
Chlorobi	Ignavibacteria	Melioribacterales	-	-
Chloroflexi	-	-	-	-
Chloroflexi	Anaerolineae	-	-	-
Chloroflexi	Caldilineae	-	-	-
Cyanobacteria	-	-	-	-
Fibrobacteres	-	-	-	-
Firmicutes	-	-	-	-
Firmicutes	Bacilli	Bacillales	-	-
Firmicutes	Clostridia	Clostridiales	-	-
Deferribacteres	-	-	-	-
Gemmatimonadetes	-	-	-	-
Nitrospirae	Nitrospira	-	-	-
Planctomycetes	-	-	-	-
Planctomycetes	Planctomycetia	Brocadiales	Brocadiaceae	-
Planctomycetes	Planctomycetia	Brocadiales	Brocadiaceae	Brocadia
Planctomycetes	Planctomycetia	Brocadiales	Brocadiaceae	Jettenia
Planctomycetes	Planctomycetia	Brocadiales	Brocadiaceae	Kuenenia
Planctomycetes	Phycisphaerae	Phycisphaerales	-	-
Proteobacteria	-	-	-	-
Protoebacteria	Alphaproteobacteria	-	-	-
Proteobacteria	Alphaproteobacteria	Caulobacterales	-	-
Proteobacteria	Alphaproteobacteria	Rhizobiales	-	-
Proteobacteria	Alphaproteobacteria	Rhodobacteraceae	-	-
Proteobacteria	Betaproteobacteria	-	-	-
Proteobacteria	Betaproteobacteria	Burkholderiales	-	-
Proteobacteria	Betaproteobacteria	Burkholderiales	Burkholeriaceae	Limnobacter
Proteobacteria	Betaproteobacteria	Comamonadaceae	-	-
Proteobacteria	Betaproteobacteria	Nitrosomonadales	-	-
Proteobacteria	Betaproteobacteria	Rhodocyclales	-	-
Protoebacteria	Betaproteobacteria	Rhodocyclales	Rhodocyclaceae	Azoarcus
Proteobacteria	Betaproteobacteria	Rhodocyclales	Rhodocyclaceae	Denitratisoma
Proteobacteria	Betaprotoebacteria	Rhodocyclales	Rhodocyclaceae	Methyloversatilis
Proteobacteria	Deltaproteobacteria	-	-	-
Protoebacteria	Gammaproteobact.	-	-	-
Proteobacteria	Gammaproteobact.	Alteromonadales	-	-
Proteobacteria	Gammaproteobact.	Pseudomonadales	-	-
Proteobacteria	Gammaproteobact.	Xanthomonadales	-	-
Verrucomicrobia	-	-	-	-

Additional scientific journal articlers were identified that discussed the microbial community within anammox reactors, but did not fully report the relative abundances of the various taxa within them. These journal articles include:

Yang et al. 2006 (only classified the anammox OTUs)
Ke et al. 2015 (only classified nitrogen-cycling OTUs)
Zheng et al. 2016 (only classified anammox OTUs)
Cho et al. 2018 (only classified anammox OTUs)
Tang et al. 2018 (classified all OTUs, but did not report their relative abundances)

Shepard's plot for Figure 5.4 (Lefcheck 2012).

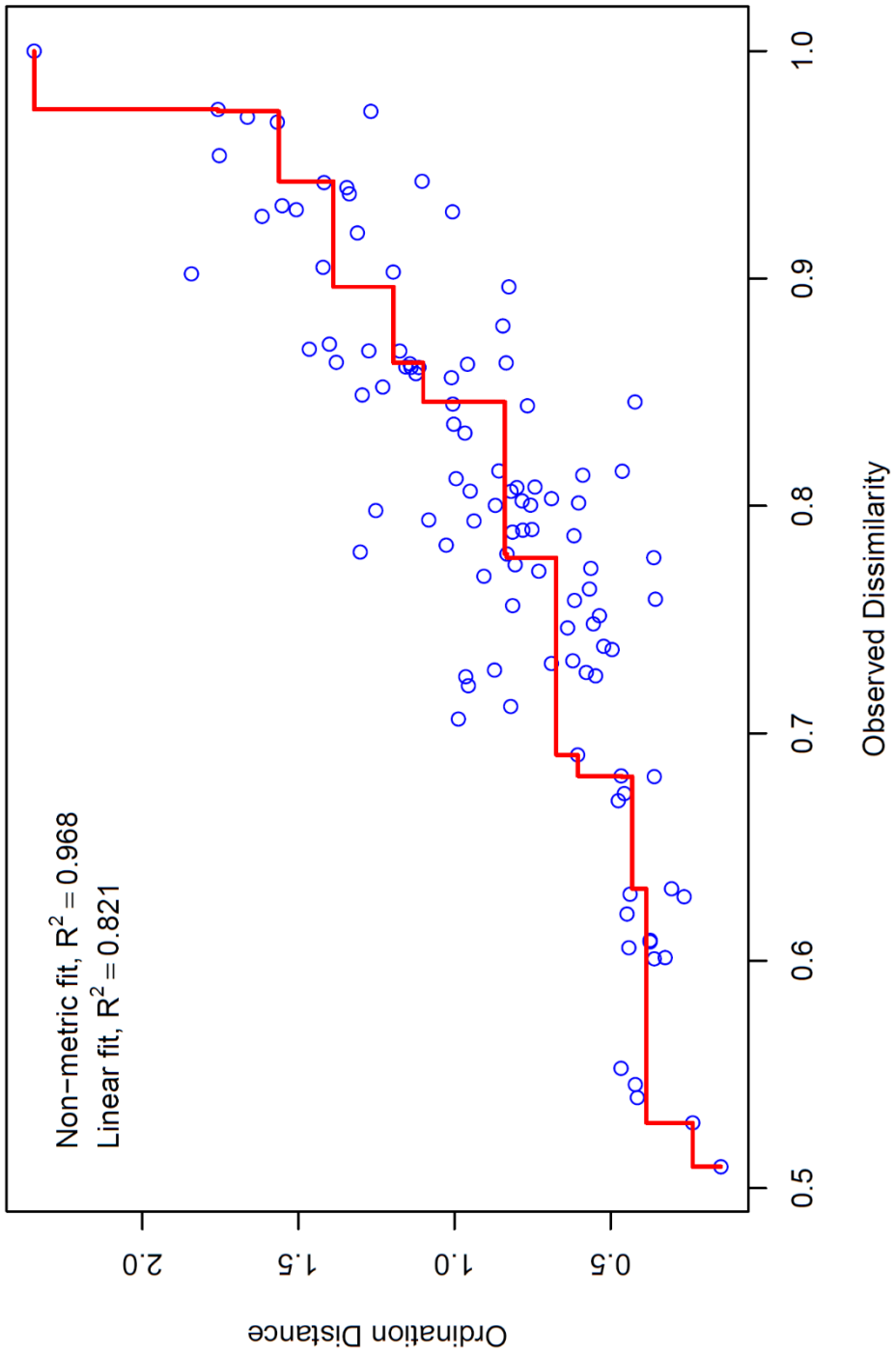

Figure 5.4, with bacterial taxa's and biological samples' names ascribed, respectively.

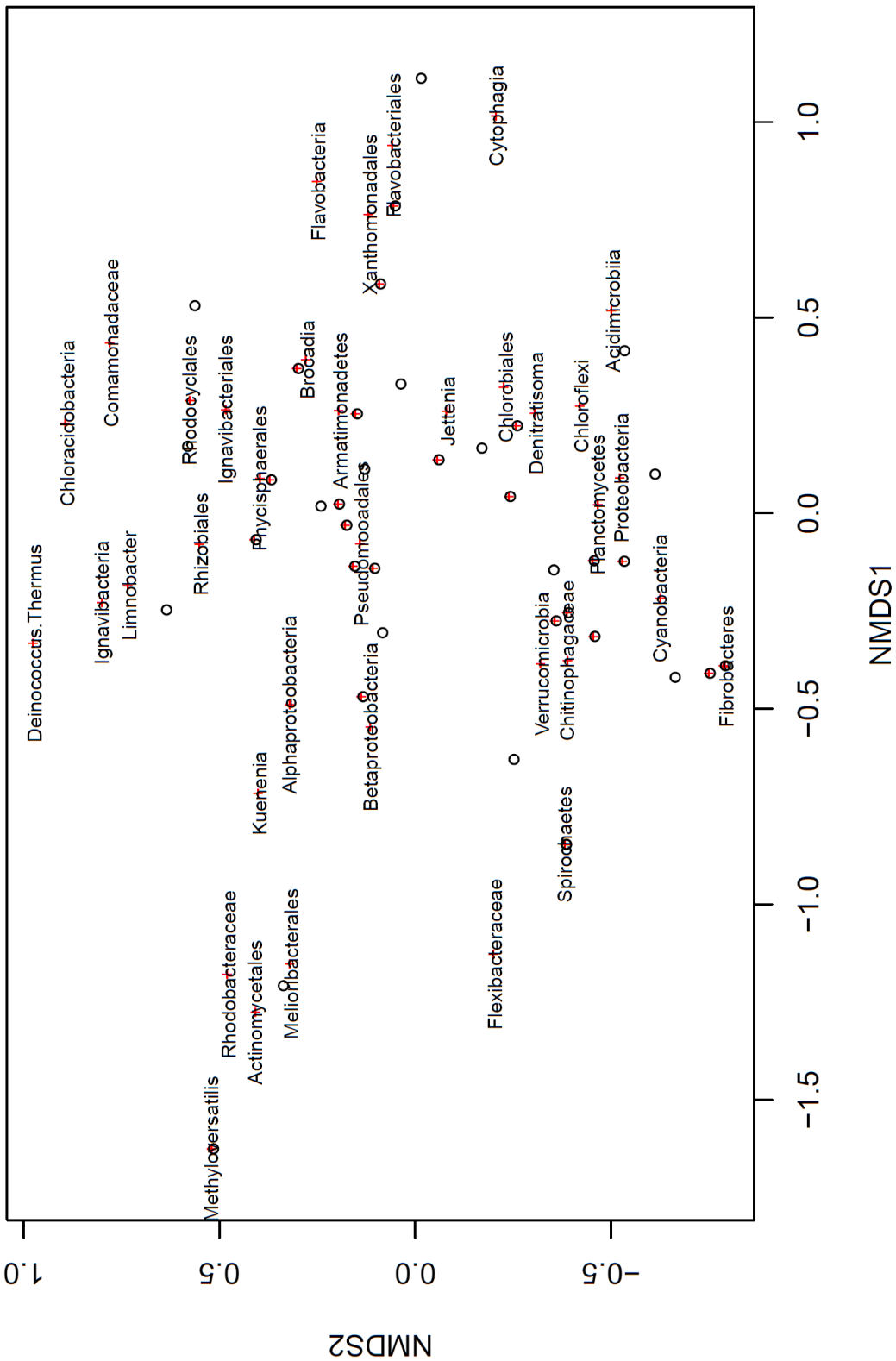

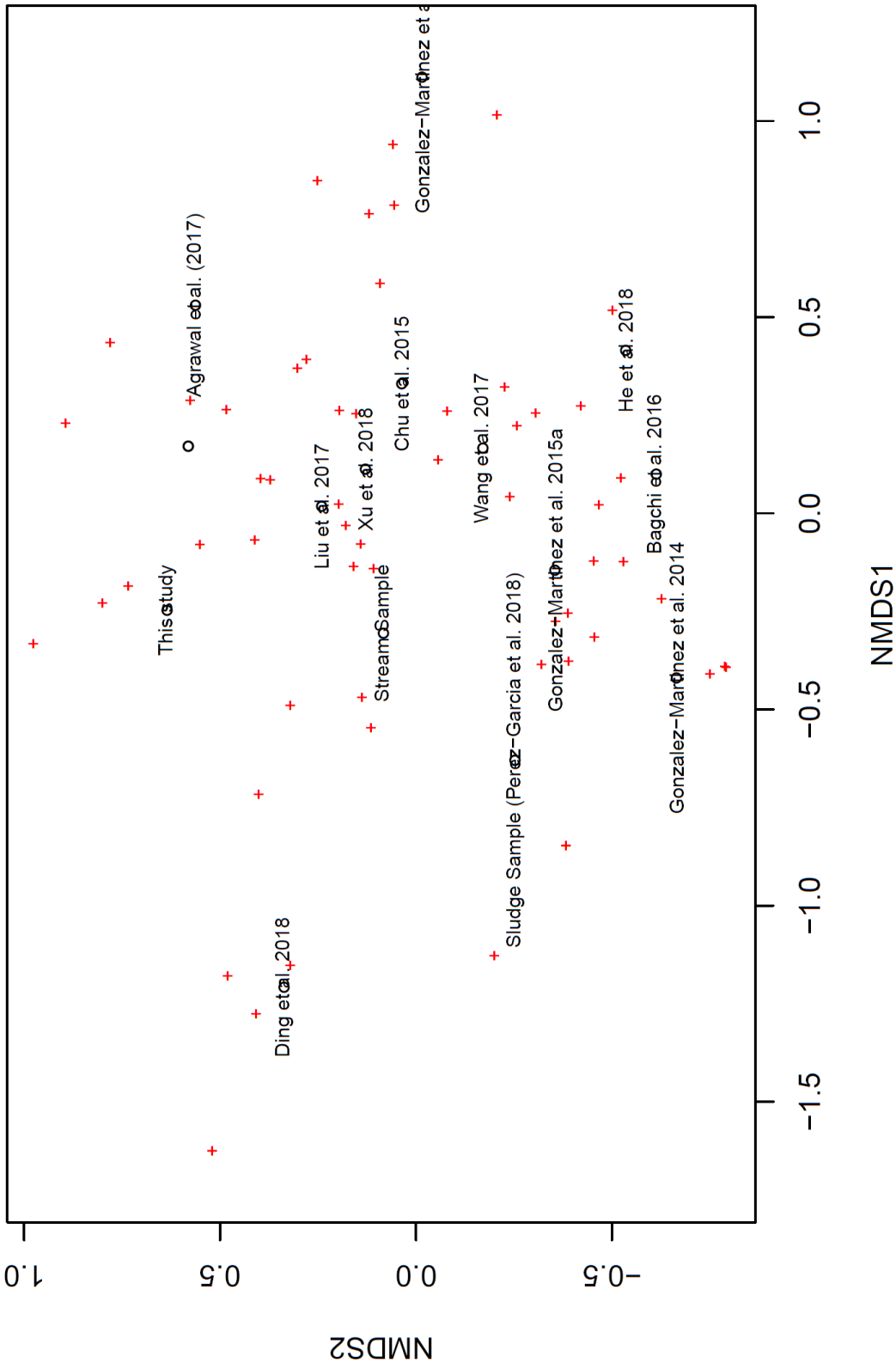
NMDS1
NMDS2
−1.5
−1.0
−0.5
0.0
0.5
1.0
−0.5
0.0
0.5
1.0
This study
Agrawal et al. (2017)
Ding et al. 2018
Liu et al. 2017
Xu et al. 2018
Stream Sample
Chu et al. 2015
Gonzalez−Martinez et a
Wang et al. 2017
Sludge Sample (Perez−Garcia et al. 2018)
Gonzalez−Martinez et al. 2015a
He et al. 2018
Bagchi et al. 2016
Gonzalez−Martinez et al. 2014

Figure 5.5, with bacterial taxa's names ascribed.